A COMPARISON OF REMOTELY-SENSED PRECIPITATION ESTIMATES WITH OBSERVED DATA FROM RAIN GAUGES IN THE WESTERN CAPE, SOUTH AFRICA.

by

Sagwati Eugene Maswanganye

Thesis submitted in fulfilment of the requirements for the degree of

MASTER of SCIENCE

in the Department of Earth Sciences, University of the Western Cape

Supervisor: Dr. Michael Grenfell

Co-Supervisor: Prof. Dominic Mazvimavi

2018

Declarations

"I declare that the thesis entitled" *A comparison of remotely-sensed precipitation estimates with observed data from rain gauges in the Western Cape, South Africa*" is my own work, that it has not been submitted before for any degree or examination in any other university, and that all the sources I have used or quoted have been indicated and acknowledged by means of complete references."

Sagwati Eugene Maswanganye 2017

Signed:……

Abstract

Precipitation data are critical for management of water resources. Precipitation can be measured through ground measurement by means of rain gauges and by remote sensing techniques. Rain gauges often give accurate measurements, however networks of rain gauges are often sparse as they are costly and cannot be placed at all the desirable locations. The alternative is remotely-sensed data which have large spatial coverage and high temporal resolution. Remotely-sensed estimates need to generate realistic and reliable data in order to be used in water resource assessments. Therefore there is need to evaluate the accuracy of remote sensing techniques. This study investigated the reliability of the following satellite derived rainfall estimates; Multi-Sensor Precipitation Estimator (MPE), Tropical Applications of Meteorology using SATellite (TAMSAT) and Climate Hazards Group InfraRed Precipitation with Stations (CHIRPS) in areas with contrasting topographical and climatic characteristics in the Western Cape Province of South Africa.

This study evaluated the accuracy of remotely-sensed precipitation estimates with ground observations from the most representative rain gauge in different two catchments at daily, monthly and yearly level. The study showed that there is general underestimation by remotely-sensed products in these catchments. For the mountainous Jonkershoek catchment, the observed annual total from March 2015 to February 2016 was 993 mm/year whereas TAMSAT and CHIRPS estimated 93 and 692 mm/year respectively. Therefore, TAMSAT and CHIRPS underestimated by 820 and 222 mm/year respectively. For the flat Heuningnes catchment located in the Cape Agulhas plains, the observed annual total from March 2015 to February 2016 was 633 mm/year whereas TAMSAT and CHIRPS estimated 114 and 532 mm/year respectively. Therefore TAMSAT and CHIRPS underestimated by 519 and 101 mm/year respectively. MPE had Missing data therefore it was analysed separately; However it also underestimated the actual amount of rainfall in both catchment.

The study further determined the ability of these remotely-sensed precipitation products to distinguish between non-raining and raining events. The findings showed that TAMSAT, CHIRPS and the MPE were poor at distinguishing between rainy and non-rainy days. TAMSAT had a possibility of detection (POD) of 0.15(15%), CHIRPS had a POD of 0.28 and the MPE had POD of 0.31 in Jonkershoek. In the Heuningnes catchment; TAMSAT, CHIRPS and the MPE had a POD of 0.16, 0.21 and 0.28 respectively. Therefore, it was concluded that the underestimation by the three remotely-sensed products is due to poor

detection of rain-bearing clouds, which may be linked to frontal and orographic rainfall which are common in the area.

Keywords: Rainfall, Remotely-sensed precipitation, satellite derived rainfall estimates, CHIRPS, TAMSAT, Multi-sensor precipitation Estimators.

Acknowledgements

First and for most, I will like to thank Dr. Grenfell and Prof Mazvimavi (Environmental and Water Sciences department, UWC) for their expertise, guidance, assistance throughout the process of writing this thesis. Thank you for being more than supervisors, in you I had mentors and father that I looked up to.

I want to extend my gratitude to Alliance for Collaboration on Climate and Earth Systems Science (ACCESS) for funding this project. Secondly I will like to extend my appreciation to Abri and South African Environmental Observational Networks (SAEON) for the provision of rainfall data for the Jonkershoek catchment.

I would like to also send my thanks you to my friends and colleagues at the EWS department (S. Siwa, Y. Mkunyana, F. Jumbi and S. Gxokwe) whom I shared the struggle with, your assistance was helpful and together we can achieve more.

A special thanks to my family (Dad, Mom, Khanyisa, Bumani, Migingiriko and Nhlalala) for your sincere support and prayers, without you I would not have made this far.

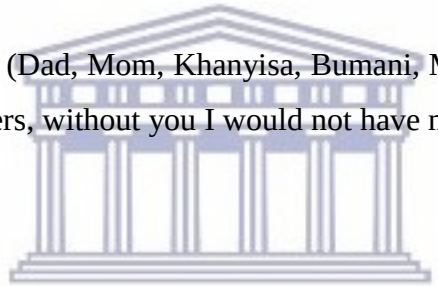

Abbreviations

CHIRPS	Climate Hazards Group InfraRed Precipitation with Stations
CSIR	Council of Science Industrial Research of South Africa
CMORPH	Climate Prediction Center (CPC) MORPHing technique
CPC	Climate Prediction Center
DWAF	Department of Water and Forestry
EUMETSAT	European Organization for the Exploitation of Meteorological Satellites
FEWS NET	Famine Early Warning System Network
GPCP	Global Precipitation Climatology Project
GSoD	Global Summary of the Day
IR	Infrared
MW	Microwave
MPE	Multi-sensor Precipitation Estimator
NRL-blended	Naval Research Laboratory's blended technique
NOAA	National Oceanic and Atmospheric Agency
PERSIANN	Precipitation Estimation from Remotely Sensed Information using Artificial Neural Networks
Ppt	Precipitation
RADAR	RAdio Detection And Ranging
RG	Rain Gauge
RFE	Rainfall Estimate
SAWS	South African Weather Service

SD	Standard Deviation
TAMSAT	Tropical Applications of Meteorology using SATellite
TCI (3G680)	Temperature Condition Index
TIR	Thermal Infrared
TRMM	Tropical Rain Measuring Mission
USGS	United States Geological Survey
VIR	Visible Infrared
VIS	Visible
WMO	World Meteorological Organisation

Measurements:

m	Metre
mm	Millimetres
m.a.s.l	Metres above sea level
km	Kilo metres
ha	Hectare

Table of contents

List of Figures

List of Tables

Chapter 1: Introduction

1.1 Background

Water is a vital and essential resource, which is increasingly becoming scarce due to rising demands. According to Rogers *et al.* (2006) the water crisis in the 21st century is much related to management than as real crisis of scarcity and stress. Other specialists suggest that theses crises are due to scarcity resulting from tremendous demand and global change. It is clear that the water crisis is a reality regardless of the reasons. This has impacted not only the ecosystem but other sectors such as food production (Pimentel *et al.*, 2004), energy and the economy. These impacts have made the management of this resource a global priority.

Water resource managers are facing challenges of river basin planning issues such as water allocation, water pollution control, and disaster/drought response. Water availability varies over time and in space (Pahl-Wostl, 2007). Water resource managers and users need information about the spatial and temporal variation of available water. Water Resource Management (WRM) requires information about the entire hydrological cycle (Sivapalan *et al.*, 2003). However, the major emphasis has been placed on precipitation as input, Evapotranspiration (ET) accounts for losses into the atmosphere, river flows mostly accounts for water available for animal and human use, ground water flows as an important storage and the effects of human activities (Dent, 2012). Water resource managers need to know the spatial and temporal variation of precipitation, evapotranspiration, river flows and the occurrence of ground water.

Most of the components of the hydrological cycle are difficult to monitor due to their complexity. For instance, the estimation of ET has always been problematic as this requires four measurement parameters when using Penman-Monteith; air temperature, atmospheric humidity, radiation and wind speed (Dent, 2012). Some components are difficult to monitor due to high spatial and temporal variation such as soil moisture (Pankey & Pankey, 2010; Qui, 2001). The spatial and temporal variations of some components are not adequately captured due to inadequate coverage of the monitoring networks. This may be due to inaccessible to sites, the cost of the monitoring equipment and vandalism of monitoring system.

Precipitation can be measured through ground measurement by means of rain gauges, and estimated from remote sensing data. The rain gauges often give accurate results when correctly installed. However, this method is expensive and labour intensive (Lakshmi, 2004), as it has to be installed, maintained and the data need to be collected as result adding more to the operational cost. Rain gauges are also vulnerable to vandalism. For these reasons, rain gauge networks are, in most cases not adequate to capture the spatial distribution and in some cases the temporal distribution as well.

There is inadequate spatial coverage by the current rain gauge networks in most parts of the world. WMO (2008) recommends at least one gauge per 100-250 km^2. However, in most parts of the world this has not been achieved. There is actually a decline in the coverage of rain gauge networks (Sivapalan *et al.*, 2003). Funk *et al.* (2015) state that in Africa (excluding South Africa) there was a decline from 2400 stations in 1980 to 400 stations after 2010. Similar declines were also observed in central southwest Asia. According to Sawunyama & Hughes (2010), the number of rainfall stations in South Africa are declining. According to Makapela *et al.* (2013) South African Weather Service (SAWS) and the Agricultural Research Council (ARC) have about 1650 and 500 rainfall stations respectively. According to the recommendation by WMO, South Africa is supposed to have about 5000 to 12000 rainfall stations. It is clear that the rain gauge coverage is inadequate.

The use of remote sensing data for estimating rainfall offers an opportunity to obtain rainfall information in areas with inadequate coverage by rain gauges. Remote sensing techniques have been used extensively since their development for weather forecasting, flood and drought prediction. However, they have their own limitations. Remotely-sensed measurements can have large uncertainty as they do not measure precipitation or any other environmental factor directly. Rather precipitation is estimated from the top of cloud temperature, as a result, the accuracy of satellite derived rainfall estimates is questionable in different physiographic settings (Ceceato and Dinku, 2010). Other biases may be due to a diurnal sampling bias, turning of the instrument or the precipitation algorithm (Smith *et al*., 2006).

The procedures for estimation of rainfall from remotely-sensed data vary in terms of the principles or theoretical concept and the input data. For example, the Multi-sensor Precipitation Estimator (MPE) uses a combination of passive microwave measurement and infrared data from geostationary satellites to estimate rainfall (Heinemann, 2002). The MPE

is mostly used for short-term weather forecasting, now-casting as well as short-term hydrological and agricultural applications (Heinemann, 2002). TAMSAT is one of the products that provide historical datasets for Africa, and like the MPE, it is not gauge dependent and it is also appropriate for near-real time applications. The Tropical Applications of Meteorology using Satellite (TAMSAT) uses a basic linear relationship between the cold cloud duration and rainfall, with a fixed calibration used regionally and seasonally (Tarnavsky *et al*., 2014). Thus rain gauge data are used for calibration but real-time gauge data are not required to produce rainfall estimates. Climate Hazards Group InfraRed Precipitation with Stations (CHIRPS) blends rain gauge data with thermal infrared estimates (Funk *et al*., 2015). CHIRPS is also relatively new in terms of providing daily estimates and started to provide it in February 2015.

Due to the variation in the remotely-sensed products, the accuracy varies from one product to product and from one place to another. However, there are large uncertainties in the estimation of precipitation in coastal regions dominated by frontal system. MPE was found not to give realistic values on the West Coast of South Africa, including the Western Cape whereas in the inland areas and the east coast, realistic yearly estimates can be obtained (Jovanovic *et al.*, 2013). For instance, Kogelberg rainfall station had yearly rainfall of 1188 mm/year whereas the MPE predicted 159 mm/year for the year 2010. Furthermore, Jovanovic *et al* (2013) concluded that the MPE proved to be unable to predict precipitation amounts where frontal and orographic rains occur. Bangira (2013) also evaluated the accuracy of MPE, in a study aimed at mapping flash flood in the Western Cape. The results indicated that the MPE underestimated the extreme rainfall events by 70% and 40% in the Berg and Breede catchments respectively.

On the study by Tote *et al.* (2015) on evaluation of TAMSAT, CHIRPS and the Famine Early Warning System Network Rainfall Estimate (FEWS RFE) throughout Mozambique. The results showed that these remotely-sensed products overestimated low rainfall and underestimated high rainfall. FEWS RFE and CHIRPS performed better than TAMSAT based on the statistical measures. However, TAMSAT detected rainfall events better than CHIRPS and FEWS RFE (Tote *et al*., 2015). The study concluded that products combining thermal infrared and passive microwave imagery perform better than infrared only products, particularly in complex rainfall areas such as coastal areas where rainfall is influenced by frontal systems.

According to Ceceato and Dinku (2010), remotely-sensed precipitation estimates for coastal and mountainous areas have considerable uncertainty because these areas receive high amounts of rainfall which is formed from local convectional systems. Therefore the clouds do not reach high altitude in the atmosphere at which they are detected as cold clouds (Ebert, 1997). This is problematic as almost all remotely sensed precipitation products assume that cold clouds have higher probability of producing rainfall than warm clouds. The purpose of this study is, therefore, to enhance knowledge about remotely sensed precipitation using MPE, CHIRPS and TAMSAT, whilst providing an understanding of the strengths and limitations of precipitation estimation in the Mediterranean climate of the Western Cape.

1.2. Research questions

i) How accurate are the remotely-sensed rainfall estimates in the Western Cape?

ii) What are the factors that affect the accuracy of remotely-sensed precipitation estimates?

1.3. Aim and objectives

1.3.1. Aim

i) The aim of the study is to improve knowledge and understanding of the accuracy and errors of remotely-sensed rainfall estimates (MPE, TAMSAT and CHIRPS).

1.3.2. Objectives

i) To assess the spatial and temporal variation of the accuracy of remotely-sensed precipitation estimates in the Western Cape.

ii) To determine the ability of the remotely-sensed precipitation products to distinguish between non-rainy and rainy events.

1.4. The significance of the study

Decision makers, planners and water resource managers need to know the amount of water available, therefore must be able to assess the input or precipitation. Rain gauges can be used to measure precipitation; however they are often sparse (Hughes, 2006). As result, there is a need for an alternative which in this case is the remotely-sensed data as detailed in the background of the study. In order for the alternative to be used, products need to generate

realistic and reliable data for water resource assessments (Ochieng, 2009). This study proposes to investigate the reliability of the MPE, TAMSAT and CHIRPS. Furthermore, to investigate the cause of the errors, this will be the initiation step towards closing the gap between the estimates and the actual ground measurements. The study will also contribute to the literature on the comparison of remotely sensed precipitation data and the actual ground measurements.

1.5. Thesis outline

Chapter 2 describes the spatial and temporal distribution of rainfall across South Africa and in the Western Cape. This chapter also describes the key rainfall generating mechanisms and how they are affected.

Chapter 3 reviews the literature on the comparison of remotely sensed precipitation and the actual ground measurements. Different methods used to obtain precipitation estimates are revised. Methods used to solve similar problems are also considered. Furthermore, the gaps in literature are identified.

Chapter 4 presents the research design and provides the description of how the required data were obtained. This will also give the description of how the data were analysed in order to obtain information from the data.

Chapter 5 presents the results on the evaluation of remotely-sensed rainfall estimates in the Western Cape. This covers both spatial and temporal distribution of the accuracy/errors in the Western Cape.

Chapter 6 also presents results on the assessment of remotely-sensed estimation of rainfall estimates at a point. This covers both spatial and temporal distribution of the accuracy/errors at a point in both the Heuningnes and Jonkershoek catchment.

Chapter 7 delivers the discussion of the results on differences between the remotely-sensed precipitation estimates and actual ground measurements from rain gauges. A discussion is also engaged on the change of the error over time, space and with elevation.

Chapter 8 concludes the study by providing answers to the research questions and furnishing a brief description of the causes of the errors. Recommendation for further studies will also be made in this chapter.

Chapter 2: Literature Review

2.1 Introduction

Precipitation is highly variable in space and time. Measurement of precipitation is crucial for planning and management of water resources. This chapter outlines the techniques used to estimate precipitation. The chapter also provides history and application of remote sensing techniques. Furthermore, the chapter reviews the techniques applied to improve and validate remotely sensed estimates of rainfall. The chapter concludes by identifying gaps in the literature and review of methods.

2.2 Historical development

According to Campbell (2002) remote sensing is the practise of deriving information about an object from a distance without coming into contact with the object. Remote sensing has long history which can be dated to the 1800s when William Herschel discovered Infrared, which led to the practice of photography (Campbell, 2002; Aggarwal, 2004). The use of remote sensing in earth observations began in 1859 when Gaspard-Felix Tournachon took an aerial photograph of a small village near Paris from an air balloon (Aggarwal, 2004; Campbell and Wynne, 2011). This was soon followed by others all around the world. In 1890, Wilbur Wright took motion photographs of the Italian landscape from an airplane. During World War I (1914-1918), aerial photographs were taken for military reconnaissance, with the intention of identifying the location of enemies (Aggarwal, 2004).

The development of remote sensing continued through World War II (1914-1945) and beyond. However, the acceptance of the use in governmental and scientific activities developed slowly due to resistance by traditionalists, imperfections in the equipment and techniques. There was also uncertainty regarding the proper use of aerial photographs (Campbell, 2002; Campbell and Wynne, 2011). In 1959, the first satellite named Explorer-6 was launched into orbit by NASA (Aggarwal, 2004). Soon after, another satellite called the TIROS Meteorological satellite was launched by NASA into orbit as the first weather satellite. Additional satellites were launched thereafter such as the LandSat with the Multi-spectral scanner in 1972, and LandSat with the Thematic Mapper in 1982 by NASA (Aggarwal, 2004). In 1997 NASA and Japan Aerospace Exploration Agency (JAXA) launched the Tropical Rainfall Measuring Mission (TRMM) which was the first space-born precipitation RADAR, carrying on board Visible (VIS), Infrared (IR) and Microwave (MW)

radiometer (Jobart, 2001). One of the latest orbiting satellites was launched in 2014 by NASA and the Japanese Aerospace Exploration Agency (JAXA) called the Global Precipitation Mission (Jackson *et al.*, 2017).

2.3 Remote sensing applications in Hydrology

2.3.1 Soil moisture estimation

Soil moisture plays a vital role in the exchange of mass and energy fluxes between the hydrosphere, biosphere and the atmosphere as it controls evapotranspiration fluxes (Albergel, 2012). Remote sensing techniques are advantageous over ground measurements, where there is a need to capture large spatial coverage and the spatial variation cannot be easily captured by ground measurements in some cases (Esien *et al.*, 2008). Satellite measurements may be more frequent than ground measurements, depending on the revisit time of the satellite. Hence, more sampling are feasible as compared to ground measurement. Remote sensing of soil moisture requires information below the surface, hence sensors that are capable of penetrating the soil layer are vital. However, remote sensing of soil moisture is mostly limited to thermal and microwave bands (Kumar and Reshmidevi, 2013). Soil moisture is typically correlated to Normalized Difference Vegetation Index (NDVI) and land surface temperature (LST) from remote sensing to ground measured soil moisture (Kumar and Reshmidevi, 2013). Many studies have shown that remotely-sensed soil moisture products have acceptable agreement with ground measurement (Peng *et al*. 2015; Albergel, 2012). Therefore, it has potential for hydrological applications and water resource management. Some of the major limitations are the poor capacity of thermal wavelength to penetrate the vegetation and the coarse spatial resolution (Kumar and Reshmidevi, 2013).

2.3.2 Evapotranspiration

One of the most important processes in hydrology is the loss of water from Earth's surface to the atmosphere called evapotranspiration (ET). On a global level, the average ET accounts for approximately 60% of the average precipitation (Li *et al.*, 2009). Hence, quantifying ET is a key for water resource assessments. According to Yebra *et al.* (2012), "remote sensing is the only feasible means of spatially estimating actual evapotranspiration (ETa) over larger regions or continents". Various approaches developed to derive ET from remotely-sensed data can be grouped into (i) those that incorporate satellite land surface temperature into a surface energy balance (SEB) model (Kalma *et al.*, 2008), (ii) those that use vegetation

indices (VIs) (Glenn *et al*.,2011), and (iii) hybrid methods that combine the surface temperature and VI data (Cailson, 2007). Therefore, SEB depends on the estimation of surface temperature from the thermal bands and the VIs depends on the estimates of the green vegetation cover over the landscape. However, VIs cannot detect soil evaporation nor vegetation stress except on a long time basis. The hybrid method is similar to soil water moisture in that it correlates VI and land surface temperature from remote sensing to ground-based estimated ET. For example MOD 16 ET uses remotely-sensed data and ground measured data to estimate ET around the globe (Mu *et al.,* 2007). MOD 16 ET has been shown to provide reliable estimates of ET (Ruhoff *et al.,* 2013).

2.3.4 Water Quality

Water quality is important for the ecosystems and water uses. Site measurement and sample collection for laboratory analyses provide accurate results for a point in time and space but does not provide temporal and spatial scales of measurement needed for management of water resources (Schmugge *et al*., 2002; Ritchie *et al*., 2003). Substances in water change the backscattering of surface water, thus the remote sensing of water quality depends on the ability to measure theses changes in spectral signature backscattered from water and relate this to water quality parameters (Schmugge *et al*., 2002). Furthermore, the remote sensing of water quality can be explained through factors that affect water quality such as suspended sediments, algae, oil and chemicals which reflect solar or thermal radiation from surface water which can be remotely sensed. Liu *et al.* (2003) state that some products such as AVHRR have shown some success at mesoscale (lakes, reservoirs, large rivers) due to the coarse spatial resolution of remotely-sensed imagery. However, the accuracy of quantification is affected by spatial variation of the parameter in consideration and its concentration levels.

2.4 Precipitation Measurement

2.4.1 Rain gauges

Non-recording rain gauges

Non-recording rain gauges such as cylindrical and ordinary rain gauges require manual observation and recording. Cylindrical rain gauges have a uniform diameter from the top to bottom and an opening at the top. Furthermore, they do not have a funnel like ordinary rain

gauges which funnels rain water in to a storage bottle. The ordinary rain gauges were designed as an improvement to the cylindrical rain gauges which have large openings resulting in substantial losses of the collected rainwater through evaporation (London Met. Office, 2000). The collected rainwater from this kind of rain gauge has be to poured into a measuring cylinder, where the observer has to read the water depth of water and record it, hence the captioning of it as a 'non-recording rain gauge'.

Recording rain gauges

These rain gauges record precipitation on a chart or data logger, and include siphon and tipping bucket rain gauges. With an autographic (Siphon) rain gauge rain water is collected in siphon collector is led into a storage tank through a vessel, as a result, the float in a storage tank moves upward. A pen connected to float marks the amount of rain water collected on a chart (JMA, 2000). For the tipping bucket rain gauge, the rain water collected is channelled through a funnel and poured in to a tipping bucket. When it reaches a predetermined amount, the bucket tips the water into a drain cylinder, causing the read switch to generate a signal for each unit of precipitation collected, and the information is recorded on a chart or data logger for the automated ones.

Errors from rain gauges

Even though rain gauges have improved to make them accurate and to make the data collection process easier, they still have errors that can be caused by environmental factors or the instrument itself. An error in a non-recording gauge may be due to evaporation losses and winds resulting in a deficit of the capture of the rainfall. According to Rooda and Dixon (2012) high wind can result in 5 to 80 percent error of the rain gauge catch. This may, however, be reduced by placing a rain gauge in a pit (ground level rain gauge) with a rim around it to avoid splash into the rain gauge. Human error can introduce inaccuracies when reading the depth of the measuring cylinder. The placement of a rain gauge plays a major role in the errors caused by wind. Therefore, during site selection for the rain gauge, the surrounding environment must be taken into consideration (WMO, 2008). However, it is unlikely that the effect of the wind can be completely avoided. What is, however, possible is that it can be minimised.

The tipping bucket rain gauge has an accuracy of 0.5 mm for precipitation of up to 20 mm per hour. An assessment of accuracy of the typing bucket rain gauge showed that the number of bucket tips decreased almost linearly with increasing precipitation intensity (JMA, 2000).

The error increases with higher precipitation intensity and can exceeded three percent for precipitation of more than 150 mm per hour, JMA, (2000). Ciach, (2003) and Molini *et al.* (2005) also confirm that high intensity rainfall can reduce the accuracy of tipping bucket rain gauge. However, Molini *et al.* (2005) states that the error is usually neglected in hydrological applications on the basis that it has little influence on the total recorded rainfall depth and secondly on the basis that occurrence of rainfall such as 150 mm per hour is rare. However the assumptions are not acceptable for some applications such as urban design as it can result in structural failure.

2.4.2 Remote sensing techniques

2.4.2.1 Passive and active techniques

Remote sensing techniques for measuring precipitation may be divided into passive techniques and active techniques. Passive remote sensing involves (i) visible (VIS) and infrared (IR) sensors and (ii) microwave sensors. These are often referred to as satellite measurements. Active remote sensing includes both space-bourne and ground-based radio detection and ranging (Radar).

2.4.2.2 Approaches to remote sensing estimation of rainfall

Single-instrument satellite rainfall estimates

Passive techniques: IR and VIS

These are satellite rainfall estimating techniques that use one- instrument to estimate rainfall. VIS and Thermal IR (10.5-12.5_m) were the first to be used and showed relatively low accuracy. The methods under single instrument satellite rainfall estimates can be divided into the following categories: cloud indexing methods, bispectral methods, life-historical methods and the cloud model-based technique (Levizzani *et al*., 2002). The cloud indexing methods technique assigns a rain rate on the basis of the relationship between cloud-top characteristics and rainfall falling from the cloud. For example, GOES precipitation index by Arkin and Meisner (1987). The techniques depend on the fraction of cloud colder than 235k (-38.15°C) in the IR with a fixed rain rate. The bispectral methods were developed to improve the IR rainfall estimates by including cloud brightness which is obtained through VIS sensor. The bispectral technique uses the relationship between cloud coldness and brightness and the probability of rainfall. Thus, a lower probability will be associated with cold but dull cloud,

while a higher probability will be associated with cold and thick clouds. The life-historic cycle is a group of techniques that requires geostationary imagery. This relies on detail-analysis of the cloud life cycle (Kidd, 2001). Cloud model-based methods like those mentioned above, relate VIS and IR to rainfall and include physics of cloud into the estimations through cloud models. One of the cloud model techniques is Convective Stratiform Technique (CST) which is one-dimensional cloud model that relates cloud top temperature to rainfall rate. Gouber (1973) used cumulus convection parameterization to relate cloud cover area to rain rate. According to Kidd, (2001) this method is complicated and is most applicable to case studies where the length of study is not long.

The advantages of the VIS and IR bands include high spatial resolution as well as the possibility of frequent temporal sampling from geostationary platforms. However there are two main problems with IR only images in estimating precipitation (Levizzani *et al*., 2002; Kidd, 2001). Firstly, clouds are considered to produce rain when cold enough (235K), but may have evolved beyond the rain stage. Secondly, cloud not cold enough may experience pre-ice –phase rain microphysics as experienced with frontal rains (Seyyedi, 2010). VIR (VIS ad IR) also referred to as bispectral reduces some inaccuracies; however, the VIS sensor is not available at night hence it can introduce a day-night bias in the estimated rainfall. The life history methods take into account the life cycle or the development of clouds, but they often screen the life cycle underneath leading to under-estimation in the morning and over-estimation in the evening (Levizzani *et al*., 2002).

Passive technique: Microwave

Clouds are non-transparent in the VIS and IR spectral range, and cloud properties are estimated from the top of the cloud. Passive microwave penetrates clouds because cloud droplets weakly interact with microwave radiation while rain drops strongly interact. Thus more direct than those based on VIS and/or IR radiation (Kidd, 2001). One of the major microwave instruments that have shown to yield more reliable information in term of instantaneous precipitation rates is the Special Sensor Microwave Imager (SSM/I). The SMM/I measures microwave radiation over a 1400 km wide swath at four separate frequencies, 19.35, 22.23, 37.0 and 85.5 GHz (Levizzani *et al*., 2002). The simplest microwave methods are based on statistical regressions using some of the brightness temperature to derive a rain index, which is then related to rainfall rate (Jobard, 2001).

The use of microwave is a more direct measure of raindrops than VIS and IR, as the microwave sensors interact with precipitation drops. However, its biggest drawback is the poor spatial and temporal resolution (Petty & Krajewski, 1996), because they are currently restricted to the polar-orbiting platform and cannot be used on geostationary satellites which can take multi shots in short periods (Joyce *et al*., 2004). Therefore, estimates are produced from one or two snapshot retrievals per day per satellite. Hence they suffer from larger sampling errors when dealing with short-term rainfall estimates (Kidd *et al.*, 2003). Table 2.1 summaries the strength and weaknesses of infrared and microwave imagers. Table 2.2 shows various satellite estimating products.

Table 2.1: Indication of strength and weaknesses of infrared and microwave imager in the precipitation estimation. Source: Heinemann (2007)

Measurement	Spatial/Temporal resolution	Retrieval accuracy
IR window channel on geostationary satellite	High	Low
Microwave measurements on low orbiting satellite	Low	Acceptable

Active technique

The most important type of precipitation measuring instruments from space is the PR (Precipitation Radar). The first of its kind to be launched in 1997 was the TRMM operating at 13.8 GHz (Levizzani *et al.*, 2002). The instrument provides vertical distribution of rainfall and aimed at obtaining quantitative measurements that contribute in improving the overall retrieval accuracy by combined use of Radar, and TRMM Microwave Imager (TMI) and VIRs instruments. Radar is expected to not only provide information about the intensity and spatial distribution; but also the rain type, storm structure, melting layer and latent heat at different heights. However, these instruments are costly, as a result, a few of them are existent in Africa.

Blended techniques

Blended techniques involve a combination of rainfall estimation techniques. The principle of this approach is to combine two sensors in order to compensate for some of the deficiencies of a single sensor method, by using data obtained from another sensor (Seyyedi, 2010).

According to Lensky and Levizzani (2008) a combination of sensors offers some improvement in precipitation retrievals. Table 2.1 shows how IR and MW can complement each other. Vicente and Anderson (1993) combined IR estimation methods for instantaneous estimation for the first time (Seyyedi, 2010 and Lavazzini *et al*., 2002).

Table 2.2: Rainfall estimates products that can be used in the southern African region. Modified from Karimi and Bastiaanssen (2015)

Product	**Main principles data**	**Spatial Reso-lution**	**Spatial coverage**	**Rainfall Gauge**	**Minimum time steps interval (temporal resolution)**	**Producer**
MPE	Meteosat 7,8,9, 10	3 km	Indian Ocean	No	15 min	EUMETSAT
CMORPH	MW estimates, IR vectors	8 km	50°N-50°S	No	30 min	NOAA/CPC
PERSIANN	MW estimates	0.25°	60°N-60°S	No	1 hr	UC Irvine
GSMap	MW estimates	0.1°	60°N-60°S	No	1 hr	JAXA
NRL-blended	MW	0.25°	60°N-60°S	No	3 hr	NRL
TCI (3G680)	MW	0.5°	37°N-37°S	No	1hr	NASA
TOVS	HIR,MSU sound retrievals	1°	Global	No	Daily	NASA
Hydro estimator	GOES IR	4 km	Global	No	15 min	NOAA
TRMM 3B42	MW estimates	0.25°	50°N-50°S	Yes	3 hr	NASA
CPC RFE 2.0	MW estimates	0.1°	20°W-55°E, 40°S-40°N	Yes	Daily	FEWS
GPCP IDD	IR estimates from geostationary	1°	50°N-50°S	Yes	Daily	NASA/GSFC
CMAP	MW	2.5°	Global	Yes	5 days	NOAA
TAMSAT	Meteosat TIR	3 km	Africa	Yes	10 days	NOAA
TRMM 3B43	MW estimates, IR geostationary	0.25°	40°N-40°S	Yes	Monthly	NASA
GPCP_V2	MW	2.5°	Global	Yes	Monthly	NASA/GSFC

	estimates, IR, TOVS					
CHIRPS	IR estimate and gauge	0.05°	50°N-50°S	Yes	Daily	USGS

Note: the abbreviations are defined in Abbreviations section (page v)

General sources of errors

Even though Blended techniques are presumed to be the most accurate and advanced, there are some general concerns about sources of errors that are not completely dealt with. The remotely-sensed precipitation technique measures rainfall indirectly through cloud properties. Firstly, a good algorithm should be able to distinguish between a raining and non-raining cloud which is difficult because there are minor differences between a raining and non-raining cloud. This causes major errors in remotely-sensed precipitation estimates (Lensky and Lavizzani, 2008). Secondly, a good algorithm should be able to qualify the amount of rainfall. It is easy to see rainfall intensity varies from place to place beneath the cloud, however satellite sees top of cloud which makes it difficult to pick up the variation in intensity (Ceccato and Dinku, 2010). This is what makes ground-based radar estimates betters (Lee *et al.*, 2005) as the measurements are done beneath cloud and as a result can measure the raindrops properties and the intensity of clouds.

A lack of ground truth data to establish reliable correlation satellite data and rainfall is still a problem in remotely-sensed precipitation estimates. Ceccato and Dinku (2010) states that satellite measurements need calibration and validation against ground-based data. This means the use of satellite technique to estimate precipitation does not do away with the need for field measurement. Accuracy depends greatly on both the calibration and the main principle data of products. (See table 2.2 for some of the products that do estimates for the southern Africa region).

2.4.3 Application of Remotely-sensed precipitation estimates

Since the first weather satellite was launched in 1960s (Campbell and Wynne, 2011; Quanwei, 1996), remotely-sensed rainfall estimates have been improving with time. The improvements has made remotely-sensed estimates more useable for various applications such as in water availability, global changes studies, now-casting, hydrological disaster management and precision agriculture.

Water availability

Remotely-sensed precipitation estimates are used in water availability studies, for instance Gaugle (1989) where remotely-sensed precipitation was used as an input for flow prediction in Africa. Najmaddin *et al.* (2017) evaluated the use of remotely-sensed precipitation estimates in a rainfall-runoff model and concluded that remotely-sensed precipitation estimates can be used in rainfall-runoff modelling in semi-arid catchments. Suwanyama and Hughes (2010) proved that remotely-sensed rainfall data can be useful to support the implementation of environmental water requirements in South Africa using real time runoff models, as it is difficult to get real time data from rain gauges.

Disaster and diseases forecasting

Remotely-sensed rainfall has been used in the predictions and assessment of disasters such as flood and drought forecasting. For example the International Centre for Integrated Mountain Development (ICIMOD) programme in Hindu Kush-Himalayan region Flood forecasting. ICIMOD uses 24hr, 48hr, and 72hr satellite rainfall forecasts over the region. The project aims to minimize loss of life and property by reducing vulnerability to floods and droughts in the region (ICIMOD, 2013). The Southern African Regional Flash Flood Guidance (SARFFG) project which is part of WMO initiative of flash flood guidance also highly depends on remotely-sensed precipitation estimations to determine small catchments with the potential to experience flash floods (de Conning, 2013).

Yamana *et al.* (2010) used satellite-based rainfall estimates to simulate potential for malaria transmission in rural Africa. The study investigated whether HYDREMATS (malaria transmission simulator) which requires 1hr resolution rainfall as an input could effectively use satellite rainfall estimates instead of ground-based data. The results indicated that satellite rainfall estimates can be used to accurately simulate the dynamics of mosquito population.

The unusual use of remotely-sensed precipitation estimation as described by Heinemann (2013) was when MPE estimates images were used as an additional tool to identify the severe precipitation by pilots which then can improve navigation decision. This application was never thought about when developing the algorithm.

Agriculture

A study by Teo (2013) is one of the examples of how remotely-sensed precipitation estimates can be useful in agriculture. The study investigated the feasibility of using remotely-sensed

precipitation estimates (RFE) and crop models for crop yield forecasting in Africa, more specifically, Gambia. The RFE driven crop yield predictions were as good as gauge driven predictions. The RFE has large coverage; therefore it can be deployed in many data-sparse region of the continent.

2.4.4 Evaluation of remotely sensed precipitation.

Many studies have been done across the globe on assessing the accuracy of remotely-sensed rainfall estimates. Wolters *et al.* (2011) for example, evaluated rainfall retrieval from SEVIRI reflectance's over West Africa using TRMM-PR and CMORPH. The cumulative frequency distributions showed CPP-PP (Cloud Physical Properties-Precipitation Properties) and TRMM-PR are generally within +/-10% of the observed data. The CPP-PP showed a very good agreement with the rain gauge data up to 5 mm h^{-}; however, overestimated at higher rain rate (5mm-16mm h^{-}). Furthermore, the study found that the results indicate the CMORPH has good agreement with cumulative precipitation and seasonal progressive of rainfall throughout the West Africa Monsoon; however the CPP-PP estimated higher amounts in the coastal areas of West Africa.

Tote *et al.* (2015) evaluated satellite rainfall estimates for droughts and floods monitoring in Mozambique. Three satellite products Tropical Applications of Meteorology using Satellite (TAMSAT), Rainfall Estimates by FEWS (RFE) and (Climate Hazards Group InfraRed Precipitation with Station data (CHIRPS) were compared. Overall the satellite products overestimated low rainfall and underestimated high rainfall amounts. The product showed better results during the wet season. CHIRPS showed better results during the cyclone season, while RFE was better than the other two during a lower decadal rainfall. The paper concluded that a product blending infrared and passive microwave imagery performs better than products using infrared only.

Mountainous areas often have complex precipitation pattern and are often associated with heavy precipitation events. Mie *et al.* (2014) investigated the performance of four widely used satellite products, Tropical Rainfall Measuring Mission (TRMM), Multisatellite Precipitation Analysis (TMPA), CPC MORPHing technique (CMORPH) and Precipitation Estimation from Remote Sensing Information using Artificial Neural Network (PERSIANN). The study concluded that none of these products can be considered ideal for detecting and quantifying heavy rainfall. All the products overestimated low precipitation and underestimated high precipitation.

In a study of mapping of flash flood potential areas in the Western Cape using remote sensing and in-situ data, Bangira (2013) compared the MPE, CMORPH, TRMM 3B42 with gauge data. The results indicated that both the MPE and CMORPH underestimated by about 70% and 40% in Berg and Breede catchments respectively, whereas the TRMM 3B42 overestimated by 10% in both catchments. In the areas with high elevation that receive high rainfall due to orographic effects, the products underestimated. TRMM 3B42 estimates were close to the ground measurement than the two (MPE and CMORPH). The study suggested that this was due to the fact that TRMM 3B42 had been bias corrected using the gauge networks over the study catchments.

Jovanovic *et al.* (2013) compared the EUMETSAT Multi-sensor Precipitation estimates to ground measurements taken in two climatic regions of South Africa. The MPE heavily underestimated precipitation by 1029 mm/year in Kogelberg. The study suggests that this is due to frontal rainfall. The MPE also underestimated as 260 mm/year as against 402 mm/year and 255 mm/year as against 390 mm/year in Sandspruit and Sandriver respectively along the coast. The study concluded that this was due to frontal rain because the product was based on top of clouds properties which are often not consistent with the amounts of precipitation in frontal systems. However, the MPE showed better estimation in the region that receives rainfall during summer seasons for instance the MPE estimated 570 mm as against observed 772 mm/year for Pretoria.

2.4.5 Area-specific calibration of remotely-sensed rainfall estimates

Evaluation gives an understanding of the accuracy of remotely-sensed rainfall products and can be used to calibrate the product for a specific area. For example, Cheema and Bastiaassen (2012) calibrated the TRMM estimates for the Indus Basin. The study addressed two questions, namely; (i) what is deviation between rainfall estimate and rain gauge measurement at differential temporal and spatial scales? (ii) how can the geographical influence on the satellite-based rainfall be described and can it be used to correct the TRMM data?. Using regression and geographic differential analysis managed to calibrate the TRMM reducing the deviation from 10.9% to 6.1% at annual level. For monthly interval the deviation decreased from 34.9% to 15.4% at 625 km^2 pre-calibration and 3125 km^2 post-calibration. The study recommended that the addition of rain gauges to the calibration can help yield even better results.

Almazroui (2010) calibrated the TRMM rainfall climatology over Saudi Arabia during 1998 to 2009. The calibration was done using 29 rain gauge data across the country. The comparison of daily estimated rainfall trends was very similar to rain gauge data. The TRMM closely follow the annual cycle on monthly scale with correlation coefficient of about 0.90. The study also made use of false alarm ratio (FAR), probability of detection (POD) and threat score (TS) to evaluate the TRMM score. It found that false alarm ratio varied across the country but was at it low at high altitude (630 m.a.s.l) and high at low altitude (18 m.a.s.l). The POD was fairly good for all high and low altitude stations. The values for the TS were between 0.07 and 0.44, which are small for low altitude coastal station. The country's average annual rainfall observed from rain gauges was 82.29 mm/year where the TRMM measured 89.42 mm/year. Thus the study suggested that TRMM rainfall be multiplied by 0.93 plus 0.04. After the calibration the error was reduced to almost 0 when compared to rain gauge data. The study concluded that the TRMM can be used in various water-related applications.

2.4.6. Review of methods used in evaluation of satellite rainfall

Various studies have experienced a need for evaluation of remotely-sensed precipitation estimation, but different methods have been used to achieve this task. In comparing remotely-sensed estimates with rain gauges data, Ochieng (2009) used correlation analysis to evaluate the accuracy of RFE. The analysis was done at dekadal (10 days), monthly, seasonal time scale. The spatial scale accuracy was based on spatial interpolation across the basin and between zones. Jovanovic *et al.* (2013**)** in comparing the MPE and rain gauges data used the difference of rainfall between the two data sets. Yearly totals of 2010 were used to produce a map of 2010 MPE estimates. Therefore, the study used visual and basics statistic to compare MPE estimates and ground measurements. Hughes (2006) compared satellite rainfall estimates with rain gauge data using correlation and regression. The comparison was generally based on visual comparison of monthly rainfalls; the study also used correlation and regression slope line between the time series. In comparison of the precipitation estimation products of HSAF, Kenyereri (2003) used correlation and a software written for Hungarian Advanced Weather workstation (HAWK) to qualify other comparison such as Possibility of Detection (POD), FAR (False alarm Ratio), Critical Success Index (CSI) and Symmetrical Extremal Depending Index (SEDI). Bangira (2013) used 90 rain gauges for the year 2008 to 2012. Inverse distance weight index (IDW) was used to show a spatial

distribution of rainfall which was compared to remotely-sensed estimate. The study also used a set of statistical error indices such as Root Mean Square Error (RMSE), Mean absolute error (MAE) and Bias also referred to as mean error.

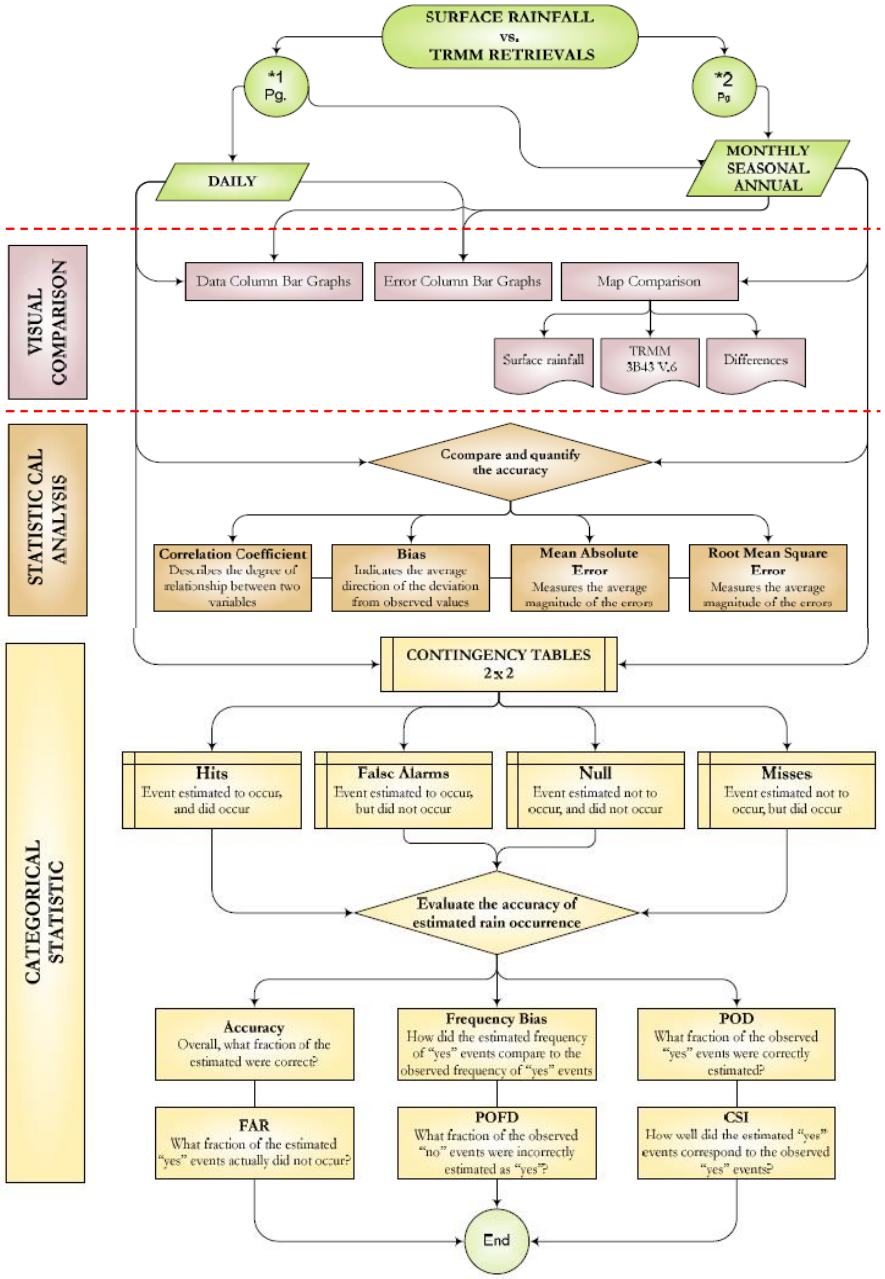

Figure 2.1: Possible analysis adopted from Gomez (2007)

In general, correlation analyses are mostly used to evaluate accuracy as shown above, however this is often used with another method or statistics. The temporal scale of analysis tends to vary depending on what the study is focusing and perhaps the amount of data available for the study. Figure 2.1 shows all the analyses that were used in the studies covered above. The figure shows that the analysis method can be divided in three; visual comparison, statistical analysis and categorical statistics. The limitation of visual analyses is that it depends so much on human interpretation. Visual analyses should not substitute statistical analyses but are very useful as they improve interpretation. Categorical statistics are useful however they do not measure or take into account the magnitude of the error, in this case the amount of rainfall, they only consider the events. Therefore they will be used for the third objective of the study which is to determine the ability of the MPE to distinguish between non-rainy and rainy day.

Various studies have experienced a need for evaluation of remotely-sensed precipitation estimation at different places and different time scale (hourly to yearly) using different kinds of analysis. The MPE which is one the advanced product has not further evaluated in the Western Cape region. The study done by Jovanovic *et al.* (2013) only compared the yearly totals of the MPE and ground measurements, hence this study will do detail evaluation of the MPE at daily and monthly totals, this study will also do event-based analysis. Furthermore, this study will also compare MPE with other products such as TAMSAT and CHIRPS.

Chapter 3: Regional Setting and Research Site Descriptions

3.1 Introduction

The study area is the Western Cape Province which is located on the southern tip of Africa. The chapter presents a description of the location, climate, topography, geology, and other features of the study area. The chapter also briefly provides a review of literature on the characteristics and factors affecting precipitation in South Africa and the Western Cape. Secondly the two catchments (Jonkershoek and Heuningnes) that the study focuses are described.

3.2 Regional setting: Western Cape

3.2.1 Location

The Western Cape Province is located on the southern tip of Africa (Figure 3.1). The province has an area of 129 462 km^2 (Maree and Govender, 2013), which makes it the fourth largest province in the country. The province is known for its tourist attraction such as Table Mountain, Robben Island and Cape Point. The main land uses are agriculture, urban area, wetlands and natural area (Maree and Govender, 2013). The Western Cape province has high variation in the topographic and climatic conditions due to its location in reference to the fold belt and the ocean.

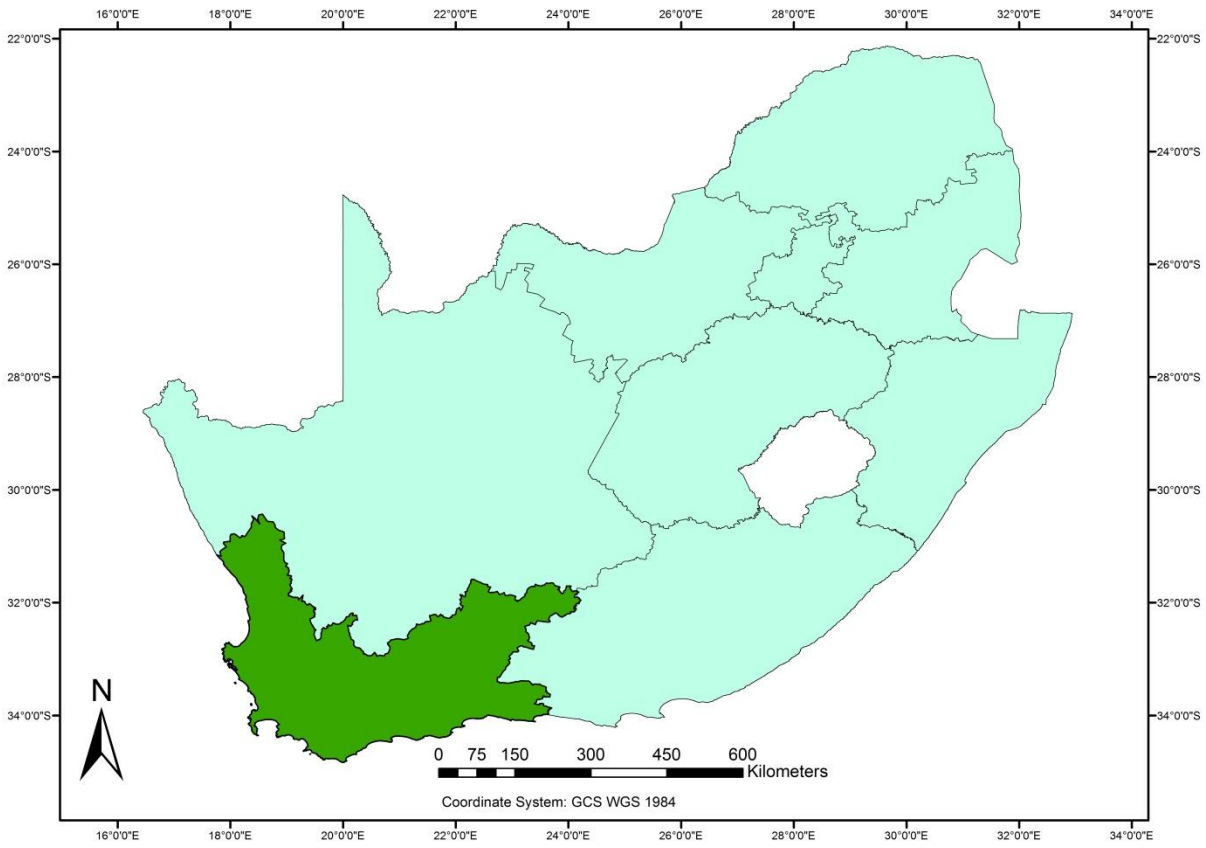

Figure 3.1: Location map of the Western Cape study area. The dark green indicates the study area, in reference to South Africa.

3.2.2 Climate of the Western Cape

The Western Cape has a Mediterranean climate with warm, dry summer, and cold, wet winter. According to Migdley (2005), this is due to the position of the subcontinent relative to low pressure systems between 40° to 50° south. These systems bring rainfall in winter by means of cold fronts and dry conditions are due to variation in westerly wave and the position of high pressure cells. Mountain ranges act as barriers, hence creating a dry interior and high coastal rainfall through orographic effects. The influence of coastal low pressure systems results in hot, dry wind from the interior which may cause wet conditions in late winter and spring. Frontal systems cause some rainfall in spring and autumn. In general the Western Cape receives an average of 600 mm per year of rainfall. However, there are areas that have high rainfall in the province such as the Jonkershoek catchment receiving an average of 1400 mm/year. The drier part of the province is the west coast which receives an average as low as 100 mm/year (Figure 3.2). The province has average temperature of 17°C, Sutherland being the coldest place with an annual average of 11°C (SAWS, 2014).

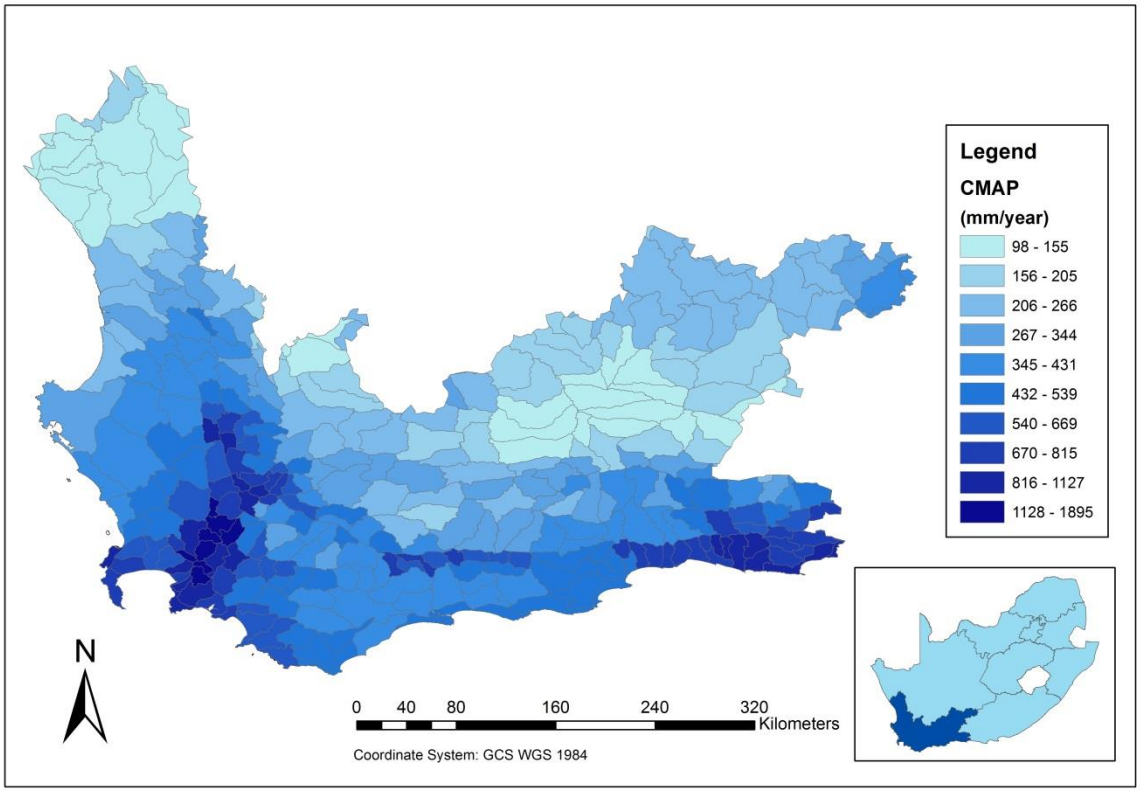

Figure 3.2: The catchment mean annual precipitation variation across the Western Cape. Data source: WRC-WR2012 (2012).

Mesoscale factors that influence rainfall over South Africa

South African weather including wind and rainfall are determined by three factors: oceans, latitude and altitude. The ocean currents have major influence on the coastal areas. The west coast is influenced by the cold Benguala current which causes rising of cold moisture above the ocean resulting in fog and very little rain on the west coast. The east coast on the other hand, is influenced by warm Agulhas current, also called the Mozambique current which causes the air to be warmer, humid and unstable, hence increases rainfall. The ocean moderates weather along the coast by reducing temperature increase in summer and increasing temperatures in winter (Sadler, 2010). South Africa is situated between 22° S and 33° S therefore the climate is dominated by the belt of subtropical high (Kalahari High, South Atlantic high, South Indian High). This belt causes descending air which results in clear skies and sunshine over the country. The latitudinal position is associated with mid-latitude cyclones which causes winter rainfall over South Western Cape. Rainfall and winds are also influenced by altitude as most parts of the country are situated in a plateau.

Seasonality of rainfall in southern Africa

Rainfall is highly seasonal over most part of southern Africa. More than 80 percent of annual rainfall in the region occurs in summer, between October and March, except in the southern cape coast which receives most of rainfall during winter. Summer rainfall decreases from the northern part of region towards the southern Cape Coast (Tyson, 2000). However, in most part of the Western Cape about 85% of the rain falls in six months from April to September (Figure 3.3).

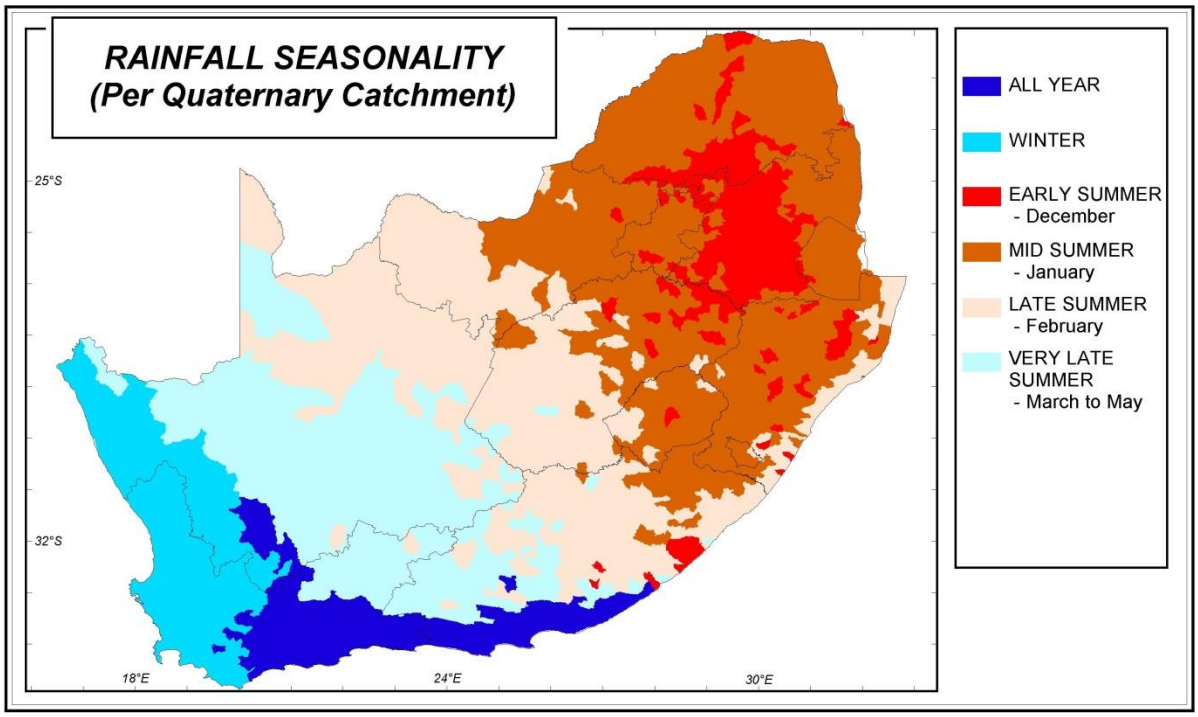

Figure 3.3: Rainfall seasonality over South Africa. Source: Schulze (1997).

3.2.3 Topography

The province has a high variety of topography, however most of the area falls within the cape fold belt with mountains from 1000 m to 2000 m.as.l (PSDF, 2005). The coastal areas have steep cliffs and sandy beaches. The Karoo which is near the interior has flat plain topography. The landscape varies from semi-desert in the west and north to forest in the southern coast of the province (Figure 3.4). There are 4 major rivers that flow in the province: Berg and Olifants which drain into the Atlantic ocean, Breede and Gouritz which drain into the Indian ocean.

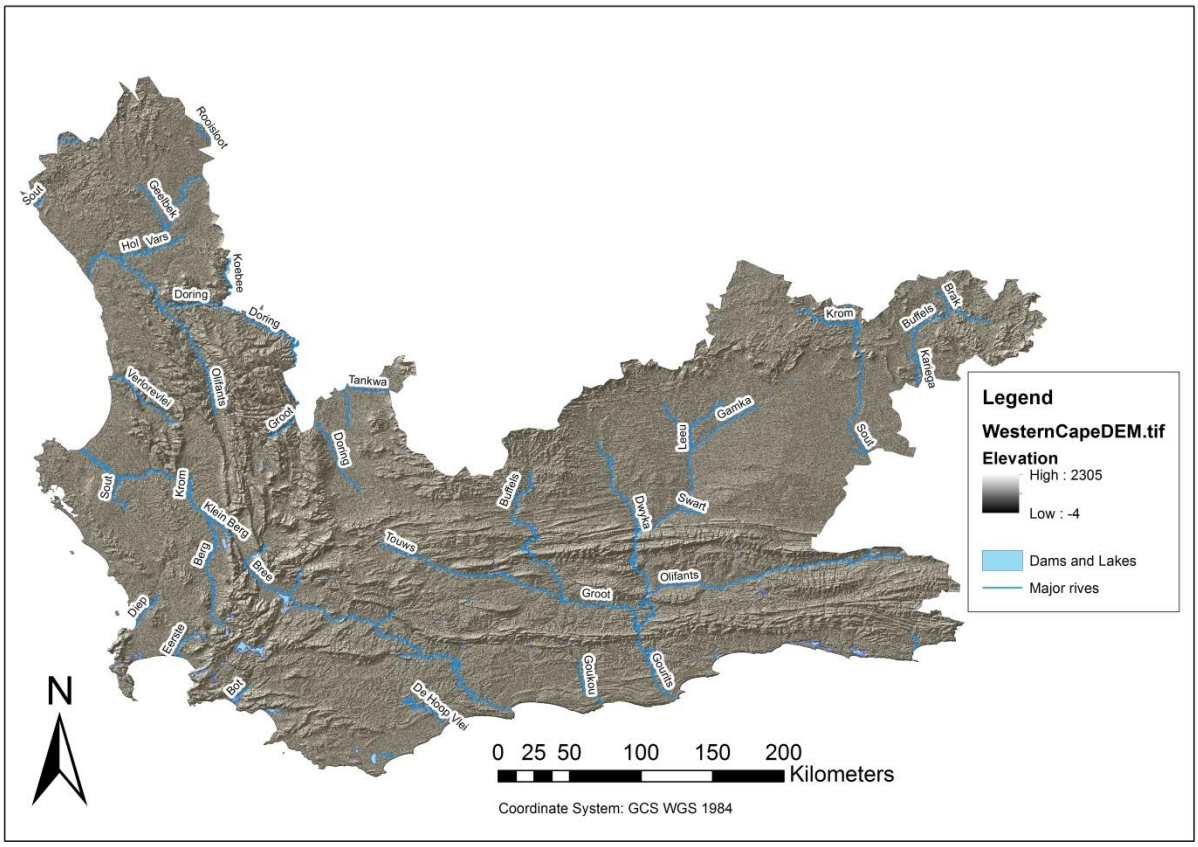

Figure 3.4: Spatial variation of elevation throughout the Western Cape with major rivers, dams and lakes. Data source: ASTER-NASA (2017)

3.2.4 Geology

The Western Cape has complex geology, however most the part of province has sedimentary rocks such as sandstone, limestone and shale. The major geological associations are Adeladie sub group which covers the entire central Karoo. The Eacea group located in the south central karoo. The Cape group often referred to as Table Mountain group is found across the whole province (PSDF, 2005). The Malmesbury group found from Cape Town to Piketberg. The Vanhynsdorp group located in Nuweru and Vanhynsdorp. The Namaqua metamorphic complex found in the Namaqua area. The eron formation which is mainly found in Oudsroom. The coastal deposits cover the coastal areas and consist of sand, dune and beach sand, etc.

3.3 Research sites

3.3.1 The Heuningnes catchment

The Heuningnes catchment is located in the Cape Agulhas area which is the southernmost point of South Africa. This is also geographic southern tip of Africa and the dividing point between the Atlantic and Indian oceans. Bredasdorp, Napier and Elim are some of the major towns in the area. The catchment covers an area of 1401 km^2 and it covers five quaternary catchments; G50B, G50C, G50D, G50E and G50F (Figure 3.5). The catchment has Agulhas plain falls within the Cape Floristic Region (CFR) and has low gradient with altitude ranging from 5 to approximately 400 m above sea level in the mountainous side. The catchment has two major rivers; Kars and Nuwejaars river. In the lower reaches of Nuwejaars river, the topography is very flat and low lying and with several pans and vleis which drains to this river. The vleis arid Voevlei and Soutpan, the Nuwejaars river flows into Zoetendalsvlei which is approximately 5 km long and 3 km wide at the middle.

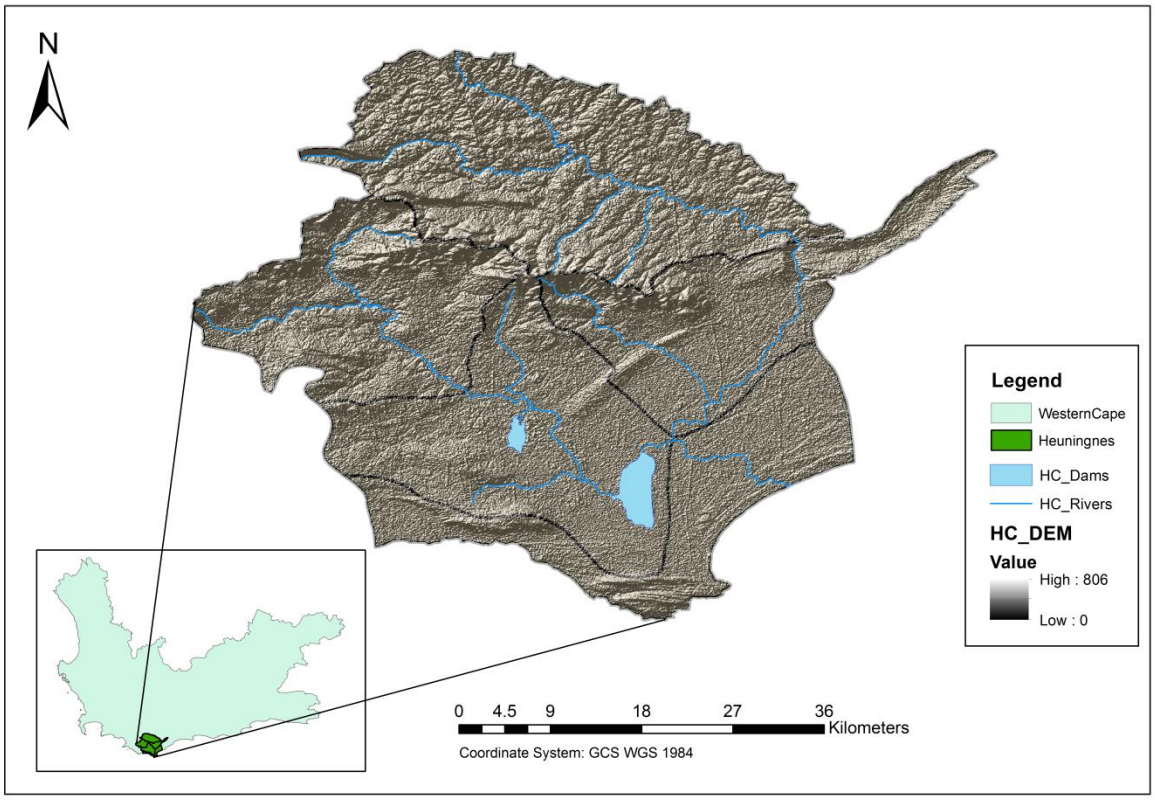

Figure 3.5: The location of Heuningnes study catchment in reference to the province indicated at bottom left; the image also shows rivers and the topography of the study area.

According to Bickerton *et al.* (1984) rainfall is mainly cyclonic and with some orographic influence on the upper reach of the catchment. Winds that bring rain are mainly from the west or south west. As a result rainfall is higher on the south side of the mountains than north facing slope. In general the catchment has rainfall of about 400 mm to 600 mm/year mostly occurring in winter. The mean temperature is approximately 17°C, January is the hottest month whereas July is the coldest month.

The permanent rain gauge networks are set up by ARC and SAWS, the rest of the network was set up for research purposes, therefore the networks are based on research objectives. For instance the Breede-Gouritz Catchment Management Agency which is responsible for the water resource management for the catchment collaborated with the University of the Western Cape in improving information base for water resource management. Therefore, the network is designed to capture rainfall variation as much as possible. Figure 3.6 presents the location of the rain gauges in the catchment.

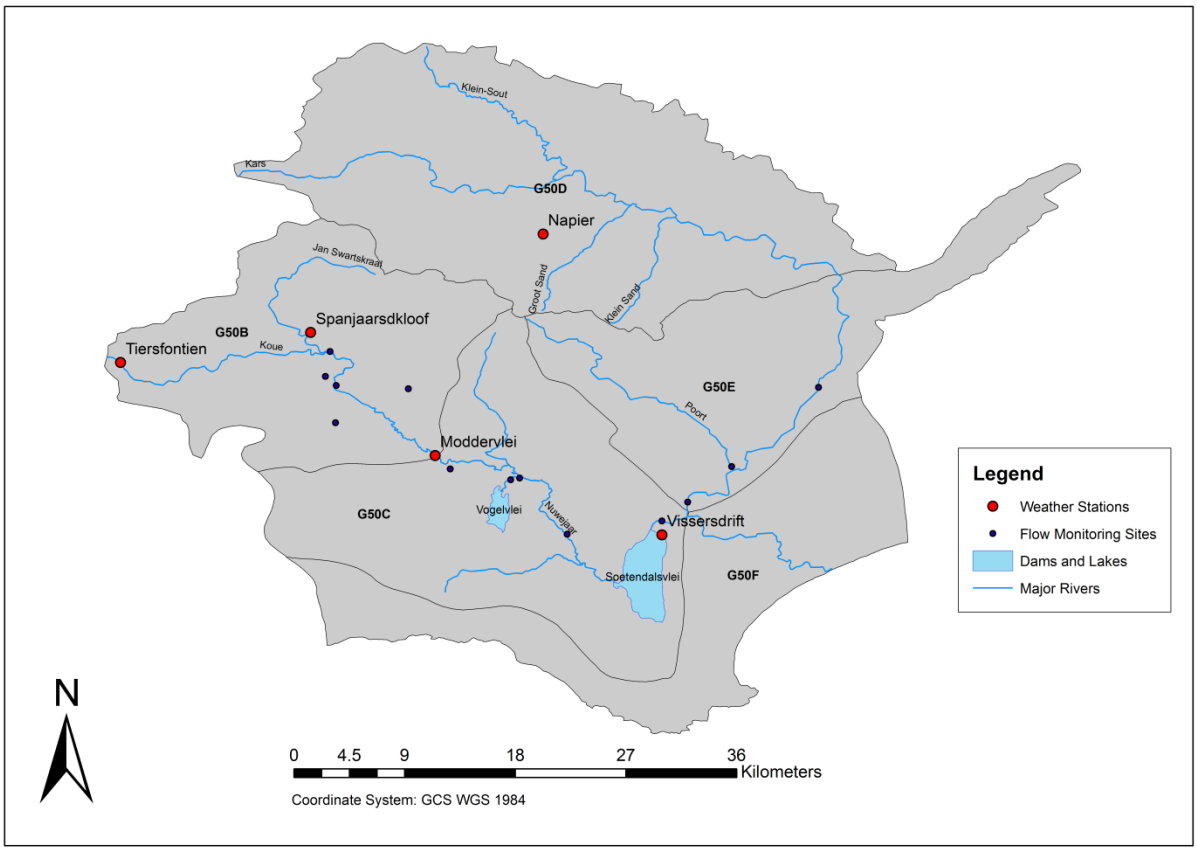

Figure 3.6: The location of the monitoring sites in Heuningnes catchment.

3.3.2 The Jonkershoek catchment

The Jonkershoek catchment (G22F) is located 10 km south-east of Stellenbosch and 60 km east of Cape Town. The catchment is approximately 65.68 km^2, with the valley that gives rise to the Eerste River which originates from the Dwarsberg Mountains and flow through Stellenbosch to False Bay. The valley is enclosed on three sides by mountains which range from 792 to 1525 m (Moses, 2008). The close side of the valley is Dwarsberg Mountain which is south east of the valley, with an open side to the north west, so the valley is orientated south east to the north west in downstream direction (Figure 3.7). The Jonkershoek area has about eight sub catchments. In between the sub-catchments is the Jonkershoek valley. The top of the mountains makes up the upper boundaries of the catchment. The catchment has very irregular and steep slopes in the upper boundaries of the mountains.

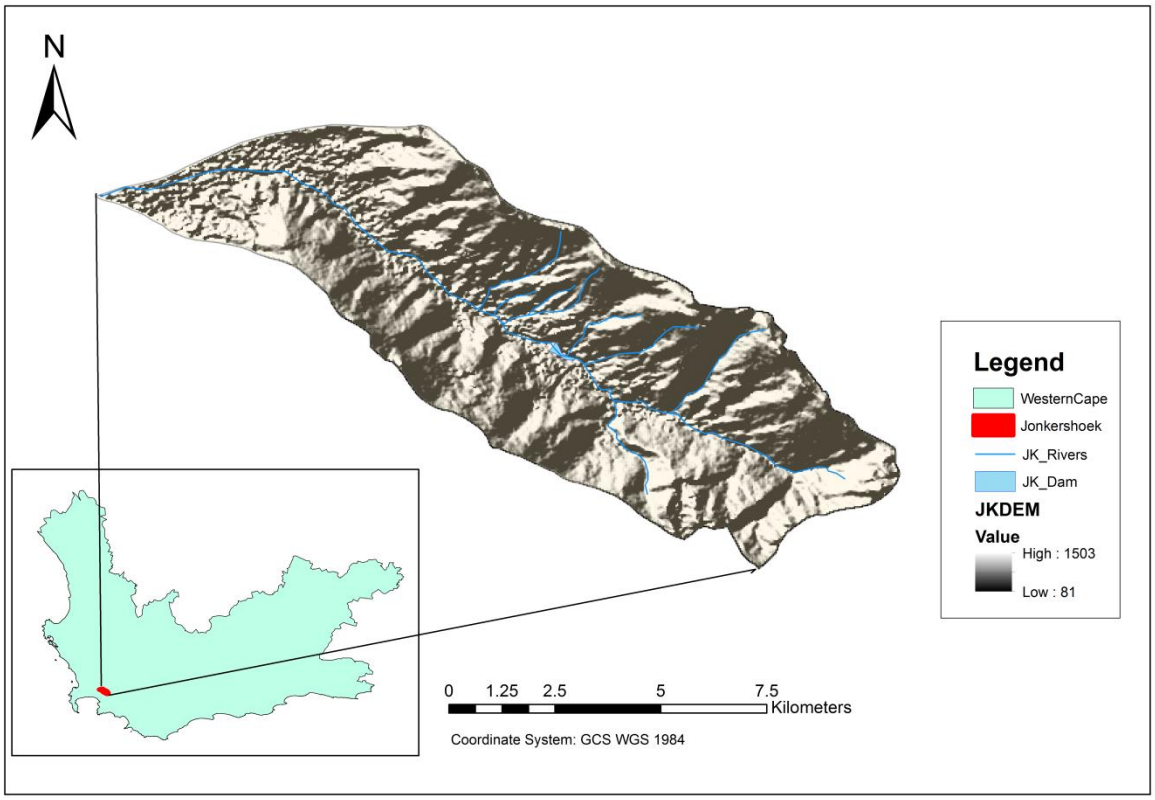

Figure 3.7: The location of Jonkershoek (G22F) study catchment in reference to the province indicated at bottom left, the image also shows rivers and the topography of the study area.

Figure 3.8: View down the Jonkershoek valley, looking at the open side (North West). (Western Cape Nature Conservation, 2002).

Jonkershoek as part of the Western Cape has a Mediterranean climate, with warm, dry summer, and cold, wet winter. Whenever rainfall occurs in summer it is as result of high pressure zone causing wind to blow up in the centre of the valley over the Dwarsberg mountain to the south east (Moses, 2008). Wicht (1969) stated that rainfall in Jonkershoek is caused by moisture carrying winds blowing from north west, this air is forced upwards at the end of the valley in south east causing the occurrence and enhancement of the rainfall over the north east and the south east. Air is forced upward over a distance of 8 km to about 1066 m above sea level. The highest peak of catchment holds a record of having the highest recorded annual rainfall in South Africa (3874 mm/year). In general, Jonkershoek has average of annual rainfall of 1390 mm/year (Moses, 2008). The hot summer is associated with south easterly winds from the warmer Indian Ocean, whereas winter is associated with strong north- westerly wind (Coetzee, 2008). The annual mean temperature is 16.1°C, with the yearly maximum of 38.1°C and a minimum of 0.7°C (Van Wyk, 1987).

The permanent network in the catchment is set up by ARC and SAWS, the rest of the rain gauge network is set up for research purposes. According to Moses (2008) the Jonkershoek catchment was established in 1935 as research catchment, with a focus of investigating the influence of afforestation on runoff. Concerns were raised from around the country about a possible decline in stream water downstream possibly due afforestation. Since, then Jonkershoek has been centre of water resource research. One of the recent additions to monitoring system are the fog monitoring stations, which were established in different elevations in one of Jonkershoek sub catchments. Currently the Jonkershoek have 19 rain monitoring station maintained by SAEON therefore the network are based on research objective. In general, the network is designed to capture rainfall variation as much as possible.

Chapter 4: Methodology

4.1 Introduction

This chapter presents the research design, including the methods used to collect, process and analyse the data in order to achieve the objectives of the study which is to evaluate the accuracy of remotely-sensed precipitation estimates with ground observation. The chapter concludes by outlining the limitations of the study.

4.2 Research design

The remotely-sensed precipitation estimates were extracted or downloaded and rainfall data from rain gauges was obtained for the study sites. The first objective of the study which is to assess the spatial variation of the accuracy of the remotely-sensed precipitation estimated required a regional analysis (Western Cape). Analyses to achieve the second and third objective of the study were done at two contrasting catchments (Heuningnes and Jonkershoek). The time period for the analysis was one-year period from March 2015 to February 2016. The study uses a comparative analysis approach. The comparisons were done at daily, monthly, seasonal and yearly timescale. The analyses were divided into three sections; graphical/visual, statistical comparison and categorical statistics. The visual comparisons were based on the differences between remotely-sensed estimates and the actual rainfall amount observed from the rain gauges. The statistical comparison was based on correlation coefficient, mean error and t-test between the observed and the estimated rainfall. The categorical statistics are events based analyses that were used to determine the ability of the remotely-sensed precipitation estimating products to distinguish between rainy and non-rainy days. Figure 4.1 provides a flow diagram of the methodology.

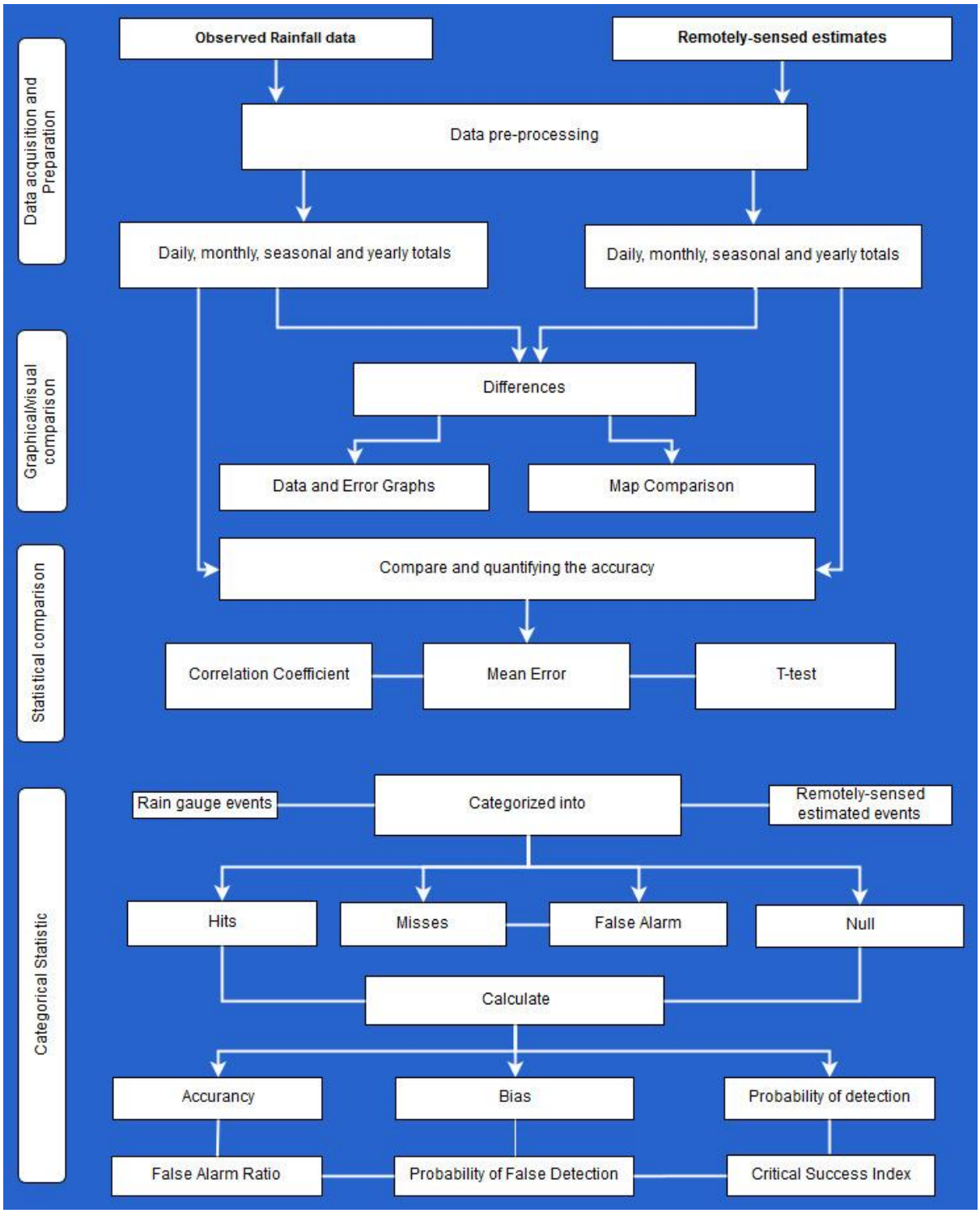

Figure 4.1: A flow diagram illustrating the methodology from data acquisition to data analysis.

4.3 Selection of the study and sampling sites

The two catchments that were used as study areas/sites were selected on the basis that they vary in topography and climatic condition in terms of the amount of rainfall they receive, as indicated in the previous chapter. The literature suggested that topography and climate conditions may have an effect on the performance of the remotely-sensed precipitation estimates (Mie *et al*., 2013). The Jonkershoek receives an annual average rainfall of 1390 mm/year (Moses, 2008), whereas the Heuningnes catchment receives 400-600 mm/year (Bickerton *et al.*, 1984). The catchments have a well coverage of the rain gauges. The Jonkershoek has 21 rain gauges, and the Heuningnes catchment has seven rain gauges stationed at different locations and elevations.

The time period for the analysis was one-year period from March 2015 to February 2016 which was decided based on i) common time for good data existence in the two catchments ii) had to have all southern hemisphere seasons (DJF, MAM, JJA, SON) in order for seasonal analysis to be done. Hence stations used in this study had to meet the following criteria; i) the station had to have daily rainfall data from March 2015 to February 2016, ii) the rain gauge station had to have good quality data (i.e., stations with data missing for more than 15% of the time were excluded). Only three and 15 stations met the criteria in Heuningnes and Jonkershoek catchments respectively (Figure 4.2). The second selection was done in each catchment to select a rainfall station that will represent the catchment. In order to select the most representative rain station, cross correlation coefficient (CC) was done and the station with the highest correlation amongst all station was regarded as the most representative. Jung *et al.* (2013) state that averaged correlation coefficient represents similarities in the properties/characteristics whereas the mean-related are more about the amount rainfall. Most of these study assessments are based on rainfall properties than the actual amount received hence, average CC was used.

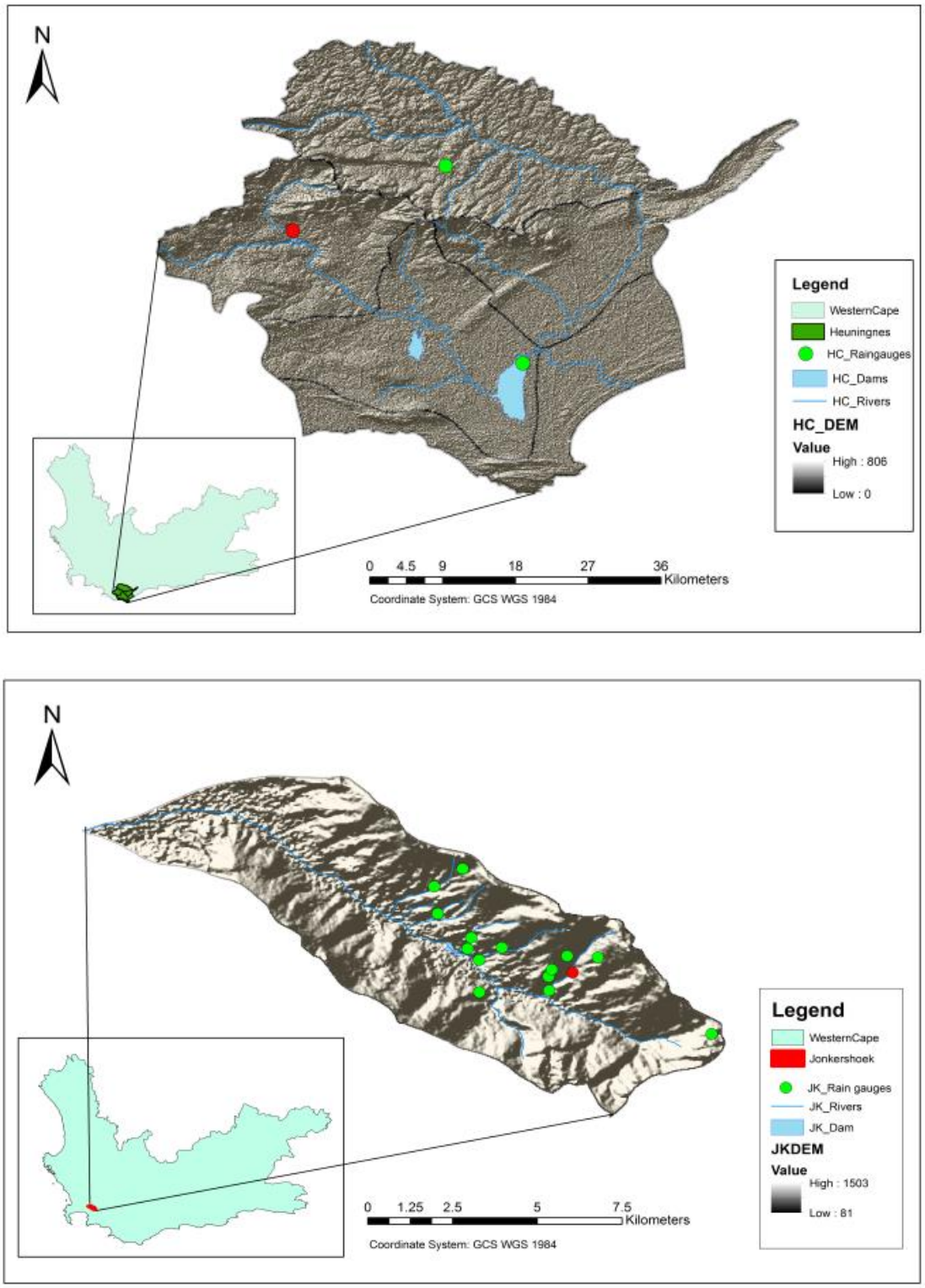

Figure 4.2: The rain gauges that were used are indicated by the green dots in the Heuningnes (top) and in the Jonkershoek (bottom), whereas the red dots indicate the rain station that were selected to represent the catchment.

4.4 Selection of remotely-sensed precipitation products

Remotely-sensed precipitation products that were used in this study were selected based on the following criteria; i) the products had to have spatial extent that covers southern Africa, ii) the products data should be freely and easily accessible, iii) the products had to vary in terms of the main principle source of data, spatial resolution and minimum time scale. This variation in the products allows for representation of the different types of products i.e blended techniques (combination of two instruments or one instrument and gauge data) and the single instrument based technique. The MPE, TAMSAT and CHIPRS met these conditions and therefore were selected for this study. The description of these products is provided in the next section.

4.5 Data collection

4.5.1 Rain gauge data

The observed rainfall data from rain gauges was obtained from the rain gauges that are placed in the study catchments (Jonkershoek and Heuningnes). Data was provided or acquired by the University of the Western Cape (UWC) for the Heuningnes, South African Environmental Observations Network (SAEON) and South African Weather Service (SAWS) provided data for the Jonkershoek. For stations in the Western Cape Province, data for 30 stations was mostly downloaded from the NOAA Global summary of the day website. The Global Summary of Data (GSoD) from National Oceanic and Atmospheric Administration (NOAA) provides freely accessible data around the world. All stations that met the requirements were used. Few stations outside the province were also selected so that the interpolated rainfall raster could cover the whole Province and gives good estimation for the outer boundaries of the province, all the rain gauge stations that were used are provided in appendix 4.1.

For most of the data used in this study tipping bucket rain gauges were used (Figure 4.3). This type of rain gauges uses two small buckets on fulcrum like seesaw. The small buckets are designed to hold an exact amount of rainfall, usually 2 mm. This system is located underneath a rain collector which funnels rainfall in the small buckets (Figure 4.3). As rainfall is collected the small bucket become unbalanced and tips down. The tipping activates an electronic signal which transmits the counts of tips to the data logger recording the counts as 2 mm of rainfall. The data logger stores the data, which is later downloaded into a

computer. It is important to note this difference as the data may come in different formats (hourly, daily or monthly). The data has to be in one format before analysis can take place.

Figure 4.3: Typical tipping rain gauge that was used in this study, when it is closed and logging (left), open rain gauge (right).

4.5.2 Remotely-sensed precipitation products

Description of Remotely-sensed precipitation estimating products

MPE

The Multi Sensor Precipitation Estimator was developed by EUMETSAT and been functional from 2002 to present. The method assumes that colder clouds are more likely to produce precipitation than warmer clouds. The method also assumes that the top of cloud temperature and the rain rate have a non-linear relationship and depends on the current weather situation (Heinemann, 2002; Dhib *et al*., 2017). The MPE uses look up tables (LUT) that were derived from Special Sensor Microwave/ image (SSM/I) on the US Defence Meteorological Satellite Program (DMSP) and IR measurement from the Meteosat first generation satellites. The DNSP was launched in 1962 but only made available to the scientific users in 1972. The METEOSAT was first launched in 1977, the mission end in 2017. However, EUMETSAT have since replaced it with the Meteosat Second Generation (MSG) which is currently in orbit. The LUT are derived based on the assumption that colder clouds produce more precipitation that warmer clouds. The LUT describes the rain rate as function of the METEOSAT IR brightness temperature (Heinemann, 2002). This means METEOSAT image applied LUT to derive rain rate in full spatial and temporal resolution.

MPE co registers data for the look up tables for derivation are accumulated in spatial windows for a specified time. The MPE uses 6-12 hours temporal windows and a spatial window of 5° latitude and 5° longitude. The raw data is provided at EUMETSAT through online data ordering system (https://www.eumetsat.int/website/home/Data/DataDelivery/EUMETSATDataCentre/index.html). However the Geo-Information Science Earth Observation (ITC) of the University of Twente provided daily estimates compiled from 15 min EUMETSAT raw data (ftp://ftp.itc.nl/pub/mpe), this study used both platforms. The EUMETSAT 15 min estimates were used when the ITC had missing data, this is explained in details in Appendix 4.2.

TAMSAT

Tropical Applications of Meteorology using SATellite and ground observation was developed by the University of Reading, United Kingdom. TAMSAT have been estimating rainfall over African since 1983 to present (Maidment *et al*., 2014). Satellite imagery is calibrated against ground observations to estimate rainfall. TAMSAT has dekadal time interval and 4 km resolution in Africa. TAMSAT is an example of cloud indexing technique using Meteosat thermal infrared (TIR) to generate cold cloud duration (CCD) fields (Maidment *et al*., 2014; Tarnavsky *et al*., 2014). The TIR data are obtained from Meteosat First Generation and Meteosat Second Generation. TAMSAT define CCD as length of time over a 10-day period when the cloud top temperature is colder than a predetermined threshold temperature. CCD is used as a proxy for rainfall. The 10 day CCD total is then linear related to rainfall.

$$R = \begin{cases} a_0 + a_1 * CCD & \text{CCD>0,} \\ 0 & \text{CCD=0} \end{cases} \qquad (4.1)$$

Where R is rain, a_0 and a_1 are zonal regression calibration coefficients. These thresholds for temperature and coefficient are area specific, these areas are known as calibration zones. The calibration is done on a monthly basis using observed data from rain gauges. TAMSAT assumes that zero CCD corresponds to zero rainfall (Maidment *et al*., 2014; Tarnavsky *et al*., 2014). Data is available at: http://tamsat.org.uk/view/estimates/index.cgi/rainfall/

CHIRPS

Climate Hazards Group Infrared Precipitation with Station data (CHIRPS) was developed by the USGS. CHIRPS incorporates satellite imagery with station data to create time series for

trend analysis and drought monitoring. The CHIRPS is a daily, pentadal and monthly product with 0.05° resolution globally (Funk *et al.*, 2015) and been providing rainfall estimates since 1981 to present. CHIRPS uses a Cold Cloud Duration from thermal infrared with a similar approach to the one of the TAMSAT. The CCD-derived estimated is then calibrated by the Tropical Rainfall Measuring Mission Multi-satellite Precipitation Analysis version 7 (TMPA 3B42 v7) on TRMM which was launched in 1977 and ended in April 2017 replaced by thee global precipitation measurement (GPM). After this calibration, the estimate is referred to as CHIRP. The estimate is then blended with interpolated station data, only after this blend, the estimate can be referred to as CHIRPS (Figure 4.4). The station data is blended through two phase processes, which yields a preliminary rainfall product with 2-day latency, sparse World Meteorological Organization's Global Telecommunication System (GTS) gauge data are blended with CCD-derived rainfall estimates at every pentad. In the second phase, which yields a final product with an average latency of about 3 weeks, the best available monthly (and pentadal) station data are combined with monthly (and pentadal) high resolution CCD-based rainfall estimates to produce fields that are similar to gridded monthly station (Becker *et al*., 2013; Funk *et al.*, 2015)

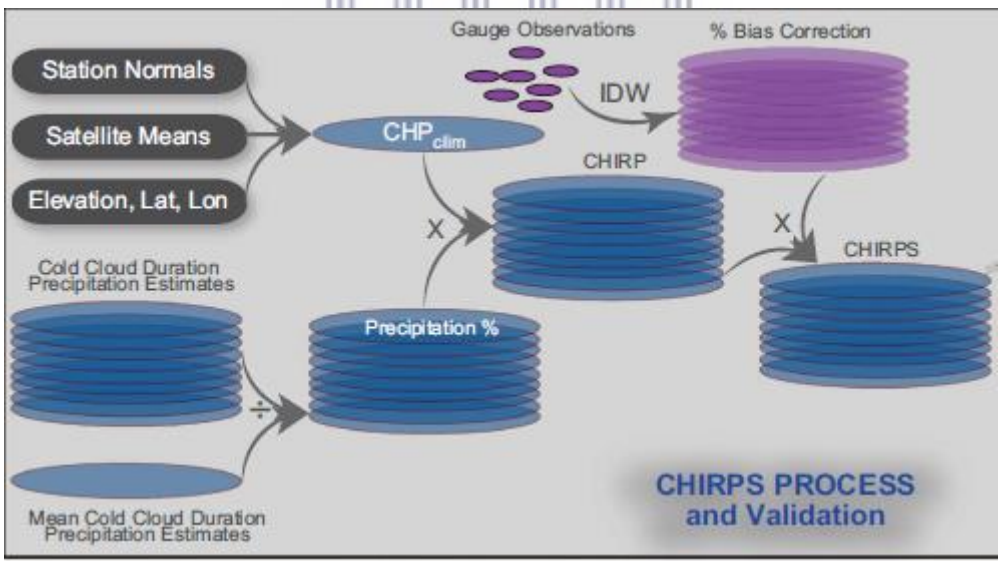

Figure 4.4: The processes of producing CHIRPS. Source: Funk *et al.*,(2015)

The TMPA 3B42 calibrated estimates are referred to as CHIRP, However the TMPA 3B42 does to some extent contain rain gauge data. Data is available at: ftp://ftp.chg.ucsb.edu/pub/org/chg/products/CHIRPS-2.0/

4.6 Data analysis

To compare remotely-sensed data and observational data from rain gauges, graphical comparison, statistical and categorical analyses were performed.

4.6.1 Assessment of the representation of the spatial variation of rainfall in the Western Cape

In order to assess the spatial variation representation by the remotely-sensed precipitation estimates, a map of the observed rainfall variation across the province had to be produced. Therefore, point rainfall gauge data had to be interpolated. Interpolation is basically the estimation of surface (rainfall) values at un-sampled points based on known surface values of the surrounding points (Childs, 2004). For this study, Inverse Distance Weighted (IDW) method was used (Equation 4.2), as it is the most commonly used and the closest to the Thiessen Polygon method which is recommended in hydrology. IDW takes into account the weighted average of the observed regionalized values (Ly *et al*., 2013). According to Garcia *et al.*, (2008) IDW has demonstrated efficiency and reliability in consistent operational usage, even in regions with noted orographic influence on precipitation patterns when compared to other methods of interpolation.

$$Zg = \sum_{i=1}^{ns} \lambda_i Zs_i \;\; ; \; \lambda = \frac{d_{oi}^{-\alpha}}{\sum_i^n d_{oi}^{-\alpha}} \qquad (4.2)$$

Where Z_g is the interpolated value at required points, Z_{Si} is observed value at point *i*, *ns* is the total number of observed points and $\boldsymbol{\lambda}$ is the weight contributing to the interpolation, *d* is the distance to observed point and α is the weighing power.

From Equation (4.2), it is clear that the number of observed points and their position have effect on the outcome of the interpolation. Hence, this study assumes that the points measured are adequate to give the accurate spatial variation of rainfall across the province of the Western Cape. The outcome of the interpolation was compared to the estimated rainfall by CHIRPS and TAMSAT at annual and seasonal level, the MPE had missing data in spring, thus excluded for some of the annual and spring analyses. All the rain gauge stations used for this interpolation are provided in Appendix 1.1.

In order to assess the spatial differences, the raster maps have the same pixel/cell size and at the same position. Therefore, the interpolated rain gauge data raster created from the procedure described above (Equation 4.2) was resampled so that it has the same cell size and

position as the remotely-sensed products before the below analyses were done. The layers were overlaid in ArcGIS and spatial analysis was used to calculate the difference between remotely-sensed and the interpolated gauge data using Equation (4.3).

$$Diff=RSr-OBSr \qquad (4.3)$$

Where *Diff* is the difference between the estimated rainfall by remotely-sensed products and the interpolated (observed) rainfall data. *RSr* is the raster layer of the remotely-sensed estimate and *OBSr* is the raster layer of the interpolated rain gauge data.

A t-test was used to determine whether there is a significant difference spatial variation between the estimated mean and the observed mean of rainfall in the Western Cape at 5% significance level.

$$t = \frac{\bar{x}_1+\bar{x}_2}{S_p\sqrt{\frac{1}{n_1}+\frac{1}{n_2}}}, \quad S_p = \sqrt{\frac{n_1{s_1}^2+n_2{s_2}^2}{n_1+n_2-2}} \qquad (4.4)$$

Where *t* is the t-statistics, $\bar{x}_1$ is the observed rainfall mean, $\bar{x}_2$ is the estimated mean from the remotely-sensed data, *Sp* is the pooled standard deviation, n_1 and n_2 are the number of observation (pixels), S_1 is the standard deviation of the observed and S_2 is the standard deviation of the remotely-sensed product. These were obtained from the raster layers through multivariate analysis in ArcGIS. A t-test assumes that the sets of data are continuous, follow a normal distribution, that mean is a good measure of central tendency and that the two samples are independent (Helshel and Hirsh, 2002).

To assess the spatial relationship between remotely-sensed estimates and the interpolated gauge data, correlation was used. Helshel and Hirsh (2002) state that correlation becomes a test for spatial or temporal variation, when one variable is a measure of time or location. In this case correlation was used as test for spatial variation. The two layers were correlated through multivariate analysis in ArcGIS, the correlation coefficient is computed as follows:

$$Corr_{oe} = \frac{Cov_{oe}}{\delta_o\delta_e}; \quad Cov_{oe} = \frac{\sum_{k=1}^{n}(Z_{ok}-\mu_o)(Z_e-\mu_e)}{N-1} \qquad (4.5)$$

Where *Corr* is the relationship between the two layers (Remotely-sensed estimate and interpolated gauge data), *Cov* is the covariance between the two layer, *δe* is the standard deviation of remotely-sensed estimated layer and *δo* is the standard deviation of the

interpolated layer. *Z* is the value of the cell (rainfall value), μ is the mean of the layer, *n* is the number of cells or pixels and *k* denotes a particular cell.

4.6.2 Assessment of the remotely-sensed estimates at a point

To determine the differences in the magnitude of observed rainfall and estimated rainfall over time, exploratory data analyses were done. This was done by plotting the estimated against observed rainfall. The difference was calculated between estimated amounts and the observed, this was calculated using Equation (4.2); error bars were used to display the differences over time. Where positive values are indication of overestimate, negative values are indication of underestimation and 0 indicates the perfect estimation.

Mean error (*ME*) also called bias measures the average of estimation error; this considers the direction of the errors. The mean error ranges from negative infinity to positive infinity and perfect score is 0. A positive score indicates that the remotely-sensed product is overestimating, while a negative score indicates that the remotely-sensed product is underestimating on average.

$$ME = \frac{1}{n}\sum_{i=1}^{n}(E_i - O_i) \qquad (4.6)$$

To assess the relationship between the estimated and observed, correlation coefficient was done. As stated that correlation coefficient can be a test for spatial or temporal variation, in this case it was used as a test for temporal trend. Correlation ranges from -1 to +1, and 1 is a perfect relationship and 0 is the worse relationship.

$$r = \frac{n(\sum OE) - (\sum O)(\sum E)}{\sqrt{[n\sum O^2 - \sum O)^2 - [n\sum E^2 - (\sum E)^2}} \qquad (4.7)$$

Where *O* is the daily, monthly totals measured by rain gauges, *E* is the daily, monthly total estimated by a particular remote-sensed product and n is number of pairs of scores.

The significance of correlation coefficient was evaluated using the t-test.

$$t = r\sqrt{\frac{N-2}{1-r2}} \quad t_{n-2} \qquad (4.8)$$

Where *r* is correlation coefficient obtained from Equation (4.2), *N* is the number of observations. *N-2* (degrees of freedom) was used to obtain the critical value of the t-distribution.

T-tests were done to determine whether there is a significant difference between estimated and observed mean over time. These were done at daily and monthly interval. The tests were done at 5% significance level using Equation (4.4), however in this case it was done to determine if there is difference in the means over time unlike in the previous case where it was used to determine the differences in space (province).

4.6.3 Assessment of the detection of rainy and non-rainy days

To assess the ability of remotely-sensed precipitation products to distinguish between rainy and non-rainy days, categorical statistics were used. These are statistics that are based on the occurrence of events and include accuracy, Bias, Probability of detection (POD), False alarm ratio (FAR), Probability of false detection (POFD) and Critical Success index (CSI) which are widely used and recommended by WMO (2008) for verification of rainfall estimates model or product. In this study these statistics were used to determine the ability of the remotely-sensed products to distinguish between rainy and non-rainy days. Daily rainfall data from rain gauges and daily estimates were used in the following analysis. In this study a rainy day was described as a day with rainfall equal to 1 mm/day or more which is recommended for this kind of study (Cai *et al*., 2015). These analyses were done on the selected station in the two study catchments. The days were categorised as Hits, Misses, False Alarm and Null where:

Hits are days when rainfall was estimated to occur, did occur

Misses are days when rainfall occurred, but was estimated not to occur

False Alarms are days when rainfall was estimated to occur and did occur

Null are days when rainfall was estimated not to occur and did not occur

Table 4.1: 2X2 Contingency table for categorical statistics modified from Seyyedi (2010) summarising the above explanations.

		Observed	
		YES	NO
Estimated	YES	HITS	FALSE ALARM
	NO	MISSES	Null

The above information was then used to describe the following statistics

Accuracy, also called proportion correct, is the fraction of correctly estimated events by remotely-sensed products: this ranges from 0 to 1 and the perfect score is 1. It can be misleading as it is heavily influenced by the most common category.

$$Accuracy = \frac{Hits+Null}{Total\ number\ of\ days} \qquad (4.9)$$

Bias gives the ratio of the frequency of estimated events to the frequency of observed events. It indicates whether the remotely-sensed products have tendency to underestimate (Bias<1) or overestimate (Bias>1). Thus it gives an indication of whether the remotely-sensed product is wet or dry bias, which is important for the correct interpretation of the other measures, in particular POD and FAR.

$$Bias = \frac{Hits+False\ Alarm}{Hits+Misses} \qquad (4.10)$$

Possibility of detection gives the fraction of observed hits events that were correctly estimated by the remotely-sensed products. It measures the ability to correctly estimate a certain category, this is only sensitive to missed and but not false alarm events. The score ranges from 0 to 1, and 1 is the perfect score. This answers the question of what fraction of the observed events occurred were correctly estimated.

$$POD = \frac{Hits}{Hits+Misses} \qquad (4.11)$$

False Alarm Ratio (FAR) gives the ratio of events that were estimated but were not observed. It ranges from 0 to 1 and the perfect score is 1. According to Lavizzani (2007) POD and FAR should always be used together as good to perfect scores are easily obtained from both even though they are completely opposite. For instance if an algorithm is wet bias, and it always estimates rainfall everywhere, all the time. The POD will be perfect (1), however the FAR will also be close to worst score (0) depending on how many rainy events occurred.

$$FAR = \frac{False\ Alarm}{Hits+False\ Alarm} \qquad (4.12)$$

Possibility of False detection (POFD) also called False alarm rate is the fraction of incorrectly estimated events that did not occur or were not observed. This is sensitive to false alarm but ignores misses. It ranges from 0 to 1 and the perfect score is 0.

$$POFD = \frac{False\ Alarm}{Null+False} \qquad (4.13)$$

Critical success index estimates the relative accuracy; unlike POD, FAR and Accuracy, it takes into account both false alarm and misses events, but it is sensitive to climatological frequency of events. This is not sensitive to null, as the result removes the consideration of correct (simple) non-rainy days which are the most common in the area under investigation.

$$CSI = \frac{Hits}{Hits+Misses+False\ Alarm} \qquad (4.14)$$

Chapter 5: Remotely-sensed estimation of rainfall in the Western Cape

5.1 Introduction

This chapter presents results addressing the first objective which is to evaluate whether remotely-sensed rainfall estimates realistically represent rainfall throughout the Western Cape. The chapter presents the differences between the interpolated gauge data and the remotely-sensed estimates. Thereafter, the effects of elevation, topography and climate on the accuracy of the remotely-sensed estimates are discussed. The chapter concludes by comparison of the seasonal differences in estimated and the interpolated gauge data. One of the remotely-sensed products (MPE) had missing data in September and October, this made it ineligible to be assessed in spring and at the annual level. The nature of the missing data is described in details in Appendix 4.2.

5.2 Comparison at annual level

As stated in the methodology, this study assumes that the interpolated rain gauge data are representative of rainfall in various parts of the Western Cape. Figure 5.1 shows the total annual precipitation from interpolated gauge data and the precipitation totals estimated by TAMSAT and CHIRPS for the year 2015/16. CHIRPS estimates have a close spatial pattern to the interpolated rain gauge data comparison to the TAMSAT (Figure 5.1). Both remotely-sensed products underestimated the total 2015/16 rainfall over most parts of the province. The interpolated gauge data had a maximum of 948.2 mm/year received in the south east of the province and had a mean of 330.9 mm/year for the province. TAMSAT estimated a maximum of 288.0 mm/year in the north east of the province and had a mean of 131.0 mm/year. CHIRPS estimated a maximum of 824.3 mm/year in the South West of the province and had a mean of 310.0 mm/year which is close to the mean of the interpolated rain gauge data.

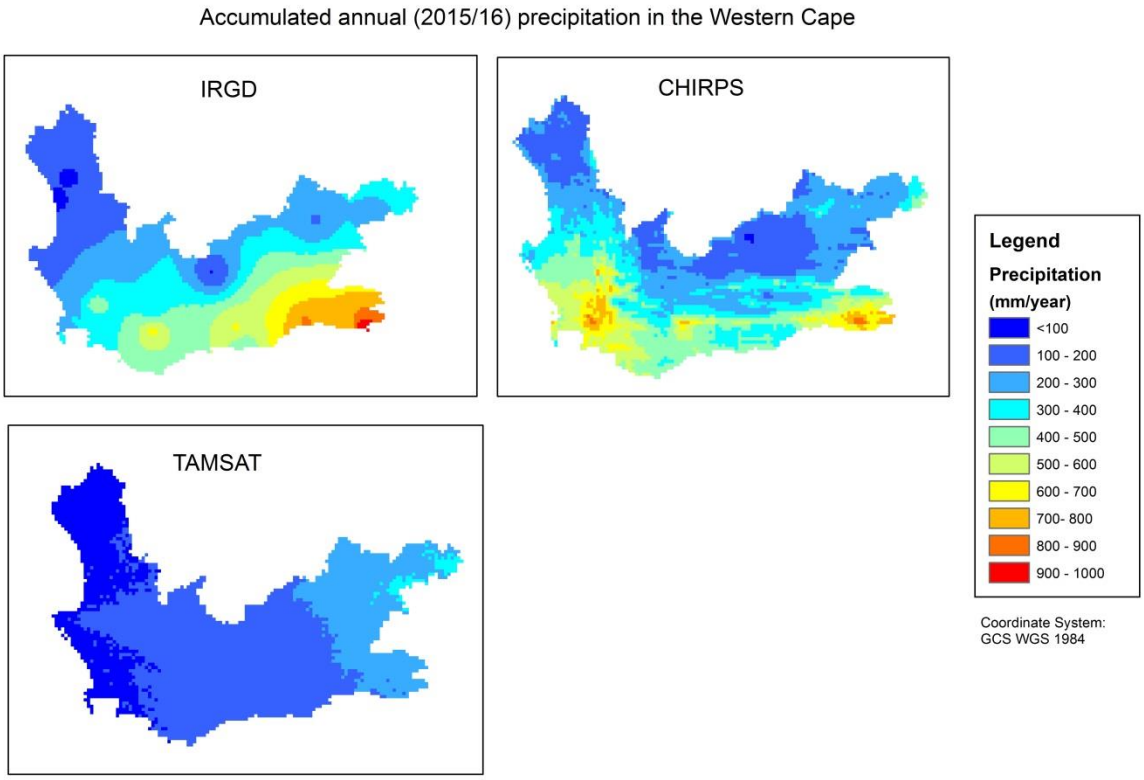

Figure 5.1: The comparison of estimated rainfall by CHIRPS and TAMSAT to the interpolated rain gauge data for the hydrological year 2015/16.

Table 5.1: The range of annual rainfall in the Western Cape Province based on rain gauge and remotely-sensed rainfall estimates

Product	Areal Min (mm/year)	Areal Max (mm/year)	S.Deviation (mm/year)	Areal Mean (mm/year)
Interpolation	89.0	948.2	172.5	330.9
CHIRPS	84.9	824.3	154.9	320.8
TAMSAT	54.0	288.0	51.8	131.0

The differences between the interpolated gauge data and the estimated annual totals by both TAMSAT and CHIRPS were obtained through map algebra (raster calculator) by subtracting the remotely-sensed rainfall estimate from the interpolated rain gauge data. CHIRPS overestimated by up to 445 mm/year in the south eastern part of the province and underestimated by up to 475 mm/year in the south western part of the province (Figure 5.2). CHIRPS compared better in the central part of the province. TAMSAT showed to have

underestimated rainfall in most parts of the province especially in the south eastern area which received high rainfall (Figure 5.3). However, the figure also shows that TAMSAT overestimated by up to 80 mm/year more in the northern part of the province which receives low rainfall (<300 mm/year). Table 5.2 shows descriptive statistics of the difference, on average CHIRPS estimated 23.2 mm rainfall less per pixel.

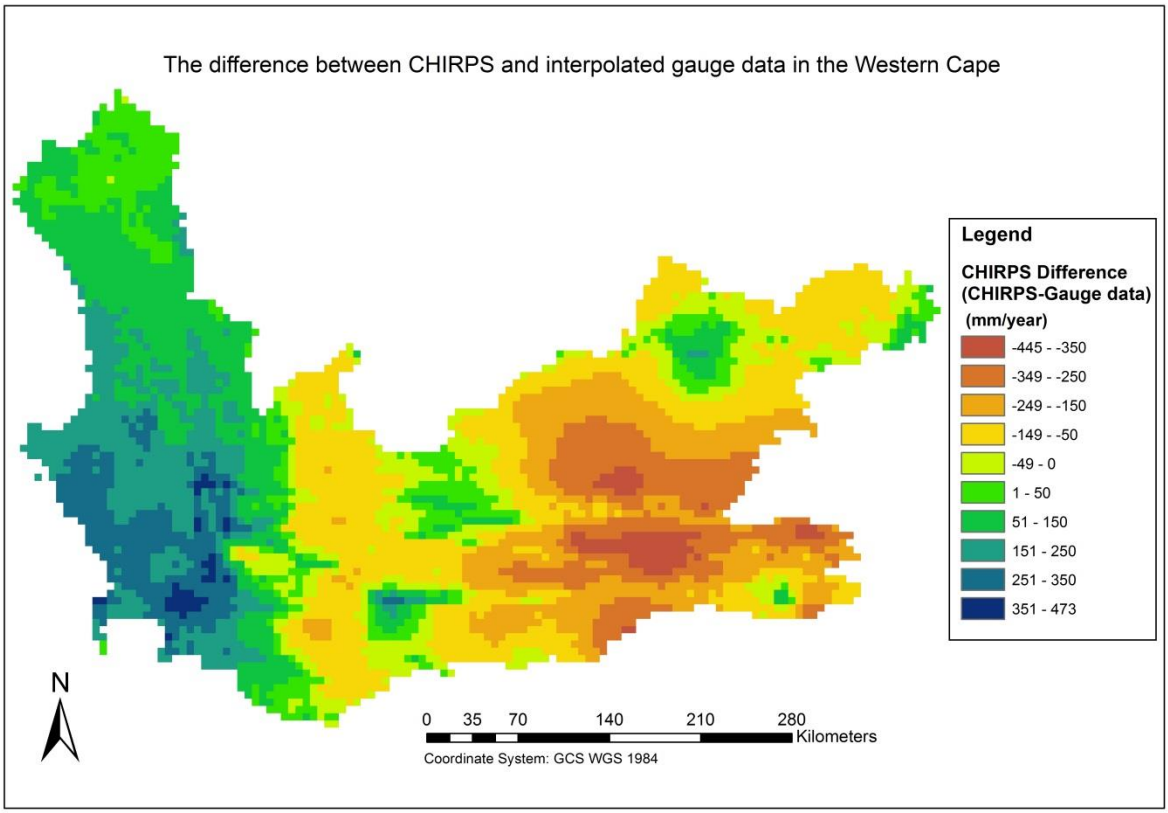

Figure 5.2: The difference between interpolated gauge data and CHIRPS estimates (CHIRPS-Interpolated) in the Western Cape (March 2015 to February 2016).

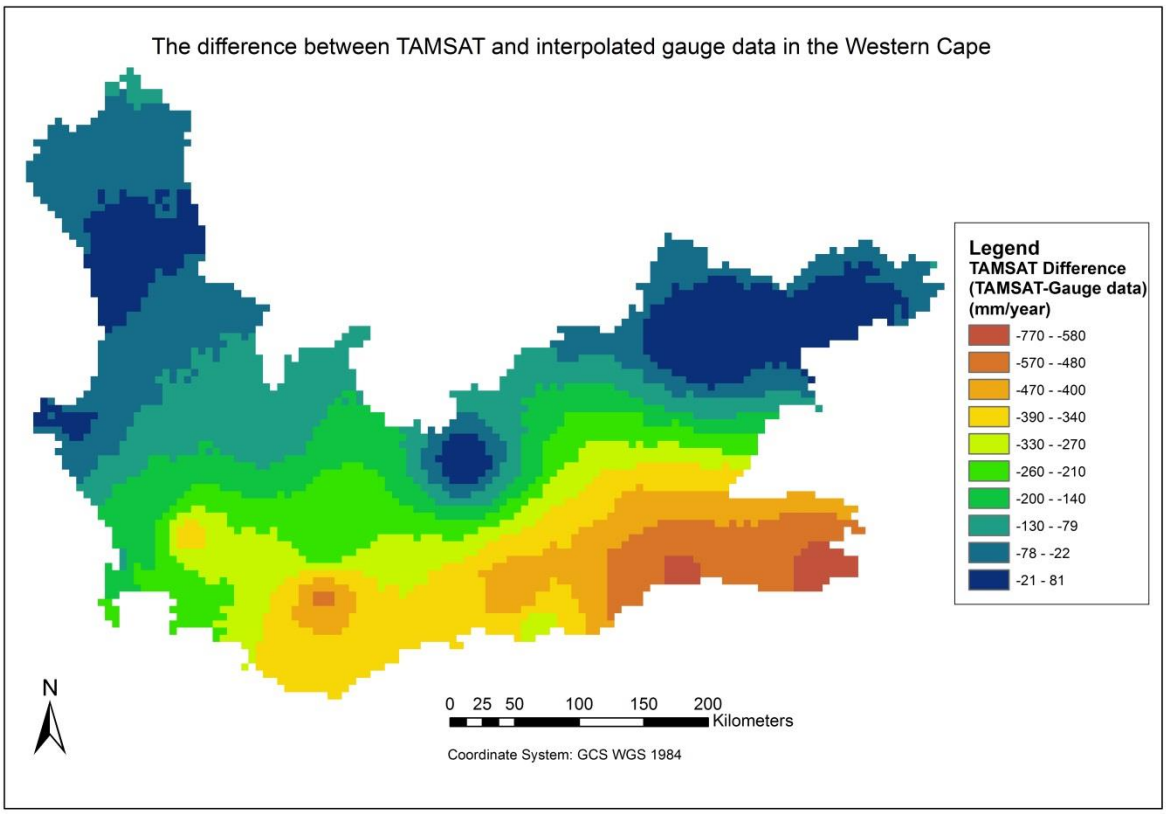

Figure 5.3: The difference between interpolated gauge data and TAMSAT estimates (TAMSAT-Interpolated) in the Western Cape (March 2015 to February 2016).

Table 5.2: Descriptive statistics of difference between the interpolated gauge data and estimated by CHIRPS and TAMSAT obtained from Figure 5.2 and 5.3. Negative values indicate underestimation and positive values indicates overestimation and a zero would have been a perfect match as compared to interpolated gauge data.

	Min(mm/year)	Max (mm/year)	S.Deviation (mm/year)	Mean (mm/year)
CHIRPS	(-)445.3	476.1	178.0	(-)23.2
TAMSAT	80.7	(-)767.5	165.7	(-)199.1

The distribution of rainfall as per estimated and observed in the province is further illustrated in Figure 5.4. Interpolated rain gauge shows that most part (24%) of the province receives between 251 and 350 mm/year. CHIRPS estimates indicate that most part (34%) of the province received between 151 and 250 mm/year. The CHIRPS estimates compare well with interpolated rain gauge data especially for rainfall greater than 250 mm/year (Figure 5.4).

According to TAMSAT most part (64%) of the province receives 50 and 150 mm/year and had no estimated greater values than 350 mm/year.

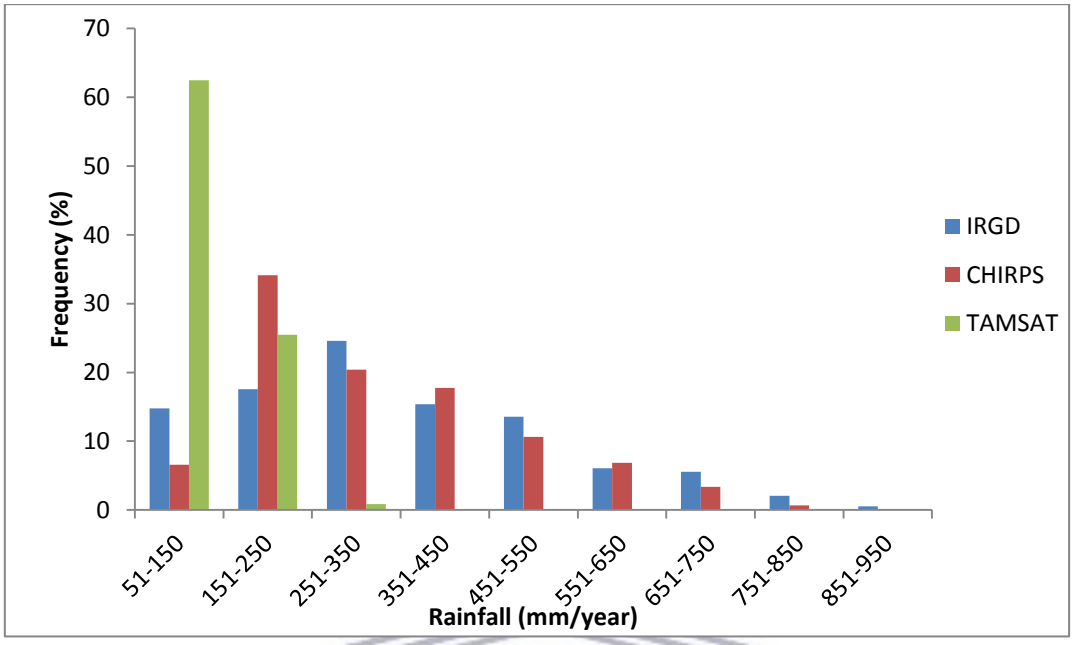

Figure 5.4: The distribution of rainfall per pixel for the interpolated rain gauge data and as estimated by CHIRPS and TAMSAT in the Western Cape.

To determine whether there is a relationship between the estimated and interpolated gauge data, correlation was used. The results showed there is a weak relationship (r=0.46) between CHIRPS estimates and the interpolated rain gauge data. However, there is a strong relationship (r=0.84) between the CHIRPS estimates and mean annual precipitation map (Figure 3.2). This might suggest great incorporation of historical gauge data. The results also show that there is a weak relationship (r=0.37) between TAMSAT estimates and the interpolated rain gauge data. TAMSAT estimates were also weakly related (r=0.17) to mean annual precipitation map. This might suggest poor calibration of the TAMSAT product in the Western Cape.

A t-test was used to determine whether there is a significant difference at 5% significance level between the mean of the interpolated rain gauge data and a) CHIRPS and b) TAMSAT rainfall estimates. The test showed (t=3.07) that at 5% significance level the areal rainfall mean as estimated using interpolated rain gauge data (330.9 mm/year) differs from the CHIRPS estimates. The test also showed (t=78.25) that the areal mean estimated by interpolated rain gauge data differed from the obtained from TAMSAT (131.1 mm/year).

5.2.2 The effects of elevation and climatic conditions on the accuracy of CHIRPS and TAMSAT at regional (provincial) level

Elevation

An analysis was done of the influence of altitude on the level of the error of remotely-sensed rainfall estimates. A correlation between elevation and the error of CHIRPS and TAMSAT was done, the results showed that there is weak to no relationship between the error of CHIRPS and TAMSAT and the elevation, r=-0.23 and 0.36 for CHIRPS and TAMSAT respectively. There was also no correlation between interpolated gauge data and the DEM (r=0.02). Therefore, there is no relationship between elevation and rainfall in this region. This indicates that rainfall might be affected by the change (increase) in elevation but not the elevation (altitude) of a point. This shows that areas with changing elevation tend to receive more rainfall than area with high elevation but flat topography.

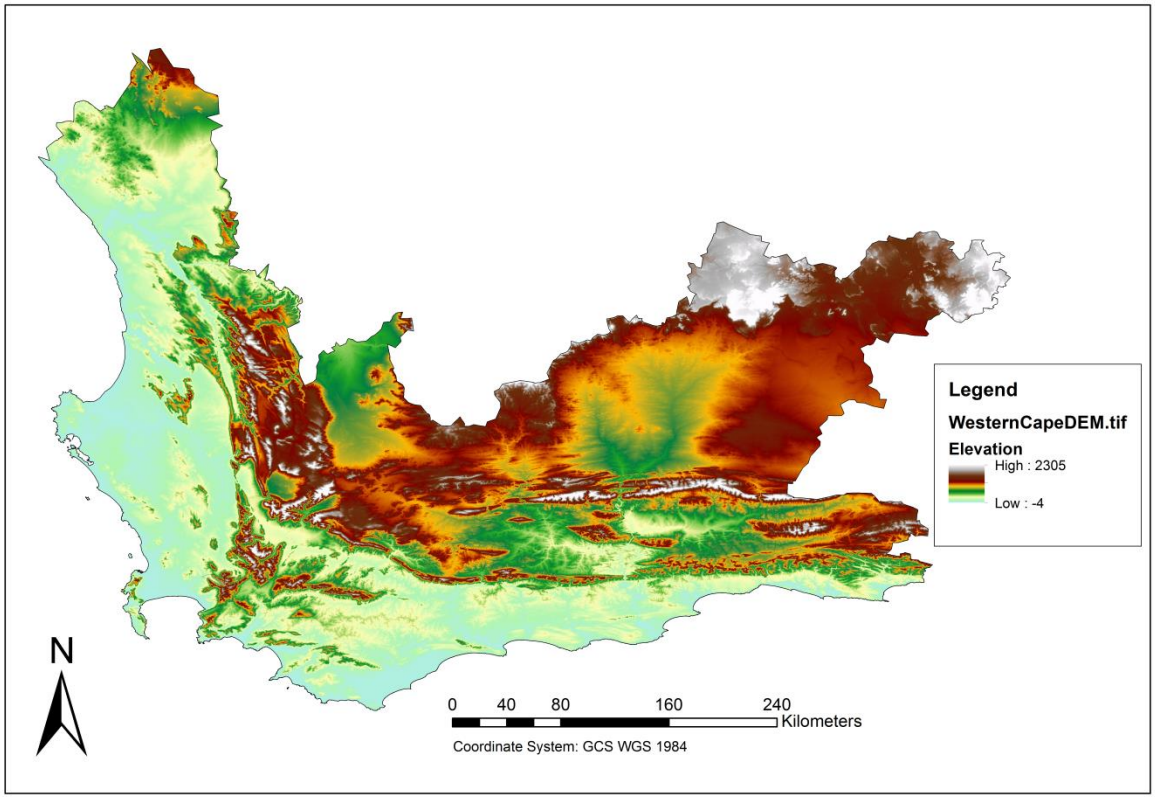

Figure 5.5: Spatial variation of elevation throughout the Western Cape. Data source: ASTER-NASA (2017)

The comparison of the DEM and remotely-sensed estimates showed to have no relationship. Studies have shown that a change in elevation (slope) may affect the accuracy of some of the remotely-sensed estimates (Gao and Liu, 2013; Basist and Bell, 1994). To determine the

effects of topography on the accuracy of the remotely-sensed products, a topography shapefile of 300 m interval was produced from the DEM (Figure 5.5), this was overlaid over the differences remotely-sensed estimates and the interpolated rain gauge data. For CHIRPS, the high change of elevation (shown by the red line in Figure 5.6) in the area commonly referred to as cape folds, appears to determine the boundary where rainfall was underestimated and overestimated (Figure 5.6 top). TAMSAT accuracy appears not to be affected by topography at a regional scale (Figure 5.6 bottom).

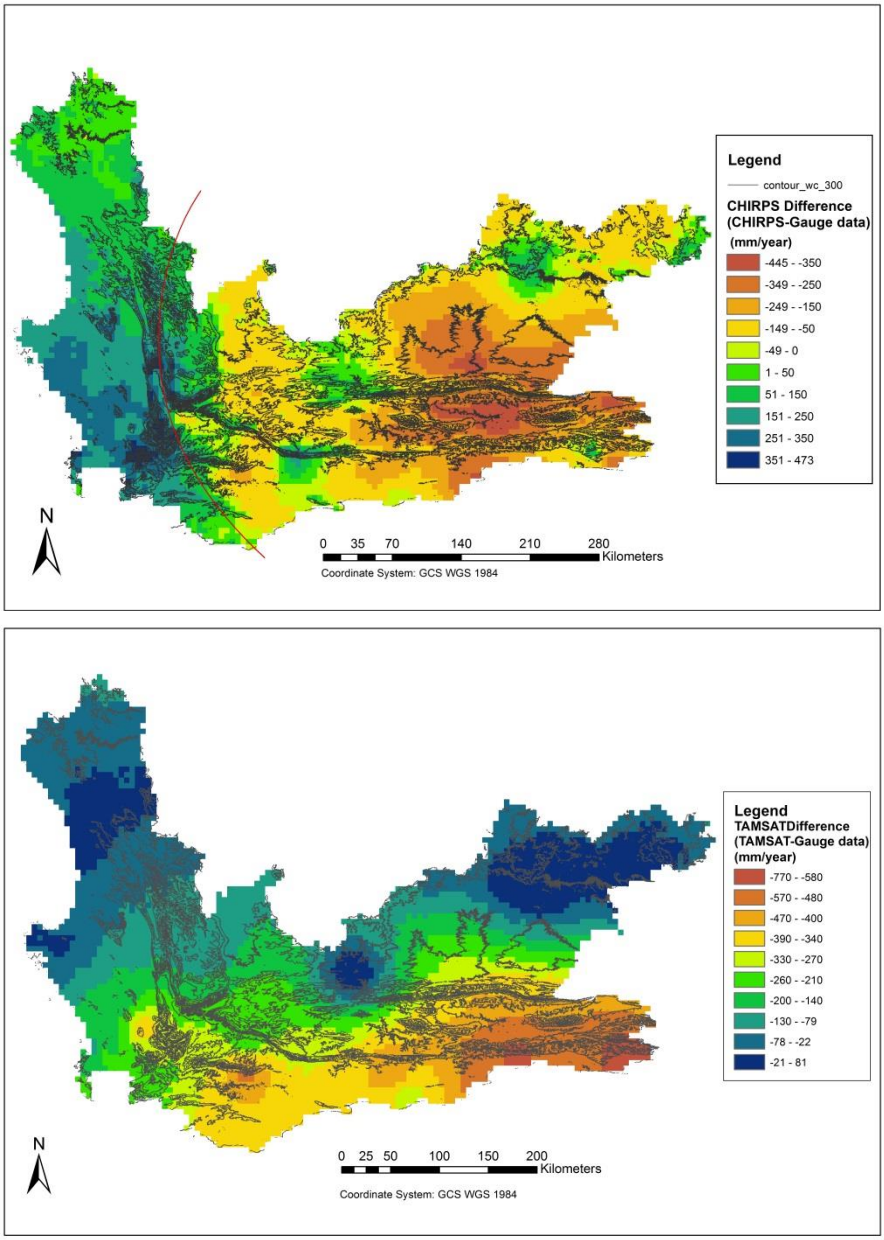

Figure 5.6: The influence of topography on the accuracy of CHIRPS (top) and TAMSAT (bottom). Contour lines were used at 300 m interval to represent a change in elevation a DEM.

Climatic condition

CHIRPS overestimated along the west coast and underestimated on the east coast of the province. According to the interpolated rain gauge data, the west coast received less rainfall than the east coast. However, the long term averages as shown by the mean annual precipitation (Figure 3.2) usually the west coast receives more rainfall in the east coast of the province. Therefore, the overestimation along the west coast and underestimation in east coast by CHIRPS might be due to the use of observed data in the calibration of CHIRPS estimates. This is further supported by the strong relationship between the (r=0.84) between CHIRPS and mean annual precipitation. A study Tote *et al.* (2015) has shown that remotely-sensed products tend to overestimate low rainfall and underestimate high rainfall values; the same pattern is observed for CHIRPS, the rainfall in the low rainfall region is overestimated and underestimated in high rainfall region. The difference in accuracy may also be due to the ocean currents as explained in the study area, the Western Cape is influenced by two different currents, with the cold Benguala associated with cold air and light rainfall influencing the west coast of the province, and Agulhas current associated with warm air and high rainfall influences the south east coast of the province. The two currents may also influence rainfall type, rainfall duration, and rainfall intensity that are received in the area. The rapid change in elevation as discussed may be a factor that determines where the influences by these currents end. TAMSAT compared better an area with low rainfall (<300mm/year) and heavily underestimated in areas with relatively high rainfall.

5.2.3 The effects of elevation and aspect in Jonkershoek

The previous section has shown that there is no relationship between rainfall and elevation at regional/provincial level, thus the accuracy is not affected by elevation. This section, however tests whether the elevation and aspect have an effect on the accuracy of remotely-sensed products at a point in a catchment. Jonkershoek is a good catchment to test this, as it has well defined slope and mountain ranges compared to the Heuningnes. Three stations at different (300, 500 and 1200 m.a.s.l) elevation in were compared to test if the elevation affects the accuracy and for this purpose, actual differences and the correlation were used below are the result.

Rainfall in the Jonkershoek increases with elevation (Figure 5.9), this is also supported by Moses (2008). Both CHIRPS and TAMSAT did not get this correct, TAMSAT has the complete opposite, rainfall decreasing with increasing elevation. CHIRPS estimated little

difference between the low part (300 m.a.s.l) of the catchment and the upper/higher parts (500 and 1200 m.a.s.l). CHIRPS also overestimated rainfall at the lower station at 300 m.a.s.l.

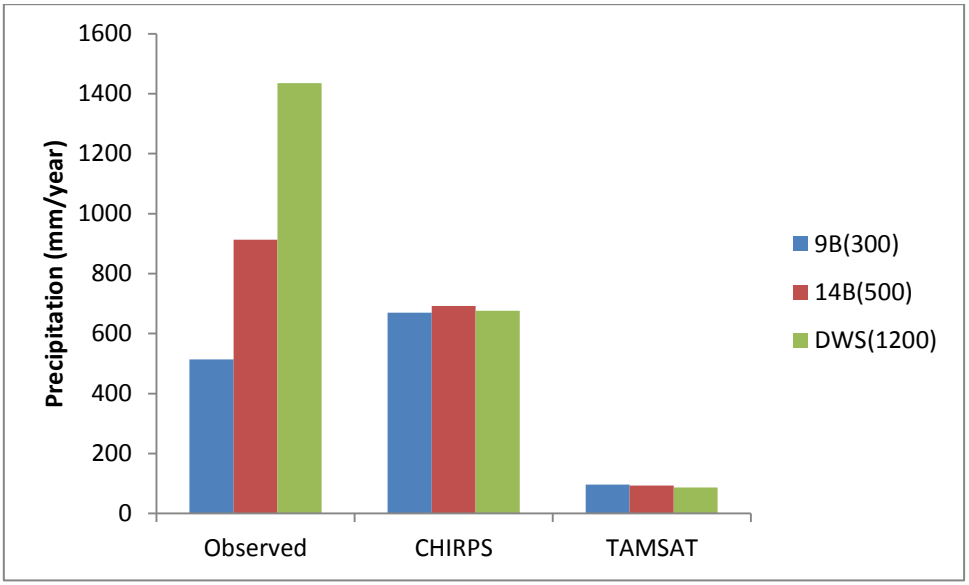

Figure 5.7: Changes in rainfall with elevation as observed, and estimated by CHIRPS and TAMSAT. Station 9B at 300 m.a.s.l, Station 14B at 500 m.a.s.l and DWS at 1200 m.a.s.l.

The monthly trends of the middle station at 500 m.a.s.l were better estimated than low (300 m.a.s.l) and high (1200 m.a.s.l) elevation station (Table 5.3). However, the high elevation station results are better than low elevation station which was unexpected.

Table 5.3: The correlation between the rain gauges at different elevation and rainfall estimated by CHIRPS and TAMSAT.

	9B (300 m.a.s.l)	14B(500 m.a.s.l)	DWS(1200 m.a.s.l)
CHIRPS	0.46	0.93	0.87
TAMSAT	0.46	0.76	0.68

The west facing slope receives more rainfall than the east facing slope (Figure 5.10), this is also supported by Moses (2008). CHIRPS did get this correct even though the difference was relatively small as compared to the observed data. TAMSAT did not get this correct instead it estimated more rainfall on east facing slope than west facing slope.

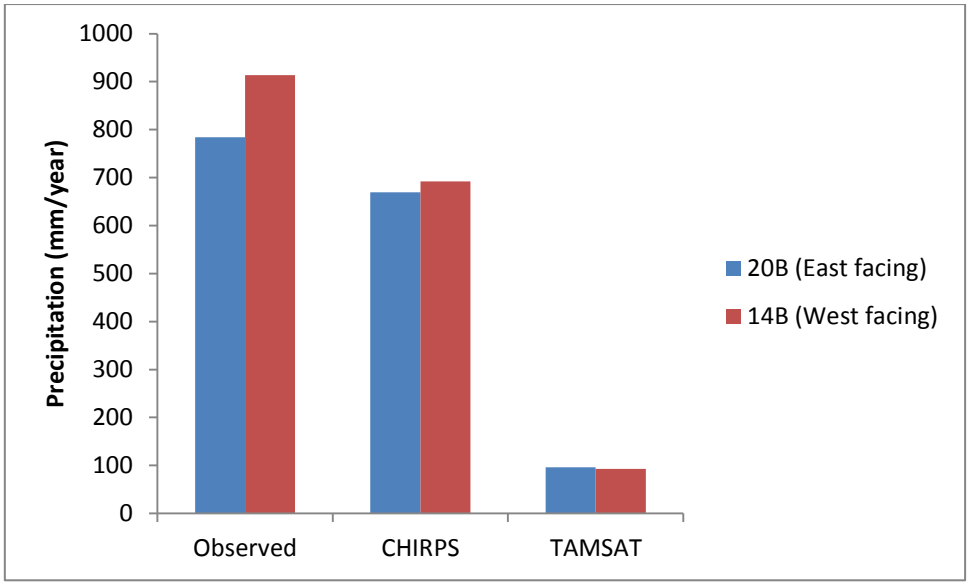

Figure 5.8: A comparison of rain received at different aspect (East and West facing slopes) of the mountain as per observed and estimated by CHIRPS and TAMSAT.

On average the rainfall temporal trends of the west facing slope correlated better to the observed than the east facing slope (Table 5.4). However, the difference is relatively small hence this may be insignificant.

Table 5.4: A comparison of correlation between estimated and observed rainfall at different aspect (East and West facing slopes) of the mountain.

Products	20B (East facing)	14B (West facing)
CHIRPS	0.91	0.93
TAMSAT	0.77	0.76

5.3 Assessment of estimation of rainfall for the various seasons

Seasons are characterised by their differences in the climate factors, such as winds and rainfall regime. Therefore, the accuracy of remotely-sensed rainfall may differs from season to season. Alazzy *et al.* (2017) showed that seasonal fluctautions have noteworthy influence on the accuracy of remotely-sensed estimates. This study did an assessment of estimation of rainfall for various seasons in the Western Cape. The interpolated gauge data show that the province received more rainfall in the south east of the province in autumn (March to May), whereas CHIRPS estimated the south west as an area with more rainfall than other parts of the province. TAMSAT and the MPE estimated north east as an area with more rainfall than other parts of the province (Figure 5.9). In winter (June to August) according to the

interpolated rain gauge data, the south west part of the province received more rainfall than any other part of the province, this is in agreement with estimates by CHIRPS and the MPE. TAMSAT estimated the opposite as south west was estimated as an area with least rainfall (Figure 5.10). In spring (September to November), both CHIRPS and TAMSAT estimated the eastern part of the province as an area with higher rainfall in spring, which coincides with interpolated gauge data, The MPE was not included as it had a significant amount of missing data (Figure 5.11). In summer (December to Febraury), TAMSAT and MPE have similar patterns, both estimated north eastern part of the province as an area with more rainfall than any part of the province (Figure 5.12). This is not in agreement with interpolated gauge data. However, CHIRPS was in agreement with the interpolated data in the south west part of the province.

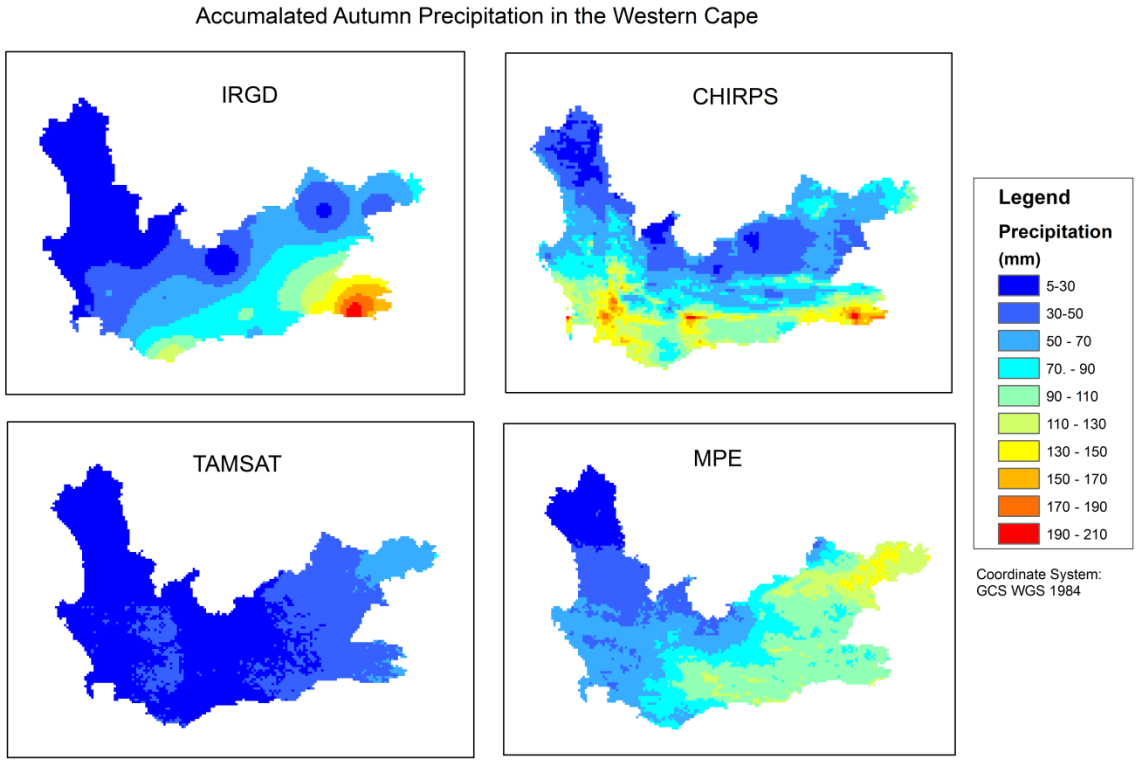

Figure 5.9: A comparison of autumn rainfall estimates (March to May 2015) in the Western Cape as interpolated rain gauge data (top left) and as estimated by CHIRPS (top right), TAMSAT (bottom left) and MPE (bottom right).

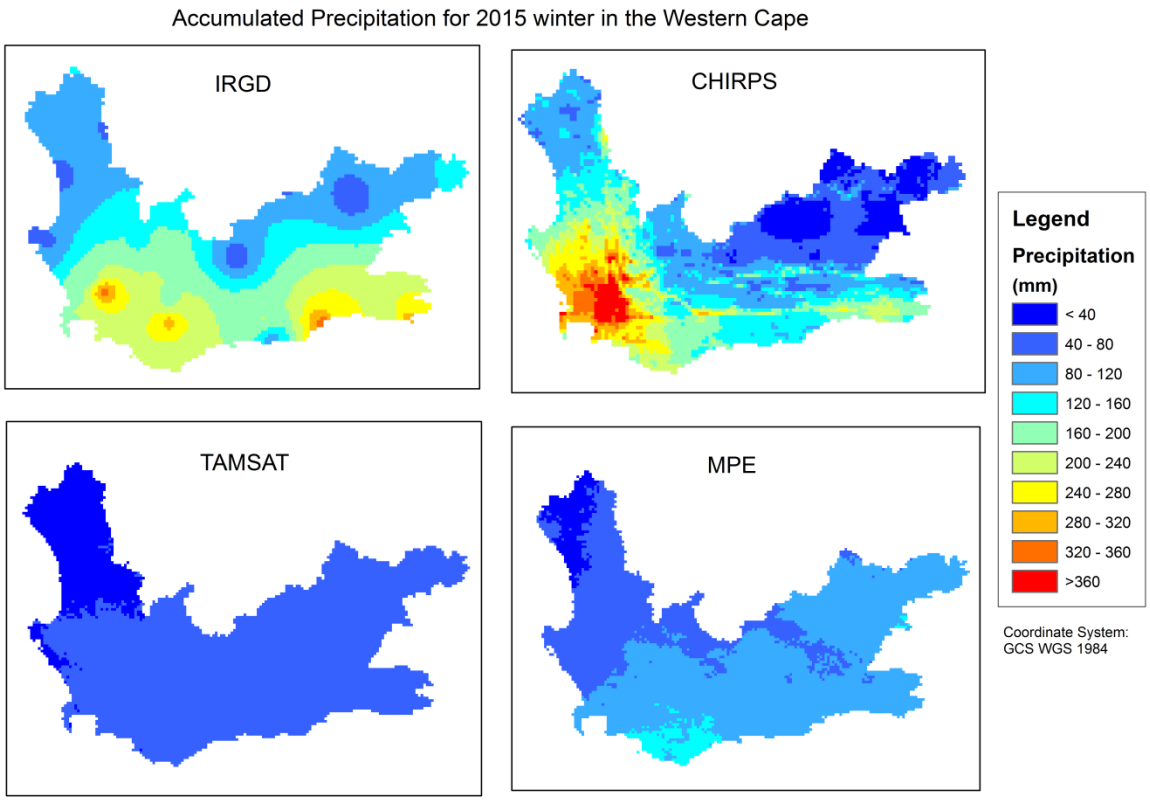

Figure 5.10: The comparison of accumulated precipitation during the winter (June to August 2015) in the Western Cape as interpolated rain gauge data (top left) and as estimated by CHIRPS (top right), TAMSAT (bottom left) and MPE (bottom right).

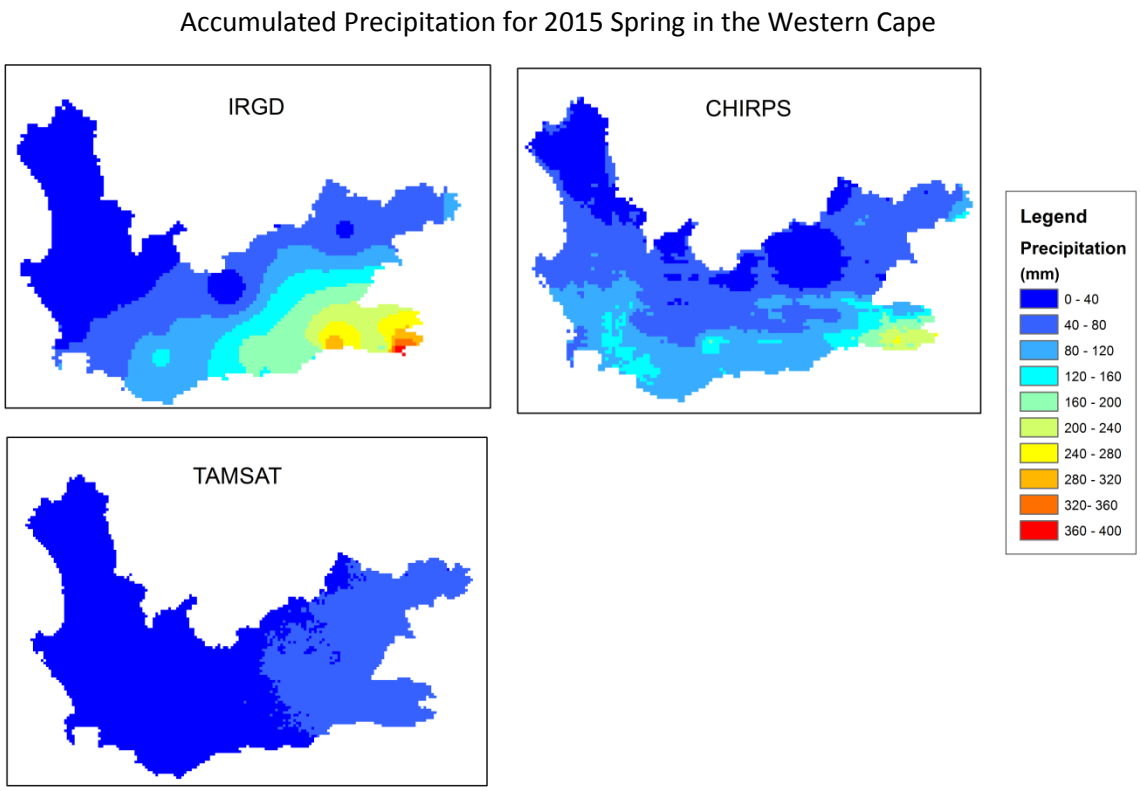

Figure 5.11: The comparison of accumulated precipitation during the Spring (September to November 2015) in the Western Cape as interpolated rain gauge data (top left) and as estimated by CHIRPS (top right) and TAMSAT (bottom left).

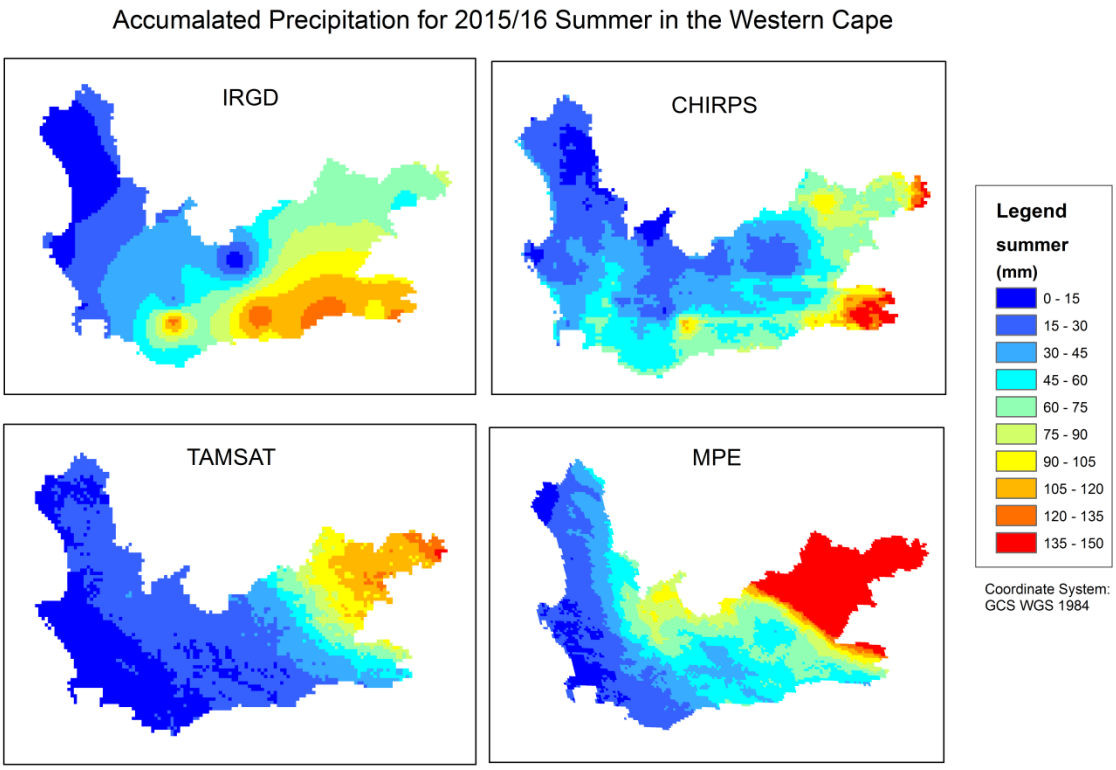

Figure 5.12: The comparison of accumulated precipitation during the summer (Dec 2015 to Feb 2016) in the Western Cape as interpolated rain gauge data (top left) and as estimated by CHIRPS (top right), TAMSAT (bottom left) and MPE (bottom right).

The remotely-sensed products underestimated the seasonal areal mean. The results showed that a general underestimation of the seasonal rainfall means by the remotely-sensed products (Figure 5.15 and Table 5.5). However, there was overestimation in autumn by CHIRPS and MPE. The MPE also overestimated rainfall in summer, suggesting that MPE has a wet bias in summer. This might be due that the MPE might not calibrated with rain gauge data for the Mediterranean climate. TAMSAT underestimated the means for all four season.

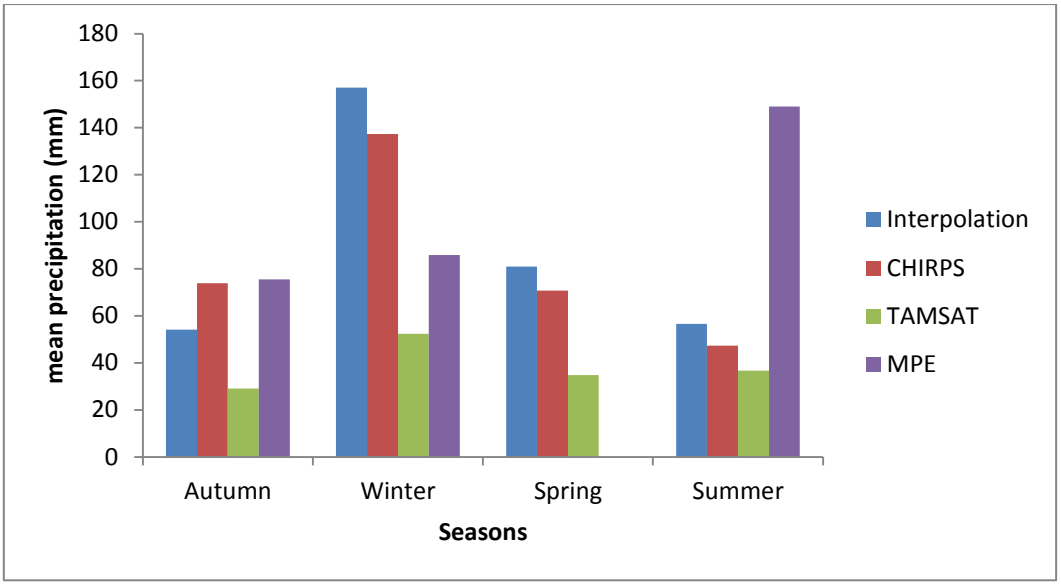

Figure 5.13: The comparison of areal seasonal rainfall means in four seasons, autumn (March to May), winter (June to August), spring (September to November) and summer (December to February) as per interpolated and estimated by TAMSAT, CHIRPS and MPE. There is no data for MPE in Spring due to missing data during that season.

Table 5.5: Comparison of the description statistics between the estimated and interpolated gauge data.

Autumn

Product	Areal Min (mm)	Areal Max (mm)	Areal S.Deviation (mm)	Areal Mean (mm)
Interpolation	5.0	210.3	37.9	54.1
CHIRPS	16.9	200.7	34.4	73.8
TAMSAT	3.0	74.0	12.6	29.1
MPE	10.0	139.0	37.7	74.5

Winter

Product	Areal Min (mm)	Areal Max (mm)	Areal S.Deviation (mm)	Areal Mean (mm)
Interpolation	57.3	344.4	56.7	157.1
CHIRPS	13.5	450.5	86.4	137.3
TAMSAT	18.0	80.0	12.2	52.4
MPE	27.0	141.0	33.1	85.8

Spring

Product	Areal Min (mm)	Areal Max (mm)	Areal S.Deviation (mm)	Areal Mean (mm)
Interpolation	5.6	386.9	69	80.9
CHIRPS	17.6	247.5	38.4	70.8
TAMSAT	13.0	68.0	12.5	34.8

Summer

Product	Areal Min (mm)	Areal Max (mm)	Areal S.Deviation (mm)	Areal Mean (mm)
Interpolation	0.01	134.1	34.4	56.5
CHIRPS	7.6	176.3	28.1	47.4
TAMSAT	2.0	149.0	33.8	36.7
MPE	4.0	293.0	83.3	149

Summary

The results clearly showed that the remotely-sensed products generally underestimate the rainfall in the Western Cape, this was shown through the actual differences between remotely-sensed estimates and interpolated rain gauge data and was further supported by the t-test. The correlation between the data showed that there is weak relationship between the interpolated rain gauge data and the remotely-sensed estimates. However, when the remotely-sensed estimates were correlated to the long term average, CHIRPS had strong relationship, which might indicate the use of historical data in the calibration of the estimates. There was no relationship between elevation and the accuracy of the remotely-sensed products, but rapid change in elevation also known as Cape Folds Belt might have been the demarcation between the area of overestimation and underestimation by CHIRPS. The climate condition might have also influenced the accuracy of remotely-sensed products. CHIRPS overestimated along west coast where the climate conditions are influenced by the cold Benguela current, the underestimation of south and eastern part of province which the climate might be influenced by the cape Agulhas current. TAMSAT accuracy did not show to be affected by elevation and climate conditions. In terms of the seasonal estimates, the remotely-sensed products tend to underestimate the seasonal rainfall. However, the MPE and CHIRPS overestimated the MPE and CHIRPS rainfall in the Western Cape. The MPE also overestimated rainfall in summer. Overall CHIRPS was better than TAMSAT and the MPE.

Chapter 6: Assessment of the remotely-sensed rainfall estimates at a point

6.1 Introduction

The previous chapter focused on the assessment of the remotely-sensed estimates over a large spatial area (Province). This chapter presents the results of the assessment of the performance of remotely-sensed estimates at a point. This was done for two catchments on the relatively flat coastal Heuningnes and the relatively small mountainous catchment of the Jonkershoek as explained in the study area and the methodology chapters. This chapter firstly assess the missing data and shows how the rain gauge stations (points) were selected. Thereafter, the daily, monthly and annual rainfall estimates in both Jonkershoek and Heuningnes are assessed; the results from the two catchments are compared in a summary at the end of each section. Lastly, the ability of the remotely-sensed products to distinguish between rainy and non-rainy days is presented.

6.2 Data quality and station selection

From the stations in Heuningnes that were selected in this study, only Spanjaardskloof had 33 days (9%) of missing data which was caused by logger battery failure. Table 6.1 presents the length of missing data in Jonkershoek, ranging from 2 to 13%. The data was filled using linear regression from a rain gauge station with the highest correlation coefficient. Linear regression was used because it is the most commonly used to fill in rainfall and most studies such as Reddy *et al*., (2008) have found that it is the most effective as compare to mean per unit and ratio estimation irrespective of the data's distribution and sample size. In this case, Napier's data which was strongly correlated (r=0.88) to Spanjaardskloof was used (Table 6.2a). Appendix 4.3 provides the correlation between all stations in Jonkershoek which was used to determine which station should be used to fill the missing on another one. The missing data in Jonkershoek were mostly due to fire damages of the stations. Appendix 4.4 provides some of the explanations.

Table 6.1: Missing data in the Jonkershoek which had to be filled.

Station	15B	8B	14B	L500	L600	L700	L800	20B	12B	9B	13B	7B
Number of missing days	32	26	29	7	22	8	8	31	20	40	37	48
Missing data (%)	8.8	7.1	8.0	1.9	6.0	2.2	2.2	8.5	5.5	11.0	10.1	13.2

As stated in the methodology, the station with the highest correlation between all the rainfall stations is the most representative of rainfall occurrence in the catchment. In the Heuningnes, table 6.2b shows that the rain gauge in Spanjaardskloof is the most related (r=0.86) to the other stations on average, therefore it was selected to represent rainfall of the catchment. In Jonkershoek, 14B which is located in Langrivier had the highest correlation on average (Table 6.3), therefore the most representative of rainfall in the catchment. Based on this selection, Spanjaardskloof and 14B were used to assess the remotely-sensed products estimates at a point.

Table 6.2a: Correlation between the rainfall stations in the Heuningnes.

	Spanjaardskloof	*Vissersdrift*	*Napier*
Spanjaardskloof	1		
Vissersdrift	0.84	1	
Napier	0.88	0.82	1

Table 6.2b: Average correlation coefficient between the rainfall stations in the Heuningnes

	Average Correlation
Spanjaardskloof	0.86
Vissersdrift	0.83
Napier	0.85

Table 6.3: The average correlation between the rain gauge stations in Jonkershoek.

Station name	Average Correlation
19B	0.924
11B	0.932
5B	0.924
15B	0.915
8B	0.922
14B	0.935
L500	0.93
L600	0.926
L700	0.926
L800	0.903
DWS	0.774
20B	0.907
12B	0.926
9B	0.655
13B	0.92

Both Heuningnes and Jonkershoek catchment received most of their rainfall during the southern hemisphere winter (Table 6.4 and 6.5). Heuningnes received less rainfall in October, whereas Jonkershoek received less rainfall in March. The Heuningnes received an average of 564 mm/year, whereas Jonkershoek received 791 mm/year for the 2015/16 hydrological year.

Table 6.4: Monthly Rainfall at the three rain gauge stations in the Heuningnes

	Spanjaardskloof (mm/month)	Vissersdrift (mm/month)	Napier (mm/month)
March 2015	80.2	79	41.4
April 2015	22.6	17.6	6.6
May 2015	31.6	15.2	11.2
June 2015	124.6	127.2	142.8
July 2015	114.2	60.2	83.4
August 2015	67.8	86.6	35.4
September 2015	79.8	68	53.4
October 2015	11.8	8.4	13.8
November 2015	46.2	63	52.6
December 2015	20.2	18.4	7.6
January 2016	23.2	13.2	9
February 2016	11.2	27.6	15.4
Total	**633.4**	**584.4**	**472.6**

Table 6.5: Monthly rainfall at the 15 Jonkershoek stations used in this study.

Month	19B	11B	15B	14B	L500	L600	L700	L800	8B	5B	DWS	20B	12B	9B	13B
Mar 2015	2.2	4.4	2.4	6.2	2.5	5.31	3.9	3.3	2.8	3.6	11.9	3.1	3.0	7.0	3.2
Apr 2015	15.8	15.4	14.3	21.1	16.3	15.2	18.3	21.1	20.6	19.0	44.2	22.8	16.0	18.5	19.8
May 2015	44.6	50.4	46.0	66.0	52.6	70.6	80.5	89.9	59.4	90.2	80.0	96.0	57.0	54.4	45.2
Jun 2015	164.8	160.4	196.4	213.4	184.2	221.8	207.8	210.6	207.2	236.8	204.7	180.0	225.2	7.00	163.8
Jul 2015	134.6	140.0	153.0	241.6	193.6	275.6	204.4	300.5	187.8	202.8	383.6	182.8	190.2	157.0	132.4
Aug 2015	56.0	72.4	63.8	129.4	81.8	124.5	131.3	147.1	77.8	108.4	250.5	70.6	79.6	69.2	56.2
Sept 2015	60.6	51.8	61.6	81.4	68.8	84.6	79.5	83.1	52.6	80.8	144.0	73.4	71.4	72.8	54.2
Oct 2015	9.8	11.8	7.4	13.2	13.2	13.2	10.2	11.2	9.6	14.6	39.1	18.4	8.6	11.6	9.4
Nov 2015	38.2	34.4	31.0	64.4	41.7	44.7	43.7	61.2	34.7	66.0	105.4	65.4	40.0	49.2	39.6
Dec 2015	29.6	29.6	35.8	38.4	27.9	34.8	28.5	31.2	30.1	32.6	71.4	42.4	39.0	36.6	25.8
Jan 16	14.6	15.4	16.4	20.0	15.0	19.1	14.5	15.7	14.9	15.8	62.2	17.4	17.0	17.0	12.0
Feb 2016	13.6	13.2	8.6	18.4	14.7	18.5	17.0	18.5	11.7	12.6	38.1	12.0	12.8	13.2	14.0
Annual Total	**584.4**	**599.2**	**636.7**	**913.5**	**712.2**	**927.8**	**839.4**	**993.4**	**709.1**	**883.2**	**1435.1**	**784.3**	**759.8**	**513.5**	**575.5**

6.3 Assessment of estimation of daily rainfall

There is a need to assess the remotely-sensed estimates at daily timescale. According to Dent (2012) daily estimates of rainfall are important for weather related applications such as flood warning and evacuation, demand scheduling and control setting (water supply and irrigation). This section will assess i) the actual differences between the estimated and observed data ii) the relationship between the two through correlation and iii) the difference between the means through the t-test.

6.3.1 Assessment of the daily differences in actual rainfall amount in the Heuningnes Catchment

There is a general underestimation by remotely-sensed products in the Heuningnes as compared to the rain gauge data (Figure 6.1), as there are more underestimated days than overestimated days. However, TAMSAT underestimated more often than the MPE and CHIRPS. The three remotely-sensed products have similar temporal patterns but differ in the magnitude of overestimation. However, CHIRPS overestimated more often as compared to the other two products (MPE and TAMSAT). CHIRPS, TAMSAT and MPE had the largest errors of 39, -48 and -34 mm/day respectively. The MPE have missing data between September 2015 and middle of October 2015. The figure also shows that MPE had no rainfall estimated in August 2015, this may be an indication that the problem that resulted in the missing data started before the period classified as missing data. The highest rainfall received was 52 mm/day, which CHIRPS overestimated and the other products underestimated. The mean error was -0.27, -1.42 and -0.8 mm/day for CHIRPS, TAMSAT and MPE respectively. This confirms that remotely-sensed products are underestimating on average.

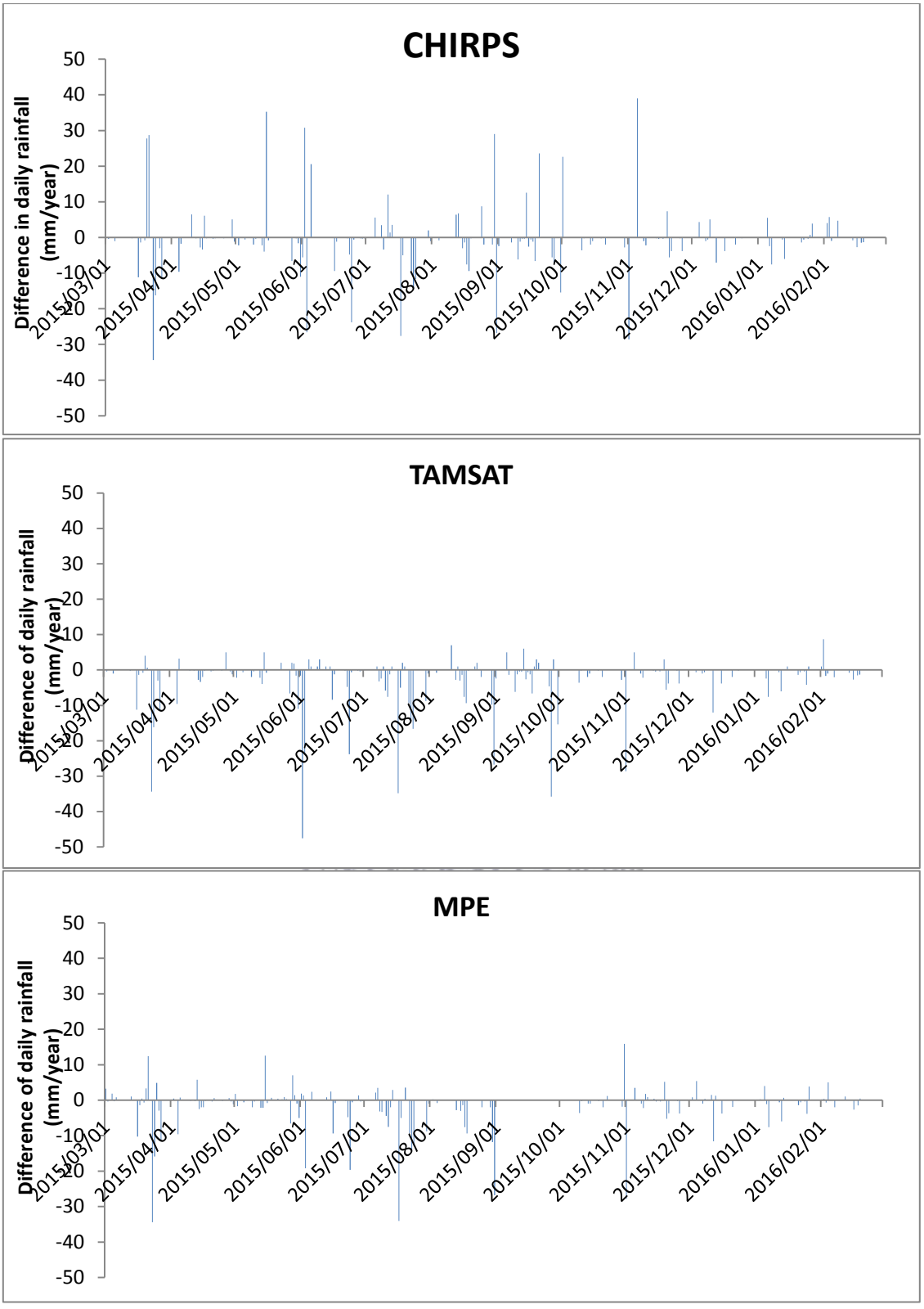

Figure 6.1: The difference between observed and the estimated rainfall by CHIRPS, TAMSAT and MPE for the year 2015/16 in Heuningnes (Spanjaardskloof). The 0 line is observed rainfall and any value above the 0 line is overestimation and any value less than 0 is underestimation.

6.3.2 Comparison of rain gauge and remotely-sensed daily rainfall in the Heuningnes Catchment

Correlation analysis was used to assess the relationship between remotely-sensed estimates and the observed data. There is weak to no relationship between remotely-sensed products and the observed data at Spanjaardskloof, in the Heuningnes catchment (Figure 6.2), CHIRPS had a correlation coefficient (r) of 0.43 and TAMSAT a correlation of 0.11. However, the correlation of the MPE was unexpectedly moderate (0.58) when the missing data is excluded. The significance of correlation showed that all these correlations were statistically differed at 95% confidence level ($p<0.05$).

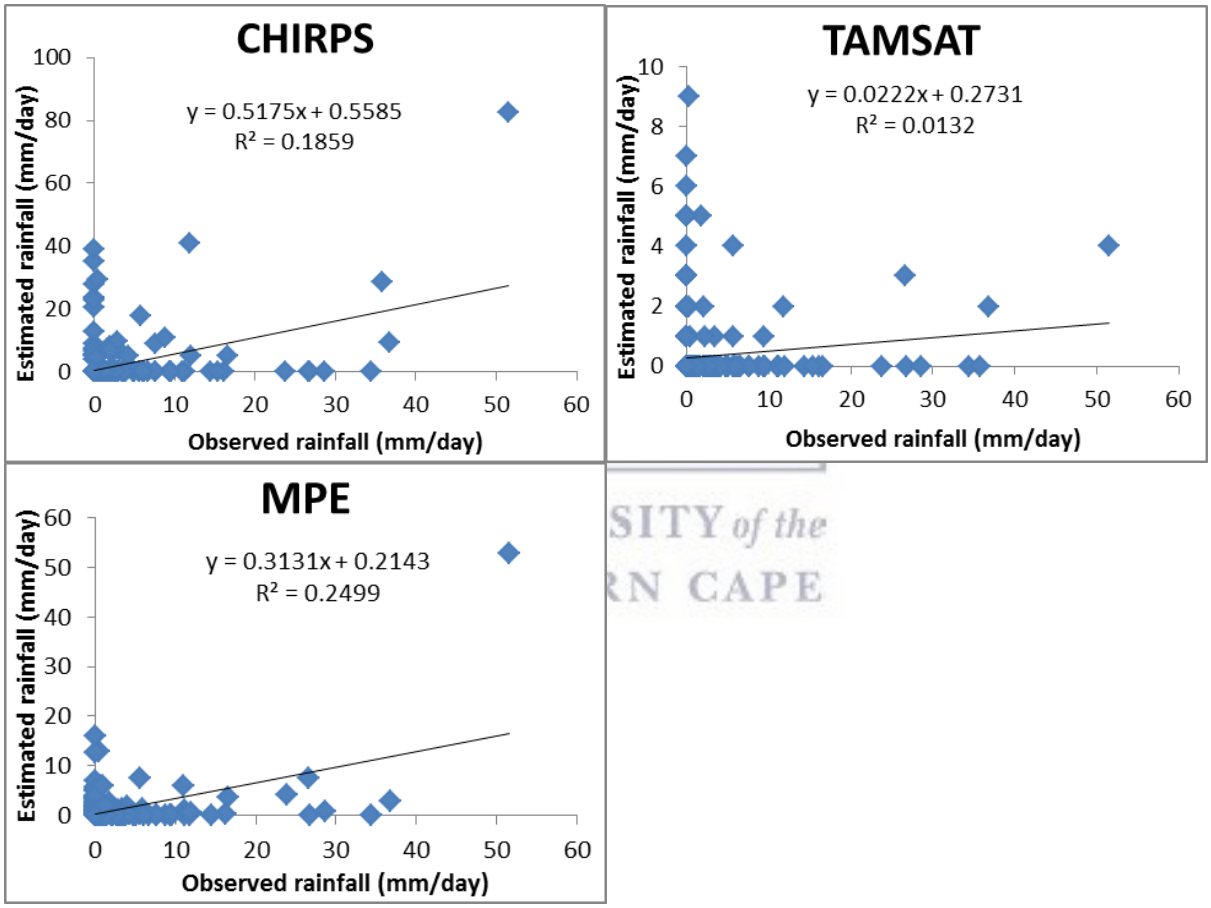

Figure 6.2: The relationship between daily observed data and estimates by CHIRPS, TAMSAT and MPE from March 2015 to February 2016 at the Heuningnes catchment (Spanjaardskloof).

A t-test was used to determine whether there is a difference between the remotely-sensed estimated mean and the observed rainfall mean at daily timescale at 5% significance level. The t-test (t=4.95) showed that at the 5% significance level the mean daily rainfall estimated using rain gauge data (1.73 mm/day) differed from that obtained from the TAMSAT data

(0.31 mm/day). The t-test (t=3.61) also showed that the mean daily rainfall estimated using rain gauge data (1.69 mm/day) differed from that obtained from MPE data (0.74 mm/day). However, the CHIRPS mean daily rainfall (1.45mm/day) did not differ significantly (t=0.81) from that of rain gauge data (1.73 mm/day).

6.3.3 Assessment of the daily differences in actual amount in the Jonkershoek Catchment

There is a general underestimation by remotely-sensed products in the Jonkershoek compared to the rain gauge data (Figure 6.3), as there are more underestimated days than overestimated days. However, TAMSAT underestimated more often than the MPE and CHIRPS. The overestimation of the three remotely-sensed products had similar temporal patterns but differ in the magnitude of overestimation. However, CHIRPS overestimated more often as compared to the other two products (MPE and TAMSAT). CHIRPS, TAMSAT and MPE had the largest errors of 113, -74 and -72 mm/day respectively. As stated before, the MPE have missing data between September and middle of October. The highest rainfall received was 76 mm/day on 17/07/2015; CHIRPS estimated no rain that day and the other products underestimated the magnitude of the event. The mean error was -0.6, -2.2 and -1.8 mm/day for CHIRPS, TAMSAT and MPE respectively. This confirms that remotely-sensed products are underestimating on average.

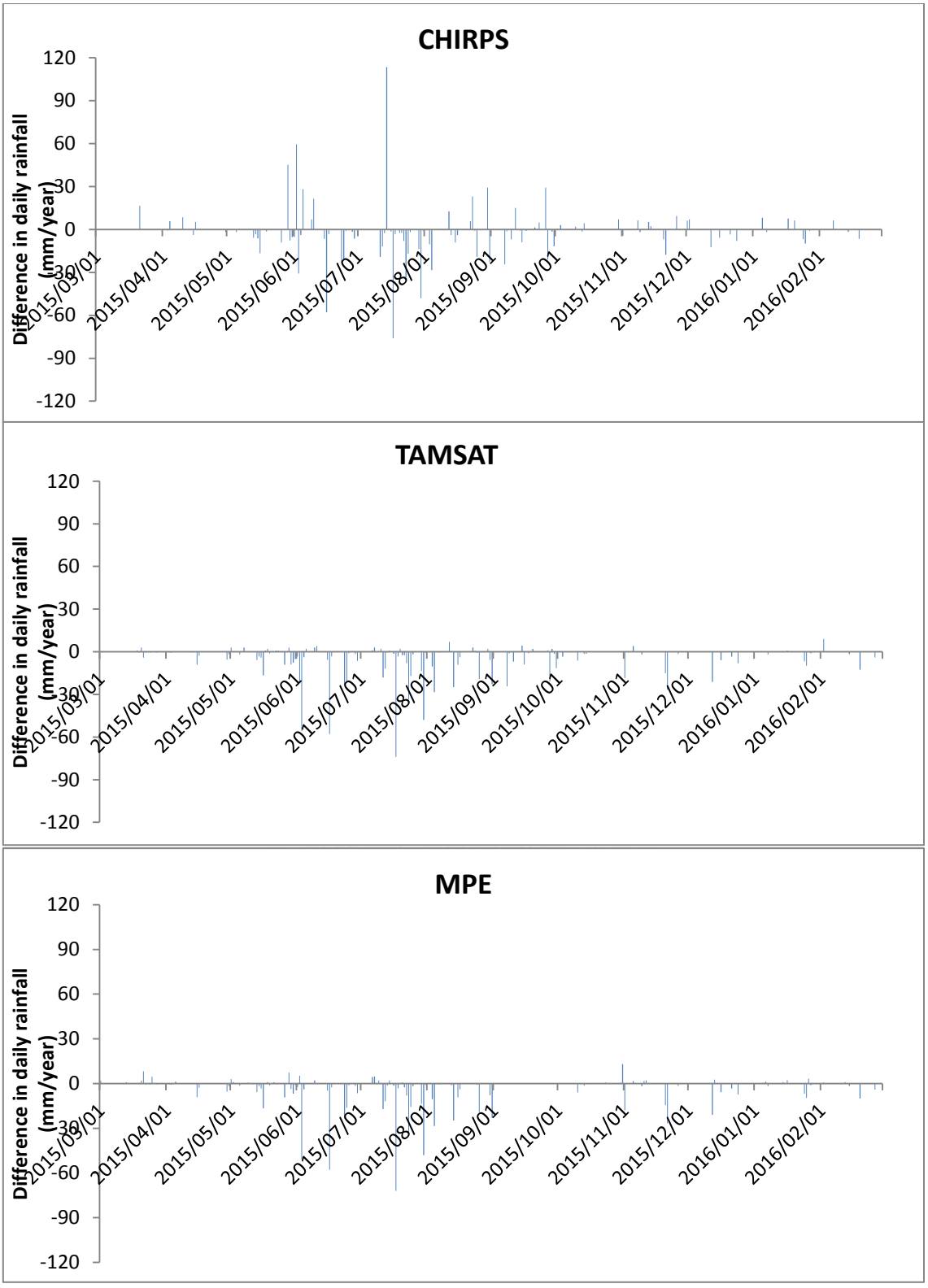

Figure 6.3: The difference between observed and estimated rainfall by CHIRPS, TAMSAT and the MPE for the year 2015/16 in Jonkershoek (14B). The 0 line is observed rainfall and any value above the 0 line is overestimation and any value less than 0 is underestimation.

6.3.4 Comparison of rain gauge and remotely-sensed daily rainfall in the Jonkershoek Catchment

There is weak to no relationship between the remotely-sensed estimates and the observed data in Jonkershoek (Figure 6.4). CHIRPS with a correlation coefficient (r) of 0.17, TAMSAT with a correlation of 0.09 and the MPE with a correlation of 0.26. The significance of the correlation showed CHIRPS and MPE correlations were statistically significant at 95% confidence level ($p<0.05$). The correlation between TAMSAT and observed data was not statistically significant, therefore there is no relationship between TAMSAT and the observed data.

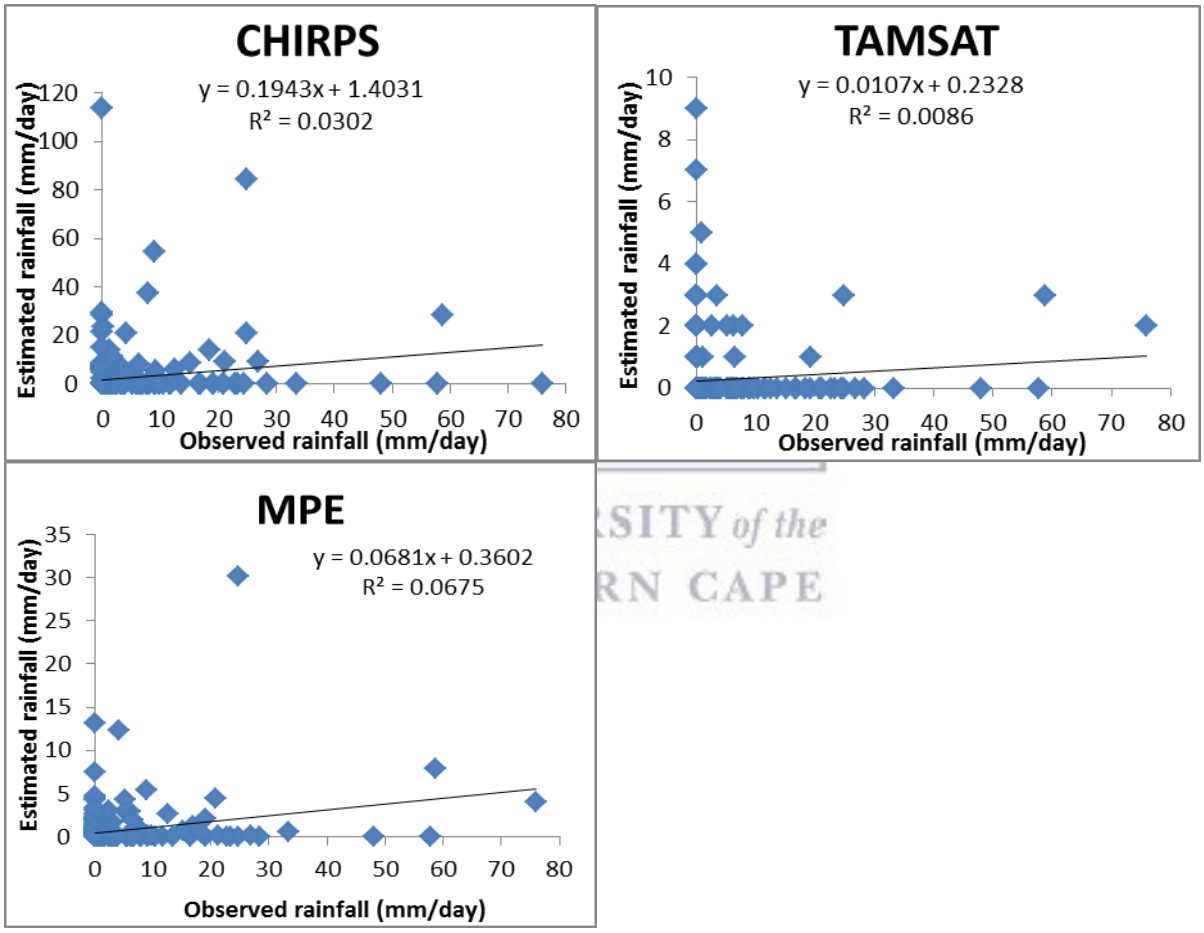

Figure 6.4: The relationship between daily observed data and estimates by CHIRPS, TAMSAT and the MPE from March 2015 to February 2016 at the Jonkershoek catchment (14B).

A t-Test was done to determine whether there is a difference between the estimated mean by the remotely-sensed products and the observed mean rainfall at daily timescale at 5% significance level. The t-test (t=5.36) showed that at the 5% significance level the mean daily

rainfall estimated using rain gauge data (2.5 mm/day) differed from that obtained from the TAMSAT data (0.26 mm/day). The t-test (t=4.53) also showed that the mean daily rainfall estimated using rain gauge data (2.5 mm/day) differed from that obtained from MPE data (0.53 mm/day). However, the CHIRPS mean daily rainfall (1.9 mm/day) did not differ significantly (t=1.06) from that of rain gauge data (2.5 mm/day).

Summary of the daily estimates assessment

The comparison of the rain gauge estimates and the remotely-sensed products (CHIRPS, TAMSAT, MPE) data showed that all three remotely-sensed products underestimated the actual rainfall. Figure 6.1 and 6.3 suggest that the remotely-sensed products might have the problem of miss-timing the daily rainfall, this is also supported by the weak relationship between remotely-sensed products and observed data. In both catchments, Heuningnes and Jonkershoek, CHIRPS performs better than the MPE and TAMSAT in terms of estimating the rainfall amount (ME=-0.27 and -0.6). However, in terms of following the temporal trends of observed data, MPE was better (r=0.58 and 0.03), suggesting that the MPE has better detection of the rainy days. This will be tested in more details in section 6.6. This again shows that correlation does not consider the gap/ differences between the estimated and observed amount but considers the trend, in this case, the temporal trends. The t-test confirmed that CHIRPS performs better than TAMSAT and MPE, in terms of the mean daily rainfall as there was no statically significant difference between CHIRPS and the observed data, whereas there was a significant difference between the observed and the other two products (CHIRPS and MPE). When the results of the two catchments are compared, the rainfall in Heuningnes was better estimated than in the Jonkershoek. This might be as result of Jonkershoek receiving more rainfall than Heuningnes and the mean error indicates that the remotely-sensed products are dry biased, hence favoring the Heuningnes. This suggests that in areas with low rainfall, the remotely-sensed products might perform better.

6.4 Assessment of monthly rainfall estimates

There is a need to assess the remotely-sensed estimates at monthly timescale. WCP (1985) states that monthly estimates of rainfall have many useful applications for the general public, agricultural, hydrological as well as climatological and numerical model needs. This section will assess, i) the actual differences between the estimated and observed data, ii) the relationship between the two through correlation, and iii) the differences between the means through the t-test.

6.4.1 Assessment of the monthly differences in actual rainfall amount at Heuningnes catchment

The assessment was from March 2015 to February 2016 at Spanjaardskloof, the most representative stations in Heuningnes Catchment as in section 6.2. The driest month based on rain gauge data was January with 23.2 mm/month observed whereas CHIRPS and TAMSAT estimated 14.34 and 2 mm/month respectively; however, CHIRPS estimated no rain for October and December (Figure 6.5). The wettest month was June with 124.6 mm/month and CHIRPS and TAMSAT estimated 103 and 22 mm/month respectively. The mean error for CHIRPS was calculated to be -8.43 mm/month and TAMSAT had a mean error of -32.78 mm/month. The MPE was excluded in this section due to missing data of 23 days overlapping two months.

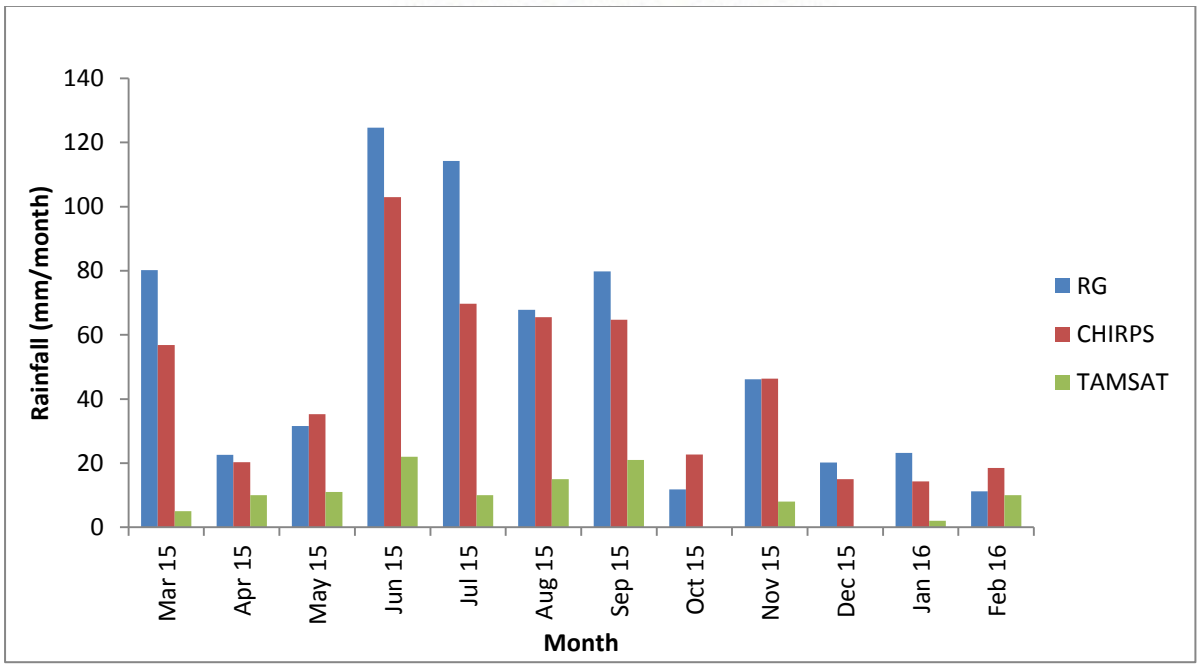

Figure 6.5: The comparison of estimated rainfall by CHIRPS and TAMSAT with observed data from rain gauge for the year 2015/16 in Heuningnes (Spanjaardskloof).

Figure 6.6 shows the difference between observed and estimated rainfall by CHIRPS and TAMSAT for the year 2015/16 at Heuningnes (Spanjaardskloof). CHIRPS overestimated during the dry (May 2015, Nov 2015 and Feb 2016). The graph also shows that TAMSAT underestimated considerably by 102.6 and 104.2 mm/month for June and July respectively, whereas CHIRPS underestimated by 21.6 and 44.5 mm/month for June and July respectively. Although there is a general underestimation by both products, CHIRPS performs better than TAMSAT. This may be caused by that TAMSAT depend solely on the remotely-sensed data whilst CHIRPS uses both satellite estimate from TRMM 3B42 and gauge data, hence errors can be reduced.

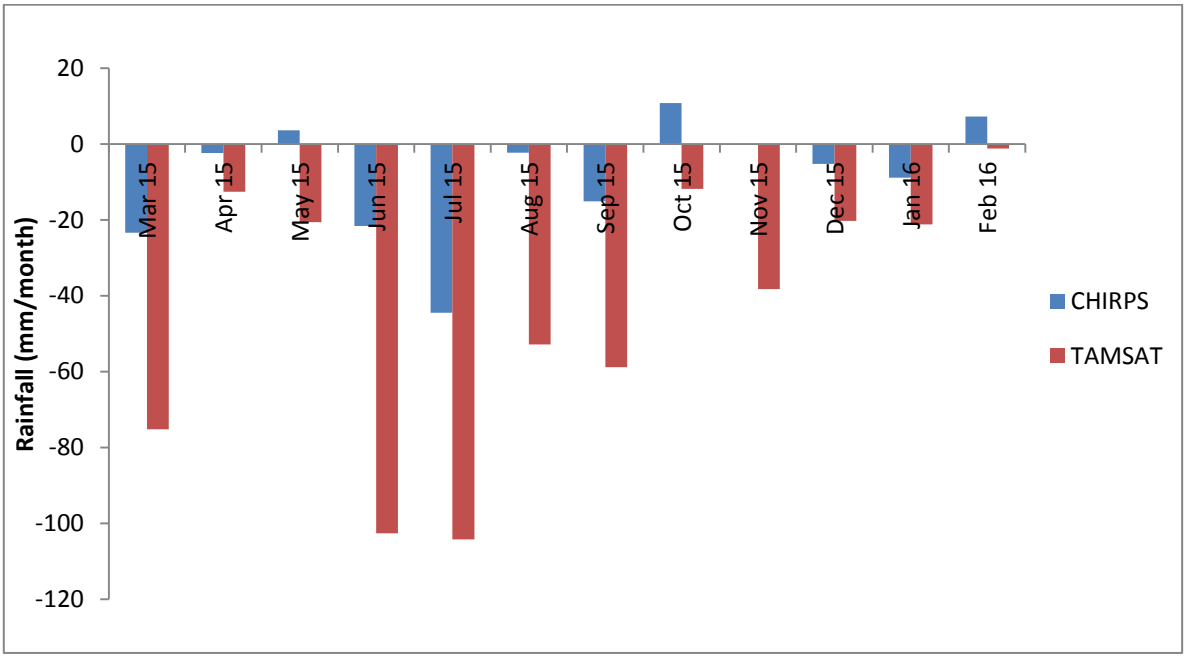

Figure 6.6: The difference between observed and the estimated rainfall by CHIRPS and TAMSAT RFE for the year 2015/16 in Heuningnes (Spanjaardskloof). The 0 line is observed rainfall and any value above the 0 line is overestimation and any value less than 0 is underestimation.

6.4.2 Association between observed and estimated monthly rainfall at Heuningnes Catchment

There is a strong relationship (r=0.95) between CHIRPS and observed monthly data at Spanjaardskloof (Figure 6.7). However, this only means the estimated values follow a similar pattern of the observed (Figure 6.5). This does not consider the difference in amount of estimated and observed values. The significance of correlation coefficient test showed that

this correlation is statically significance at 95% confidence level (P=0). Where N= 12, Df= 10, t Critical= 2.23 and calculated t was 9.6.

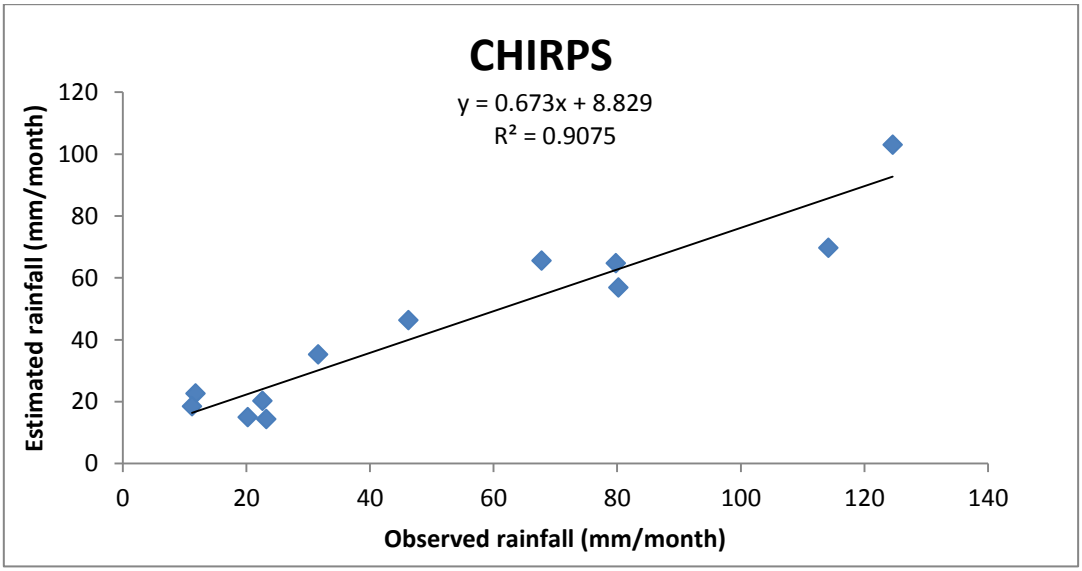

Figure 6.7: The relationship of between CHIRPS and observed data at the Heuningnes catchment (Spanjaardskloof) from March 2015 to February 2016.

There is moderate relationship (r=0.65) between TAMSAT and observed data at Spanjaardskloof (Figure 6.8). However, this only means the estimated values follows a similar temporal pattern of that of the observed (Figure 6.5). This does not consider the differences between the estimated and observed amount. The significance of correlation coefficient test showed that this correlation is statically significance at 95% confidence level (p=0.02). Where N=12, Df= 10, t Critical= 2.23 and calculated t was 2.27.

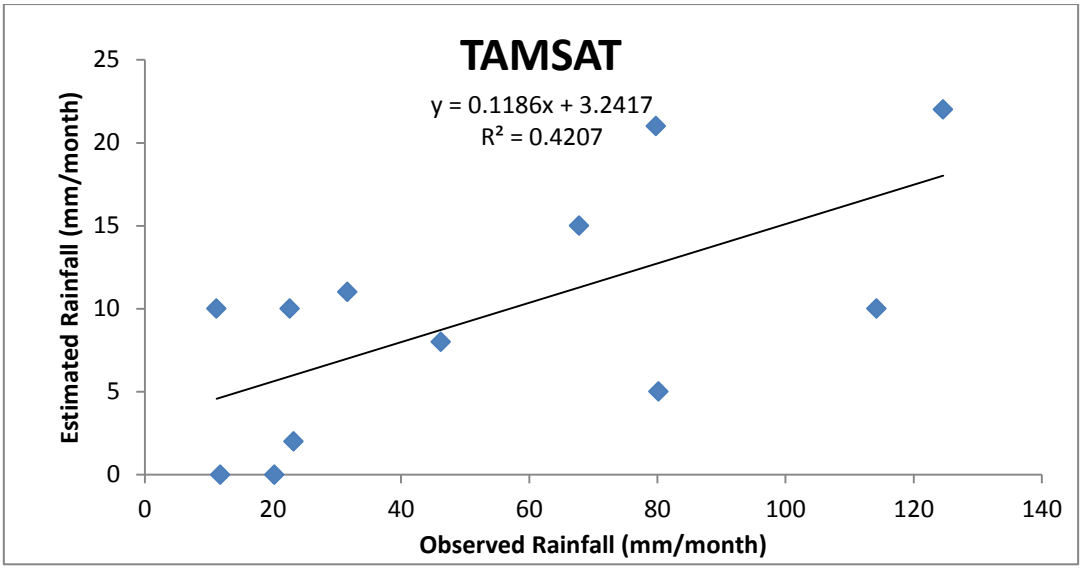

Figure 6.8: The relationship between TAMSAT and observed data from rain gauge at Heuningnes (Spanjaaarsdkloof) from March 2015 to February 2016.

The MPE had missing data that overlaps two months (Sept and Oct). However, when the missing data is excluded, the correlation between MPE and rain gauge data was unexpectedly moderate (0.58). The significance of correlation showed that all the correlations were statistically significant at 95% confidence level ($P<0.05$). Ten months were used to obtain these results. Hence, the MPE was not included in the assessment of the actual amount which does not take into account the number of sample unlike correlation and the t-test.

A t-test was done to determine whether there is a difference between the estimated mean by the remotely-sensed products and the observed rainfall at monthly timescale at 95% confidence level. The t-test ($t=4.23$) showed that at the 5% significance level the mean monthly rainfall estimated using rain gauge data (52.78 mm/month) differed from that obtained from the TAMSAT data (9.5 mm/month). The t-test ($t=2.5$) also showed that the mean monthly rainfall estimated using rain gauge data (48.6 mm/month) differed from that obtained from MPE data (24.04 mm/month). However, the CHIRPS mean daily rainfall (44.35 mm/month) did not differ significantly ($t=1.88$) from that of rain gauge data (52.78 mm/month).

6.4.3 Assessment of the monthly differences in actual amount at Jonkershoek

A comparison of estimated monthly rainfall by CHIRPS and TAMSAT with observed data from March 2015 to February 2016 was done using rain gauge (RG) 14B. The driest month was March 2015 with 6 mm/month observed whereas CHIRPS and TAMSAT estimated

21.21 and 4 mm/month respectively (Figure 6.9). The wettest month was July with 242 mm/month where CHIRPS and TAMSAT estimated 113.49 and 14 mm/month respectively. From the results below, CHIRPS mean error was calculated to be -18.84 mm/month and TAMSAT had a mean error of -68.21 mm/month.

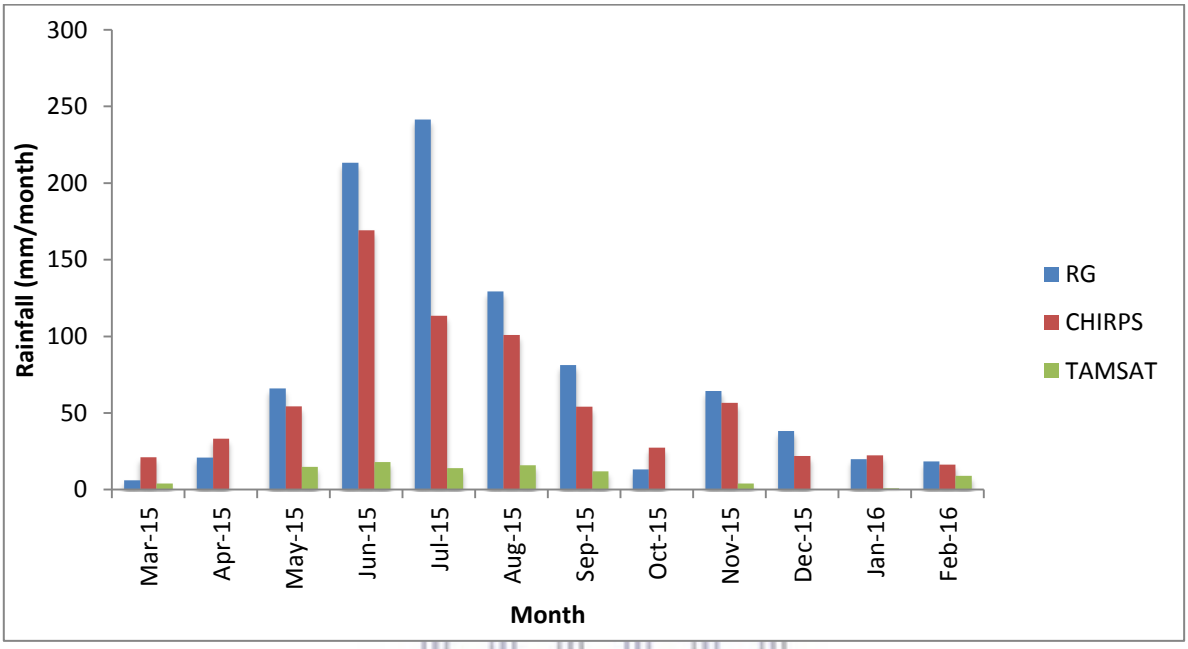

Figure 6.9: The comparison of estimated rainfall by CHIRPS and TAMSAT with observed data from rain gauge 14B in the Jonkershoek for the year 2015/16.

Figure 6.10 shows the difference between observed and estimated rainfall by CHIRPS and TAMSAT RFE for the year 2015/16 at the Jonkershoek catchment (14B). CHIRPS overestimated during March, April, October and January 2016. TAMSAT heavily underestimated by 195 and 228 mm/month for June and July respectively, whereas CHIRPS underestimated by 44 and 128 mm/month for June and July respectively. However, there is general underestimation by both products. CHIRPS performs better than TAMSAT, this may be caused by that TAMSAT depend solely on the remotely-sensed data whilst CHIRPS uses both satellite estimate from TRMM 3B42 and gauge data, hence errors can be reduced.

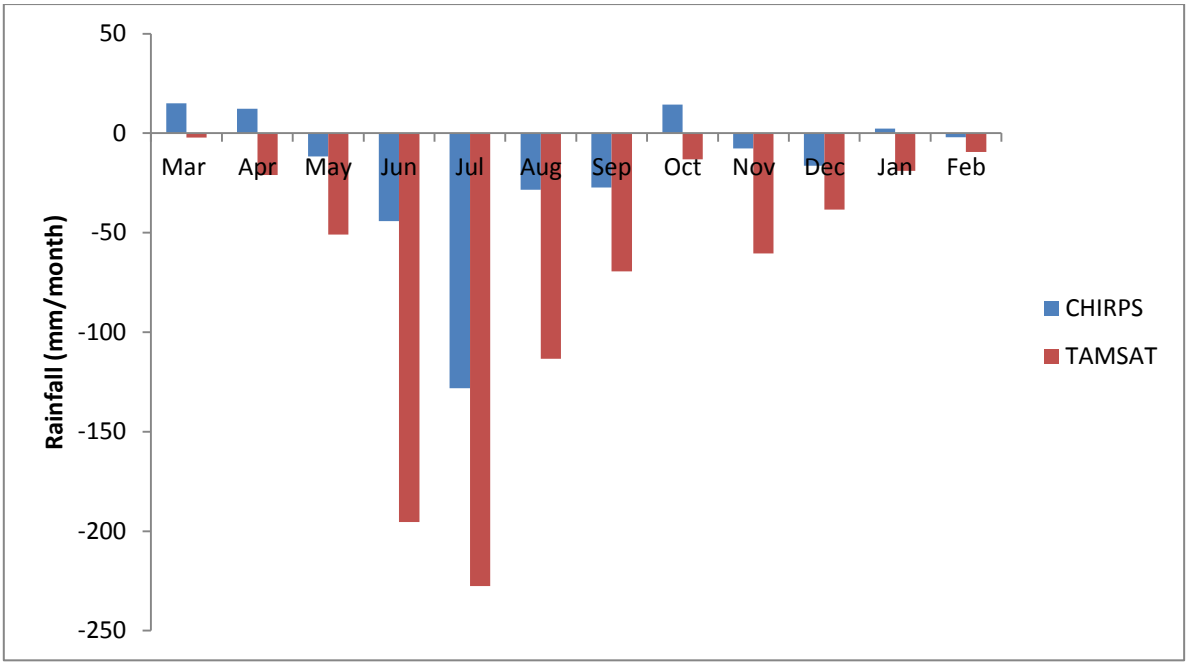

Figure 6.10: The difference between observed and estimated rainfall by CHIRPS and TAMSAT RFE for the year 2015/16 at Jonkershoek (14B). The 0 line is observed rainfall and any value above the 0 line is overestimation and any value less than 0 is underestimation.

6.4.4 Association between observed and estimated monthly rainfall at Jonkershoek

At the monthly interval, there is a strong relationship (r=0.87) between CHIRPS and observed data from the selected rain gauge station (14B) at Jonkershoek (Figure 6.11). However, this only means the estimated values follow a similar pattern to the observed (Figure 6.9). This does not consider the magnitude of the difference between the estimated and observed values. The significance of correlation coefficient test showed that this correlation is statistically significant at 95% confidence level (P=0.00). where N=12, Df= 10, t Critical= 2.23 and calculated t was 3.29.

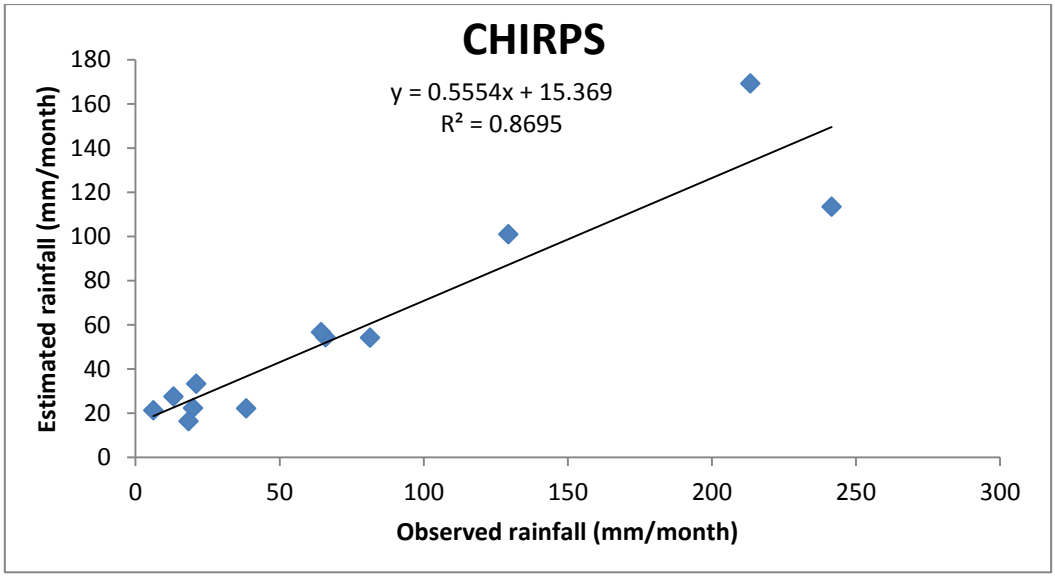

Figure 6.11: The relationship coefficient between CHIRPS and observed data from rain gauge in Jonkershoek, station 14B.

There is a strong relationship (r=0.73) between TAMSAT and observed data from 14B at Jonkershoek (Figure 6.12). However, this only means the estimated values follows a similar pattern to the observed (Figure 6.9). The significance of correlation coefficient test showed that this correlation is statistically significant at 95% confidence level (p=0.004). Where N=12, Df= 10, t Critical= 2.23 and calculated t was 4.86.

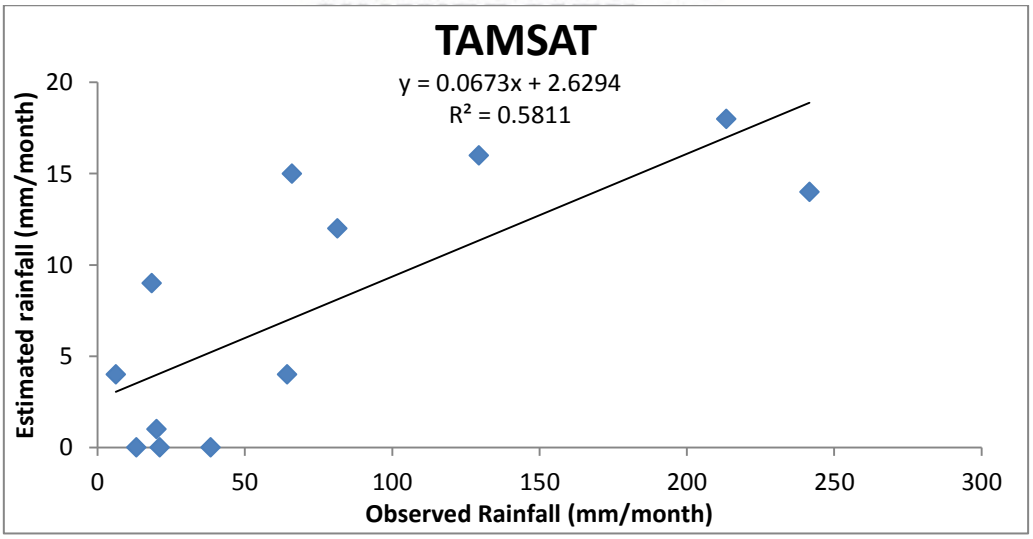

Figure 6.12: The relationship between TAMSAT and observed data from rain gauge 14B in the Jonkershoek catchment.

The MPE had missing data that overlaps two months (Sept and Oct). However, when the missing data is excluded, the correlation between MPE and rain gauge data was unexpectedly

moderate (0.7). Ten months were used to obtain these results. Hence, the MPE was not included in the assessment of the actual amount which does not take into account the number of sample unlike correlation and the t-test. The significance of correlation showed that all the correlations were statically significant at 95% confidence level ($P<0.05$).

A t-Test was done to determine whether there is a difference between the estimated mean by the remotely-sensed products and the observed rainfall at monthly timescale at 5% significant level. The t-test ($t=3.2$) showed that at the 5% significance level the mean monthly rainfall estimated using rain gauge data (76.12 mm/month) differed from that obtained from the TAMSAT data (7.75 mm/month). The t-test ($t=2.7$) also showed that the mean monthly rainfall estimated using rain gauge data (81.81 mm/month) differed from that obtained from MPE data (15.86 mm/month). However, the CHIRPS mean monthly rainfall (57.64 mm/month) did not differ significantly ($t=1.63$) from that of rain gauge data (76.12 mm/month).

Summary of the monthly estimates assessment

The comparison of the monthly actual amounts estimated by the remotely-sensed products (CHIRPS and TAMSAT) and the observed data shows that the three remotely-sensed products underestimated the actual rainfall. The MPE had missing data that overlapped two months (Sept and Oct), therefore was not included in the assessment of actual amounts. However, included in the other assessment (r and t-test) as the take into the sample size(n). The results showed that there is moderate to good relationship between the products and observed data. CHIRPS performed better than the TAMSAT and the MPE. TAMSAT had the poorest performance and the t-test showed that there is a statistically difference between the mean estimated by TAMSAT and the observed mean, the same was observed for the MPE. When the results of the two catchments are compared, rainfall in Heuningnes was better estimated than the Jonkershoek. This might be as result of Jonkershoek receiving more rainfall than Heuningnes and the mean error showed that remotely-sensed products are dry biased, hence favoring the Heuningnes. This suggests that in areas with low rainfall, the remotely-sensed products might perform better. However, when considering the relationship, Jonkershoek was better estimated whereas, in terms of the differences in the means and the t-test, results are similar for the two catchments.

6.5 Assessment of annual rainfall estimates

6.5.1 The actual differences between estimated and observed annual rainfall in the Heuningnes catchment

All three products underestimated the yearly total rainfall in Heuningnes (Figure 6.13). 633.4 mm/year was observed where CHIRPS estimated 532.23 mm/year, TAMSAT estimated 114 mm/year and the MPE estimated 240 mm/year. Therefore, CHIRPS underestimated by 101.17 mm/year (16%), TAMSAT by 519.4 mm/year (82%) and the MPE by 393.4 mm/year (62.11%) and by 656 mm/year (58%) when the likewise deletion is applied.

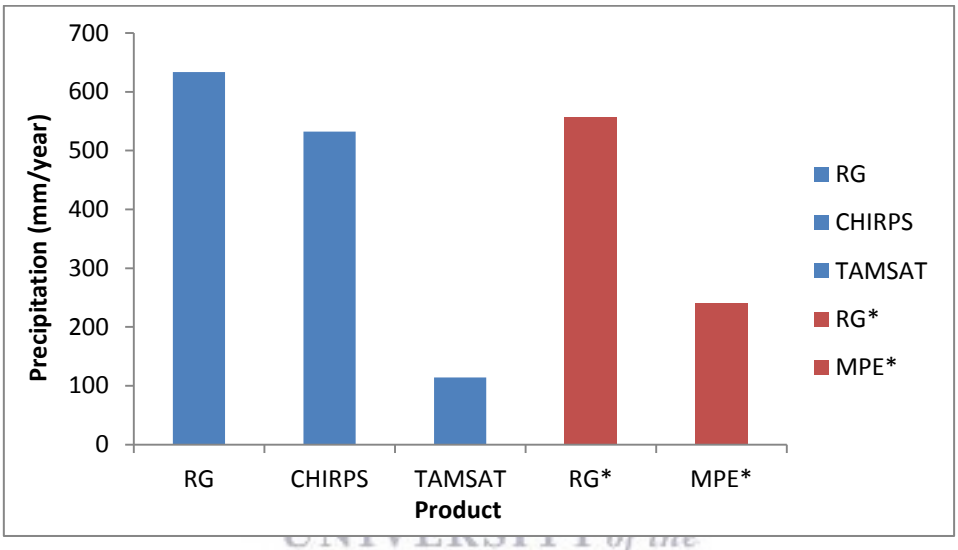

Figure 6.13: A comparison of the observed rainfall data from rain gauge (RG) in Spanjaardskloof and the remotely-sensed estimated by CHIRPS, TAMSAT and MPE for the year 2015/16. The red bars represent the results of the MPE when missing data is excluded from the comparison. * indicates that there were missing data.

6.5.2 The actual differences between estimated and observed annual rainfall in the Jonkershoek catchment

The comparison between the observed and the estimated rainfall by CHIRPS, TAMSAT and MPE from 2015 March to 2016 February shows all three products underestimated rainfall in Jonkershoek (Figure 6.14). 913.47 mm/year was observed whereas CHIRPS estimated 691.05 mm/year, TAMSAT estimated 95 mm/year and the MPE estimated 173 mm/year. All the remotely-sensed products underestimated rainfall, CHIRPS by 222 mm/year (24.35%),

TAMSAT by 818.49 mm/year (89.60%) and the MPE by 740.49 mm/year (81.06%) and by 656 mm/year (79%) when the likewise deletion method is applied.

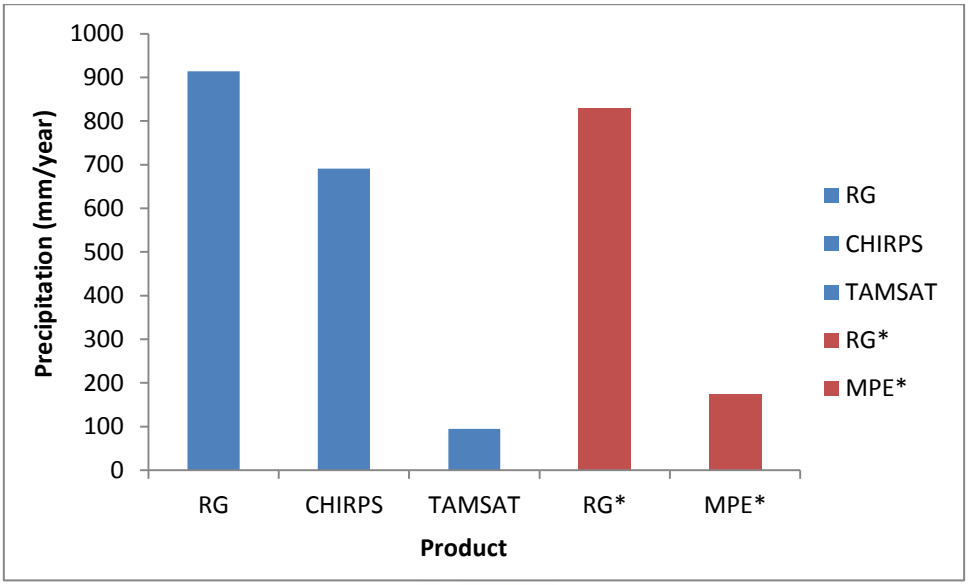

Figure 6.14: A comparison of the observed data from rain gauge (RG) 14B and the remotely-sensed estimated rainfall by CHIRPS, TAMSAT and MPE for the year 2015/16 at Jonkershoek. The red bars represent the results of the MPE when missing data is excluded from the comparison. * indicates that there were missing data.

Summary of the annual estimates assessment

Jonkershoek received more rainfall than Heuningnes, and all three remotely-sensed products underestimated the yearly total. However, CHIRPS had better estimates compared to TAMSAT and MPE in both catchments. In this regard, rainfall at Heuningnes was estimated better than in Jonkershoek. This might suggest that the products are dry biased, therefore favouring a catchment with less rainfall; this will be tested in details later in the study.

6.6 Assessment of the detection of rainy and non-rainy days

There was a need to establish whether underestimation or overestimation is due to the problem of rainy or non-rainy not being accurately detected. This was done through categorical statistics which is calculated through hits, misses, false alarms and null. Hits are days when rainfall was estimated to occur, and did occur. Misses are days when rainfall occurred but it was estimated not to occur. False Alarms are days when rainfall was estimated to occur and did occur. Null are days when rainfall was estimated not to occur and did not occur.

6.6.1 The Heuningnes Catchment

TAMSAT had 14 hits, 72 misses, 28 False Alarm and 252 null days out of 366 days (Table 6.6). Rainy day is defined as rainfall equal or greater than 1 mm/day as it is commonly used threshold for this statistics (Cai *et al.,* 2015) and TAMSAT can only estimate a minimum of 1 mm/day. The accuracy was 0.7 whereas the perfect score is 1; this indicates 70% of all (rainy and non-rain) days were detected correctly by TAMSAT. The bias of 0.45 indicates that TAMSAT underestimates the frequency of the rainy days. False Alarm Ratio (FAR) of 0.69 indicates 69% of the estimated rainy day by TAMSAT, did not occur. Possibility of False Detection (POFD) of 0.11 indicates that 11% of the observed non rainy days were detected incorrectly. Possibility of detection (POD) was found to be 0.14 whereas the perfect score is 1, this means that there is 14% chance that a rainy day will be detected as rainy day by TAMSAT. This clearly shows that TAMSAT misses a significant number of rainy days, therefore underestimation can be linked to the power of distinguishing between rainy and non-rainy days.

Table 6.6: Categorical statistics results for TAMSAT at Spanjaardskloof, Heuningnes.

	Hits	Misses	False Alarm	Null
Mar	0	8	1	22
Apr	1	4	1	24
May	0	9	3	19
Jun	4	4	6	16
Jul	3	9	4	15
Aug	2	8	5	16
Sep	2	9	5	14
Oct	0	5	0	26
Nov	0	6	2	22
Dec	0	6	0	25
Jan	0	7	1	23
Feb	1	6	1	21
Sum	13	81	29	243
Total	366			
	TAMSAT Score	Perfect Score		
Accuracy	0.7	1		
Bias	0.45	1		
POD	0.14	1		
FAR	0.69	0		
POFD	0.11	0		
CSI	0.66	1		

CHIRPS had 20 hits, 74 misses, 13 False Alarm and 259 null days out of 366 days (Table 6.7). Rainy day is defined as rainfall equal or greater than 1 mm/day as stated above. The accuracy was 0.76 whereas the perfect score is 1, the possibility of detection was found to be 0.21 whereas perfect score is 1. This means that there is 21% probability that a rainy day will be detected as rainy day by CHIRPS. This clearly shows that the CHIRPS misses a significant number of rainy days, therefore underestimation can be linked to the power of distinguishing between rainy and non-rainy days.

Table 6.7: Categorical statistics results for CHIRPS at Spanjaardskloof, Heuningnes.

	Hits	Misses	False Alarm	Null
Mar	0	8	1	22
Apr	1	4	0	25
May	0	9	1	21
Jun	1	7	1	21
Jul	7	5	1	18
Aug	3	7	2	19
Sep	2	9	1	18
Oct	0	5	1	25
Nov	0	6	2	22
Dec	2	4	1	24
Jan	1	6	2	22
Feb	3	4	0	22
Sum	20	74	13	259
Total	366			
	CHIRPS Score	Perfect Score		
Accuracy	0.76	1		
Bias	0.35	1		
POD	0.21	1		
FAR	0.39	0		
POFD	0.05	0		
CSI	0.69	1		

MPE had 20 hits, 51 misses, 33 False Alarm and 196 null days out of 328 days (Table 6.8). This only when rainy is defined as rainfall equal or greater than 1 mm/day as the TAMSAT can only estimate a minimum of 1 mm. The accuracy was 0.72 whereas the perfect score is 1, the possibility of detection was found to be 0.28 whereas the perfect score is 1. This means that there is 28% probability that a rainy day will be detected as rainy day by MPE. This clearly shows that the MPE misses a significant number rainy days, therefore underestimation can be linked to the power of distinguishing between rainy and non-rainy days.

Table 6.8: Categorical statistics results for MPE at Spanjaardskloof, Heuningnes

	Hits	Misses	False Alarm	Null
Mar	2	6	6	17
Apr	2	4	3	21
May	1	8	3	19
Jun	4	3	4	19
Jul	3	9	4	15
Aug	0	9	0	22
Sep	0	0	0	0
Oct	2	3	1	17
Nov	1	3	5	21
Dec	2	4	3	22
Jan	1	6	3	21
Feb	4	3	2	20
Sum	22	58	34	214
Total	328			
	MPE Score	Perfect Score		
Accuracy	0.72	1		
Bias	0.7	1		
POD	0.28	1		
FAR	0.61	0		
POFD	0.14	0		
CSI	0.51	1		

6.6.2 The Jonkershoek Catchment

TAMSAT had 12 hits, 72 misses, 23 False Alarm and 259 null days out of 366 days (Table 6.9). Rainy day is defined as rainfall equal or greater than 1 mm/day. The accuracy was 0.74 whereas the perfect score is 1, the possibility of detection was found to be 0.14 whereas the perfect score is 1. This means that there is 14% probability that a rainy day will be detected as rainy days by TAMSAT. This clearly shows that the TAMSAT misses significant a number rainy day, therefore underestimation can be linked to the power of distinguishing between rainy and non-rainy days.

Table 6.9: TAMSAT categorical statistics results for the Jonkershoek Catchment (14B).

	Hits	Misses	False Alarm	Null
Mar	0	1	2	28
Apr	0	5	0	25
May	1	9	7	14
Jun	4	8	3	15
Jul	3	12	5	11
Aug	2	9	3	17
Sep	2	8	3	17
Oct	0	4	0	27
Nov	0	5	0	25
Dec	0	4	0	27
Jan	0	4	0	27
Feb	0	3	0	26
Sum	12	72	23	259
Total	366			
	TAMSAT Score	Perfect Score		
Accuracy	0.74	1		
Bias	0.42	1		
POD	0.14	1		
FAR	0.66	1		
POFD	0.08	0		
CSI	0.67	1		

CHIRPS had 21 hits, 63 misses, 20 False Alarm and 262 null days out of 366 days (Table 6.10). Rainy day defined as rainfall equal or greater than 1 mm/day. The accuracy was 0.77 whereas the perfect score is 1, the possibility of detection was found to be 0.25 whereas the perfect score is 1. The worst month was July where CHIRPS only estimated one rainy day whereas it missed all 15 rainy days and 113 mm was estimated for one day. The better detected months were March and October which are dry months.

Table 6.10: CHIRPS categorical statistics results for the Jonkershoek Catchment (14B).

	Hits	Misses	False Alarm	Null
Mar	1	0	0	30
Apr	3	2	2	23
May	1	9	0	21
Jun	2	10	3	15
Jul	0	15	1	15
Aug	3	8	2	18
Sep	1	9	3	17
Oct	3	1	1	26
Nov	4	1	2	23
Dec	1	3	2	25
Jan	0	4	3	24
Feb	2	1	1	25
Sum	21	63	20	262
Total	366			
	CHIRPS Score	Perfect Score		
Accuracy	0.77	1		
Bias	0.49	1		
POD	0.25	1		
FAR	0.49	1		
POFD	0.07	0		
CSI	0.61	1		

MPE had 22 hits, 42 misses, 28 False Alarm and 208 null days out of 328 days (Table 6.11). Rainy day is defined as rainfall equal or greater than 1 mm/day. The accuracy was 0.77 whereas the perfect is 1, the possibility of detection was found to be 0.31 whereas the perfect score is 1. This means that there is 31% chance that a rainy day will be detected as rainy day by MPE. This clearly shows that the MPE misses a significant number of the rainy days, therefore underestimation can be linked to the power of distinguishing between rainy and non-rainy days.

Table 6.11: MPE categorical statistics results for the Jonkershoek Catchment (14B)

	Hits	Misses	False Alarm	Null
Mar	1	0	4	26
Apr	0	5	2	23
May	4	4	5	18
Jun	7	5	1	17
Jul	6	6	4	15
Aug	0	13	0	18
Sep	0	0	0	0
Oct	1	2	2	18
Nov	1	4	3	22
Dec	1	3	1	26
Jan	0	4	5	22
Feb	1	2	2	24
Sum	22	48	29	229
Total	328			
	MPE Score	Perfect Score		
Accuracy	0.77	1		
Bias	0.73	1		
POD	0.31	1		
FAR	0.57	0		
POFD	0.11	0		
CSI	0.48	1		

Summary on the detection of rainy days

The remotely-sensed products do well in the scores that includes null days (Accuracy, POFD), this might be because the remotely-sensed products are dry biased as they tend to estimate more non-rainy days than rain-days, hence null should be easier as the non-rainy days are the most common in this climatic region. The dry biased of these products is confirmed by the Bias scores below 1 (ranging from 0.42 to 0.75) for both the Heuningnes and Jonkershoek catchments, this means that the remotely-sensed products are underestimating the rainy days. The rainy days were also poorly detected (POD of 0.14 to 0.31) for the two catchments; this shows that there is up to 31% chance that a rainy day will be detected by the remotely-sensed products in the Western Cape. However, there is a little chance (up to 14%) that the remotely-sensed products can falsely estimate rainfall and it does not occur; this can also be linked to the dry biasness of the products. When all the scores are included, the remotely-sensed products performance is moderate (CSI=0.46 to 0.69). When

comparing the two catchments, rainy and non-rainy days were better distinguished in the Jonkershoek than on Heuningnes. The MPE performed better than CHIRPS and TAMSAT.

6.6.3 Effects of daily rainfall magnitude on the detection of rainy and non-rainy days

The previous sections have shown underestimation of the quantity of rainfall by the remotely sensed precipitation product. The last section has also shown that one major cause is the poor detection of rainy day. This section investigates whether the detection of rainy days is related to the rainfall magnitude.

6.6.3.1 The Heuningnes Catchment

The Heuningnes had 94 rainy days of which 61 had a magnitude between 1 and 5 mm/day, 16 had magnitude from 5 to 10 mm/day, 9 had magnitude greater than 10 to 20 mm/day, 4 had greater than 20 to 30 mm/day, 4 had magnitude greater than 30 mm/day. To do a similar assessment on the MPE, the deletion method was applied to compensate for the MPE's missing data. Hence, after deleting, Heuningnes had 84 rainy days of which 55 had magnitude between 1 and 5 mm/day, 14 had magnitude greater than 5 to 10 mm/day, 8 had magnitude greater than 10 to 20 mm/day, 4 had greater than 20 to 30 mm/day, 3 had intensity of greater than 30 mm/day.

The ability of TAMSAT to distinguish between rainy and non-rainy days generally improves as rainfall magnitude increases (Figure 6.15) with a correlation of 0.65 between rainfall magnitude and correctly detected rainy days. Although there is positive relationship, the relationship is not well defined as magnitude of 5 to 10 mm/day was better than 10-20 mm/day. However, the higher magnitude (>20 mm/day) are better detected (also refer to Appendix 6.1). The significance of correlation coefficient test also confirmed that the correlation is not statistically significant.

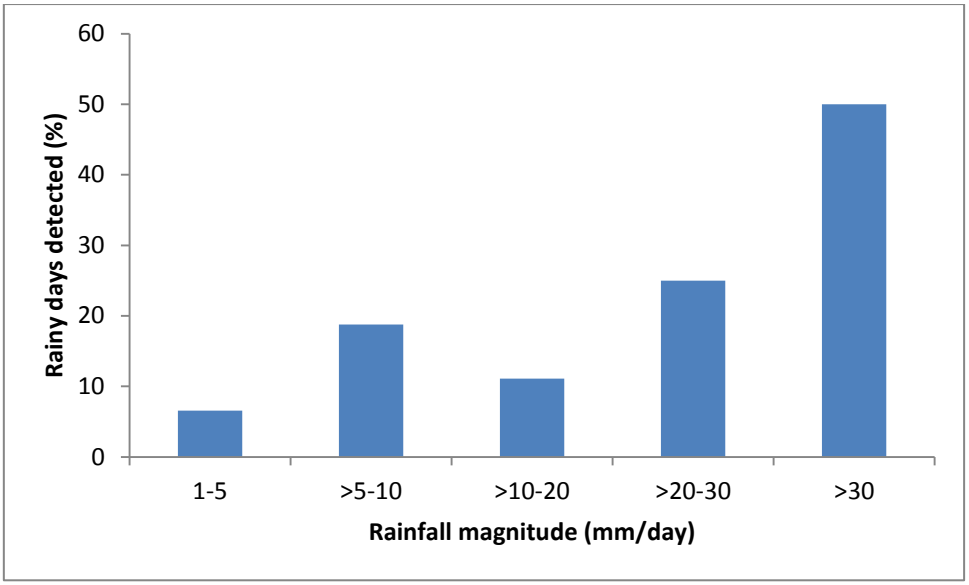

Figure 6.15: The percentage of rainy days correctly detected by TAMSAT at various rainfall magnitudes at Spanjaardskloof in the Heuningnes catchment.

In Heuningnes, the ability of CHIRPS to distinguish between rainy and non-rainy days generally improves as rainfall magnitude increases (Figure 6.16) with correlation of 0.25 between rainfall magnitude and correctly detected rainy days. Although the relationship is positive, it is however not well defined as 4 rainy days with magnitude of 20 to 30 mm/day were not estimated (also refer to Appendix 6.2). The significance of correlation coefficient also confirmed that the correlation is not statistically significant.

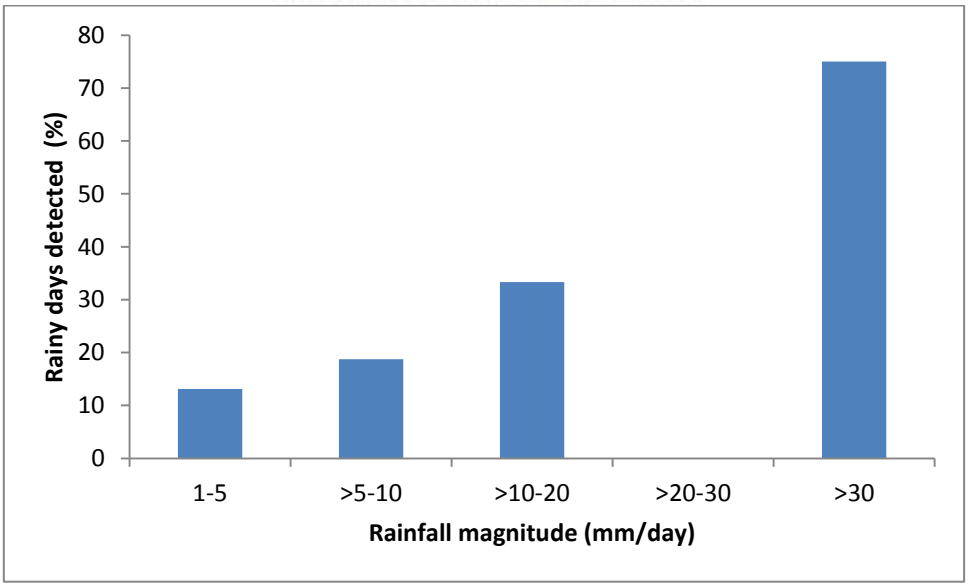

Figure 6.16: The percentage of rainy days correctly detected by CHIRPS at various rainfall magnitude at Spanjaardskloof in the Heuningnes catchment.

In Heuningnes, the ability of MPE to distinguish between rainy and non-rainy days generally improves as rainfall magnitude increases (Figure 6.21) with a correlation of 0.88 between rainfall magnitude and correctly detected rainy days. However, the relationship is very inconsistent as rainy days with magnitude of 1 to 5 mm/day were detected better than those greater 5 to 10 mm/day. Rainy days with magnitude greater than 20 to 30 mm/day were also detected better than rainfall greater than 30 mm/day (also refer to Appendix 6.3). As strong as the correlation is, the significance of correlation coefficient also confirmed that the correlation is not statistically significant.

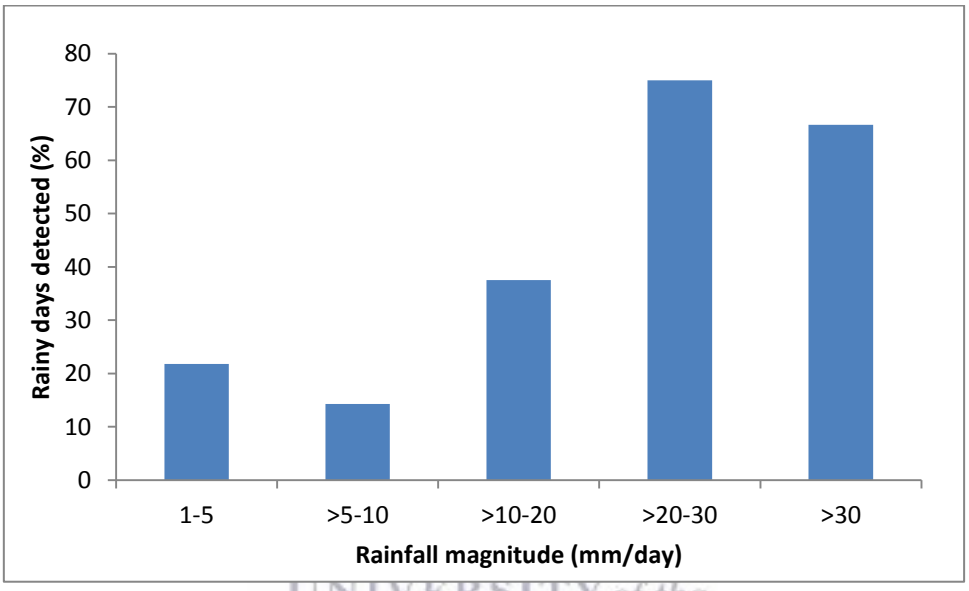

Figure 6.17: The percentage of rainy days correctly detected by the MPE at various rainfall magnitude at Spanjaardskloof in the Heuningnes catchment.

6.6.3.2 Jonkershoek

The Jonkershoek had 82 rainy days, 36 days had magnitude from 1 to 5 mm/day, 22 days had magnitude greater than 5 to 10 mm/day, 11 rainy days with magnitude greater than 10 to 20 mm/day, 10 days with magnitude greater than 20 to 30 mm/day, 5 days with magnitude greater than 30 mm/day. For MPE which had missing data, deletion method was applied, thereafter, Jonkershoek had 73 rainy days, 33 days had magnitude between 1 to 5 mm/day, and 19 had magnitude greater than 5 to 10 mm/day, 9 rain days with magnitude greater than 10 to 20 mm/day, 7 days with magnitude greater than 20 to 30 mm/day, 5 days with magnitude greater than 30 mm/day.

In Jonkershoek, the ability of TAMSAT to distinguish between rainy and non-rainy days improves as rainfall magnitude increases (Figure 6.14) with a correlation of 0.58 between rainfall magnitude and correctly detected rainy days. Even though the relationship is positive, it is not well defined as magnitude between 5 and 10 mm/day was detected better than 10 to 30 mm/day (also refer to Appendix 6.4). The significance of correlation coefficient test also confirmed that the correlation is not statistically significant.

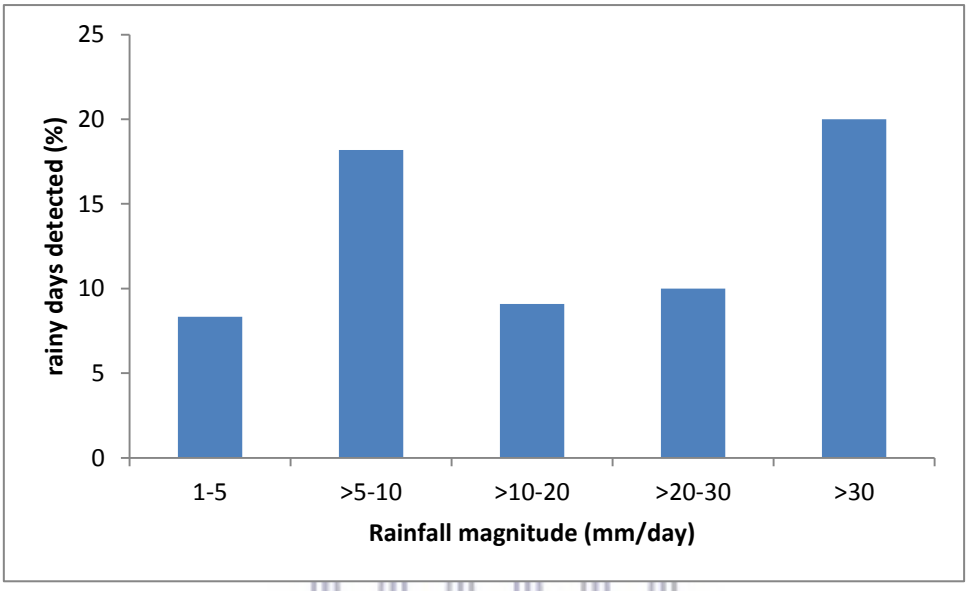

Figure 6.18: The percentage of rainy days correctly detected by TAMSAT at various rainfall magnitude at Jonkershoek.

In Jonkershoek, the ability of CHIRPS to distinguish between rainy and non-rainy days generally improves as rainfall magnitude increases (Figure 6.19) with a correlation of 0.86 between rainfall magnitude and correctly detected rainy days. There is relationship even though it is not perfectly defined as magnitude from 5 to 30 mm/day were better detected than rain with magnitude greater than 30 mm/day (also refer to Appendix 6.5). The significance of correlation coefficient test also confirmed that the correlation is not statically significant.

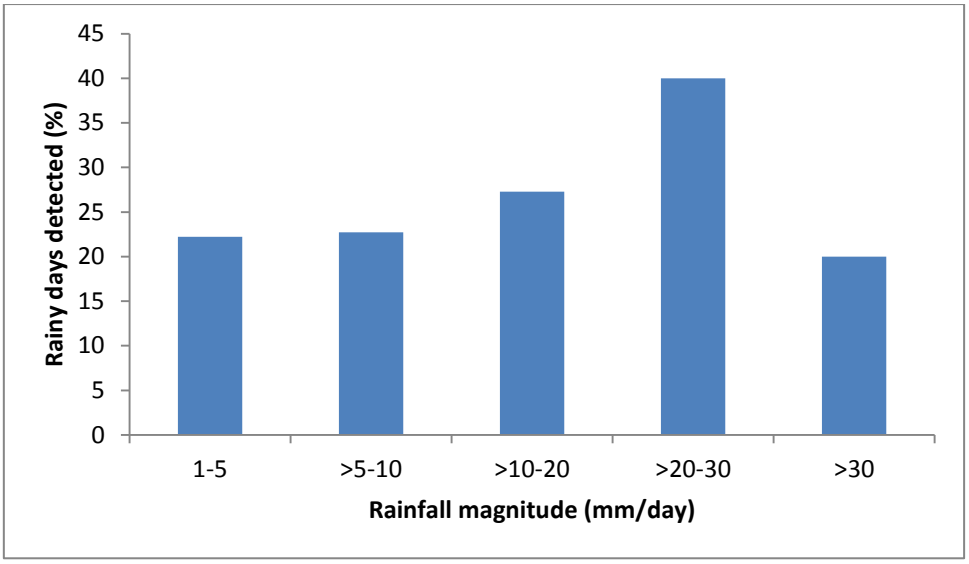

Figure 6.19: The percentage of rainy day correctly detected by CHIRPS at various rainfall magnitude at Jonkershoek.

In Jonkershoek, the ability of MPE to distinguish between rainy and non-rainy days generally increases rainfall magnitude (Figure 6.20) with a correlation of 0.75 between rainfall magnitude and correctly detected rainy days. However, the relationship is inconsistent as rainfall magnitude increases with correct rainy days detection until 20 to 30 mm/day were rainy days were poorly detected compare to days between 5 and 20 mm/day (also refer to Appendix 6.6). The significance of correlation coefficient also confirmed that the correlation is not statically significant.

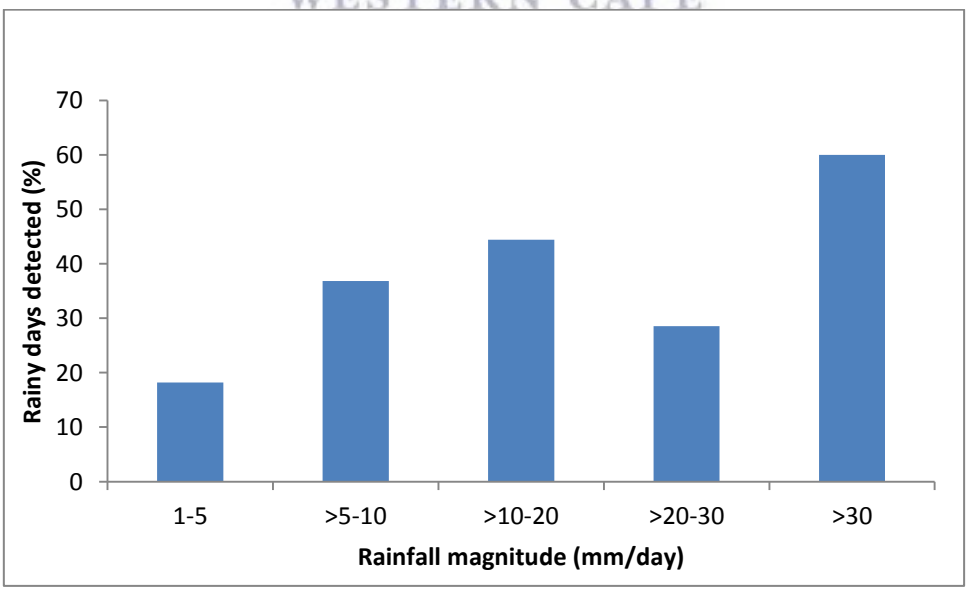

Figure 6.20: The percentage of rainy day correctly detected by MPE at various rainfall magnitude at Jonkershoek.

Summary of the effects rainfall magnitude on the detection of the rainy-days

The previous sections (6.6.1 and 6.6.2) have shown that poor detection of rainy days is a major cause of the underestimation of the rainfall by remotely-sensed products. This section determined whether there is a systematic relationship between correctly detected rainy days and the magnitude. The results have shown that there is a positive relationship, meaning that in high magnitude rainfall tend to be detected better; however the relationship is not well defined in both the Heuningnes and Jonkershoek catchments. The significance of correlation have that the relationships are not statistically significant, even when the correlation is greater than 0.7. Jonkershoek had more intense rainfall as compared to Heuningnes catchment, only 16% of the rainy days that were greater than 10 mm/day, whereas Jonkershoek had 31% of the rainy days with magnitude greater than 10 mm/day (Figure A5).

Chapter 7: General Discussion

The study showed that all remotely-sensed products used in this study generally underestimated the actual amount of rainfall at both provincial and catchment level. This is consistent with the findings of Jovanovic *et al.* (2013) and Bangira (2013), which explained the observed underestimation by the limited potential for the satellite product algorithms to quantify rainfall from frontal systems. The producers of the MPE data have acknowledged that the performance is very poor when it comes to frontal rainfall (Heinemann *et al.*, 2002). Meanwhile, De Coning and Poolman (2011) have shown that in the Western Cape rainfall is predominantly from frontal systems. The underestimation may also be linked to the fact that these techniques do not measure rain drops directly but relates cloud properties to rain rates (Ceceato and Dinko, 2010).

At the regional/provincial level, the remotely-sensed products also generally underestimated rainfall, however CHIRPS overestimated along the west coast of the province and underestimated in the eastern part of the province. This might be attributed to the climate conditions of two parts may be influenced by two different ocean currents. The west coast is influenced by the Bengaula currents from the Atlantic ocean, whereas the eastern part of the province may be influenced by the Cape Agulhas currents from the Indian ocean. The accuracy of the TAMSAT appears not to be affected by these climatic differences. At provincial level, there is a weak relationship between the accuracy of the remotely-sensed products and elevation, therefore the elevation of pixel does not affect the accuracy of the remotely-sensed products. However, an overlay of elevation contours showed that the area of high change in elevation often referred to as the Cape Fold mountains might demarcates the area of overestimation and underestimation for CHIRPS which was not the case with TAMSAT.

At the catchment level, the results also showed good association between the estimates and the observed data at monthly level. This could be due to great monthly calibrations of the products, hence the estimates had a similar temporal trends to the observed data. TAMSAT daily estimates are not calibrated against historical gauge data. This may be also due to the fundamental principles that the more it rains the more the cloud occurrence. Therefore, there will be more cloud coverage/occurrence during the wet seasons than dry seasons. This means that the errors decreases with increasing time scale, hence the estimates were better at monthly than daily intervals which is consistent with findings by Cai *et al.* (2015). TAMSAT

producers have also acknowledged that estimates accuracy improves over increasing temporal scale.

The t-test showed that there is no significant difference between the CHIRPS estimates and observed data at both daily and monthly level. This means that CHIRPS estimates are more accurate and can be used in less sensitive hydrological practices such as an input for hydrological models. For instance, Funk *et al.* (2015) showed that CHIRPS can be used to support effective hydrological forecasts and trend analysis in Ethiopia using a Variable Infiltration Capacity Model. Tou *et al.* (2016) also used CHIPRS as input for the SWAT model and the streamflow estimations were satisfactory. In the absence of observed data, the remotely-sensed estimates can be used, especially CHIRPS. However, this must be done with caution. The t-test showed that there is a significant difference between the observed and TAMSAT and MPE estimated values at both daily and monthly timescale.

The results clearly showed that CHIRPS performs better than TAMSAT and the MPE in all measures that were used in this study. This might be due to the fact that CHIRPS incorporates gauge data hence CHIRPS daily estimates are only made available at the end of each month (Funk *et al.*, 2015). When gauge data are incorporated, they reduce the initial remotely-sensed errors caused by the sensors or the algorithm itself. TAMSAT only uses the gauge data to calibrate but it is not blended into the estimates. This means that TAMSAT only relies on sensors and the algorithm which ultimately determines the amount of rainfall. Like TAMSAT, MPE also relies on its retrievals (Microwave and Infrared) and its algorithm. This is consistent with Lensky and Levizzani, (2008), Seyyedi, (2010) which indicated that blended techniques should be better as they reduced errors/deficiencies from single sensors.

The MPE was better than TAMSAT, even though MPE had missing data which highlights that one of the weaknesses of blended technique as it is vulnerable to have missing data, due its multiple sources of input data. As a result, absence of one input means that the product is unavailable for that time. The errors of these remotely-sensed products may be reduced through calibration, for instance TAMSAT errors might be reduced by downscaling of the calibration zones. Figure 7.1 shows TAMSAT's calibration zones for May; three calibration zones cover the whole of South Africa (Figure 7.1), whereas Kruger (2010) have shown that South Africa has approximately 23 climate zones.

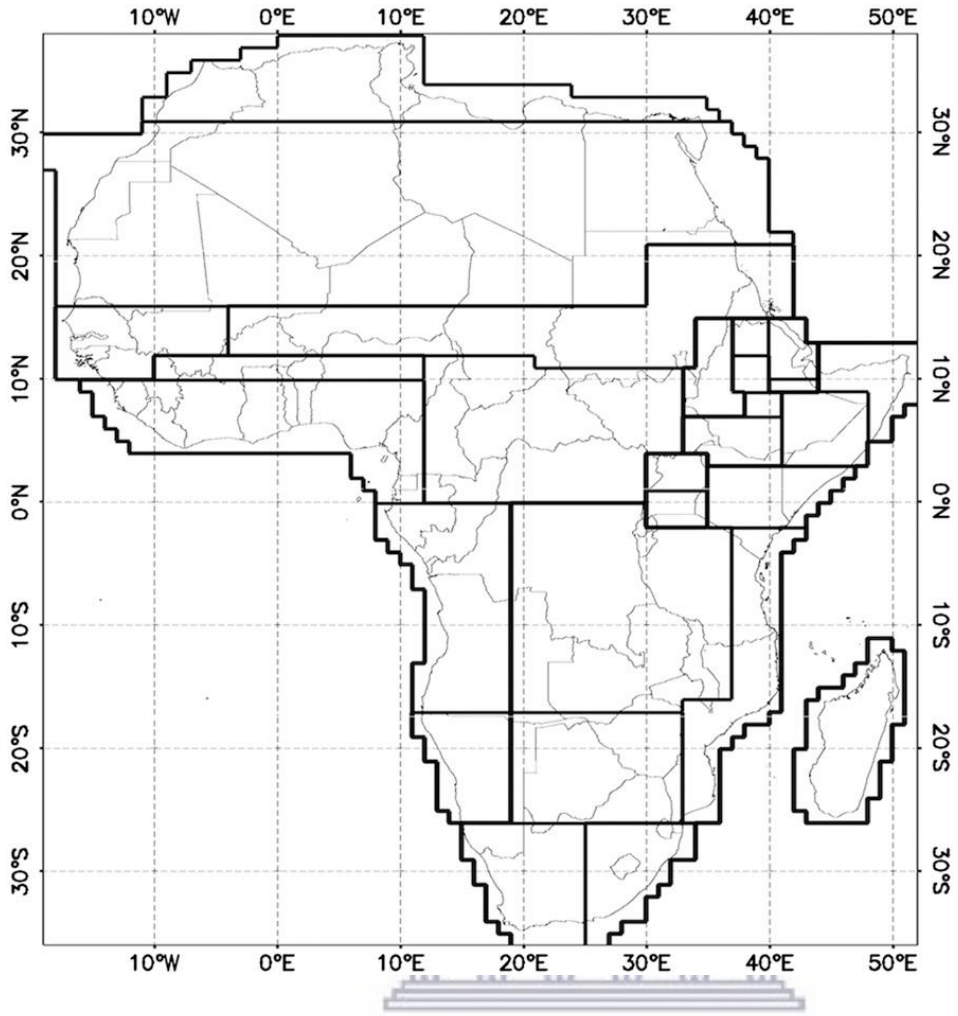

Figure 7.1: TAMSAT's calibration zones for May. South Africa is cover by three calibration zones, Tarnavsky *et al*. (2014).

The study further investigated the ability of the remotely-sensed estimates to distinguish between rainy and non-rainy days. In general, the results showed that all three products had weak ability (14 to 31%) to distinguish between rainy and non-rainy days in both catchments. Furthermore, an investigation into whether the magnitude of rainfall affects the ability of the remotely-sensed products to detect rainy days correctly was carried out, with the assumption that it might be easier to detect heavy rainfall than low rainfall days. The results showed that smaller/light magnitude rainfall (<5mm/day) are not as correctly detected as heavy magnitude rainfall (>30mm/day). However, the relationship is not well defined. Therefore, it cannot be concluded that increase in rain magnitude does increase the probability of remotely-sensed products to detect a rainy day. There might be another factor playing a role in detection of rainy days such as rain type and cloud type.

However, when the results of the two catchments are compared, the mountainous catchment (Jonkershoek) rainfall was detected better than the relatively flat catchment (Heuningnes) which was unexpected as many studies have implied that remotely-sensed estimates tend to be poor in the mountainous areas (Ceccato and Dinku 2010; Mie *et al*., 2014) due to the fact that mountains tend to have complex rainfall patterns. Mie *et al.* (2014) also stated that the four products tested in their study are not ideal for detecting rainfall in mountainous catchments.

Even when considering most of the above mentioned other accuracy measures (Correlation Coefficient at monthly timescale, Accuracy, Bias, POFD) excluding correlation coefficient at daily timescale and the accuracy measures related to actual amounts, Jonkershoek rainfall is estimated better. The results also showed that there were more rainy days in the Heuningnes catchment meaning that underestimation of these products favours Jonkershoek as it has less rainy days. Secondly Jonkershoek had more intense rainfall compared to Heuningnes, for instance 65% of the rainfall received in Heuningnes had magnitude of less than 5 mm/day, whereas in the Jonkershoek only 43% were under 5 mm/day. Another possibility might be due the cloud dwelling longer in the Jonkershoek as cloud can be trapped by the terrain. Orographic effects may increase the magnitude of thick, cold cloud which the algorithms relate to rain rate. Whereas in Heuningnes, clouds move freely without being trapped hence will move over an area quicker, before the measurement of the required information needed for estimation are captured. Due to movements of clouds, required information might be inaccurately extracted than that of the stationary or slow cloud. It is easier to extract information from a standing object than moving object. Ganguly (2012) states that extraction of information from a moving object requires very high resolution remote sensing sensors.

The study showed that on large scale (Provincial), the remotely-sensed product have similar spatial distribution of precipitation as the interpolated gauge data (Chapter 5). Furthermore, the study did a basic analysis using the Jonkershoek catchment to determine the effects of elevation and aspect on remotely-sensed precipitation estimates at a catchment level. The observed data showed that rainfall increases with elevation; this is also supported by Moses (2008). The results showed that remotely-sensed products were unable to detect this spatial pattern correctly. This might be due the spatial resolution of the products. The pixels might be too large to capture the Jonkershoek rainfall variation (Figure 7.2). In testing the effects of the aspect in Jonkershoek, the west facing slopes receive more rainfall than the East facing slopes as established by this study and others such as Moses (2008). CHIRPS did capture this

spatial pattern correctly, but TAMSAT failed as it estimated the opposite. Therefore, in-situ effects such as the two assessed here (elevation and aspect) on rainfall are complex for remotely-sensed precipitation products to get spatial pattern correctly especially in a small mountainous catchment like the Jonkershoek.

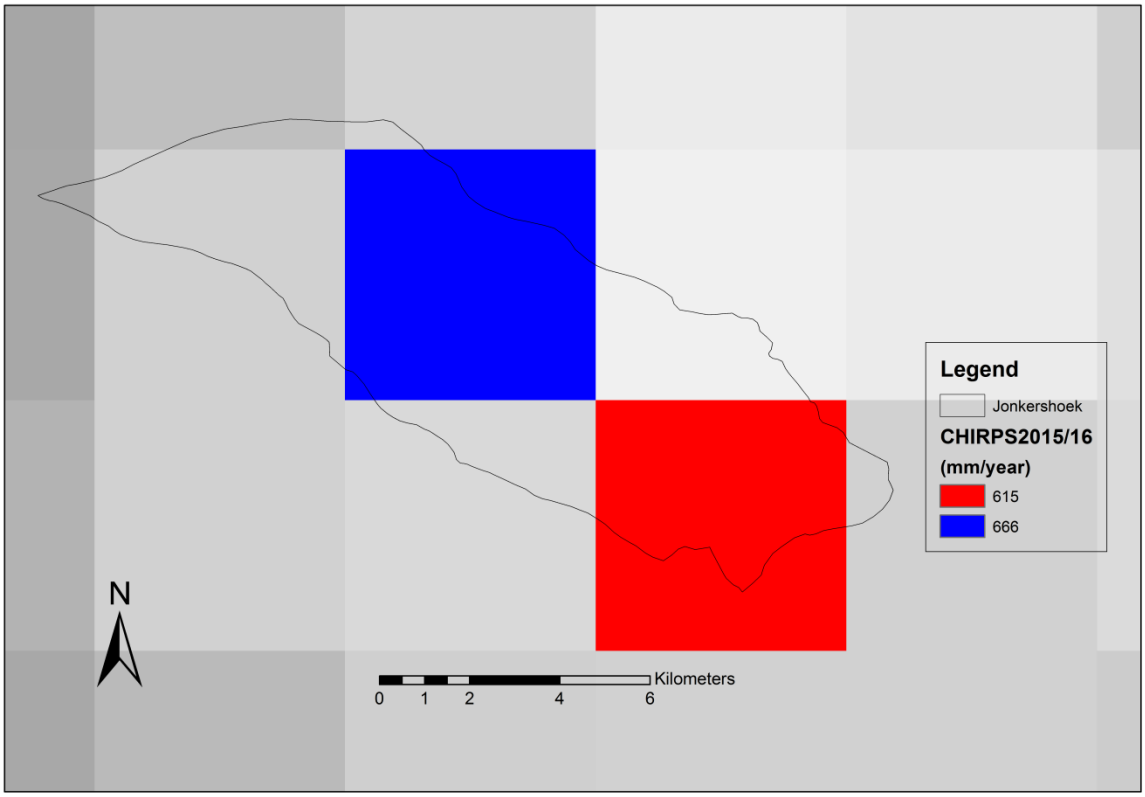

Figure 7.2: The actual spatial resolution of CHIRPS. The pixel might be large to capture the variation of rainfall in Jonkershoek catchment.

Chapter 8: Conclusion

The study showed that remotely-sensed products generally underestimated the actual rainfall amount in the Western Cape, at both provincial and catchment level. The study also showed that there was a good association between the estimated and the observed rainfall at monthly level, however there is a weak association at daily level. CHIRPS performed better than the TAMSAT and the MPE. The MPE was however, better than TAMSAT with its missing data. Therefore, blended techniques estimates are better than single instrument derived estimates. The remotely-sensed products unexpectedly showed better estimations in the mountainous catchment (Jonkershoek) than in the relatively flat catchment (Heuningnes). In determining the ability of remotely-sensed products to distinguish between rainy and non-rainy days, the remotely-sensed products were poor in distinguishing between rainy and non-rainy days as this miss a large number of rainy days. CHIRPS detected rainy days better than TAMSAT in both catchments, the MPE was also better than TAMSAT in this regards. Rainfall magnitude does affect the ability of remotely-sensed products to distinguish between rainy and non-rainy day as an increase in the rainfall magnitude usually increases with the possibility of detection of the rainy days but at times this relationship can be very inconsistent as shown by the results. Rainfall of Western Cape is complex due to the effects of frontal systems hence difficult to estimate; therefore remotely-sensed estimates should be used with caution as errors can be high as in the case of TAMSAT. The remotely-sensed estimates should not replace rain gauges because (i) even remote sensing estimation need to be calibrated using the rain gauge data (ii) remote sensing does not capture the complexity of rainfall and cannot be used in act requiring high level of accuracy such as the one rain gauge provides. Therefore, remotely-sensed estimates should not replace rain gauges or go away with field measurement but can assist in areas that have no observed data.

Recommendation

Remote sensing of precipitation is a growing field of science and needs to be evaluated. New satellites are being launched that are specialised in measuring precipitation such as the TRMM, GPM, and the Meotesat Third Generation (MTG) that will be launched soon. South Africa is also anticipating its first operational earth observing satellite in the next 5 years (Makapela *et al.*, 2015). More work is also being done to improve the algorithms of the estimates. Hence, there will be continuous improvement of remotely-sensed estimates. Thus, continuous evaluation of these products is needed especially in complex climates. The issue

of missing data in remotely-sensed estimates need to be investigated especially how to fill them.

References

Aggarwal S., 2004. Principles of remote sensing. *Satellite Remote Sensing and GIS Applications in Agricultural Meteorology*, pp.23–38.

Alazzy A.A., Lu H., Chen R., Ali A.B., Zhu Y., Su J., 2017. Evaluation of satellite precipitation products and their potential influence on hydrological modelling over the Ganzi River Basin of the Tibetan Plateau. *Advances in Meteorology*, 2017(2017). 23p

Albergel C., de Rosnay P., Gruhier C., Muñoz-Sabater J., Hasenauer S.,Isaksen L., Kerr Y. and Wagner W., 2012. Evaluation of remotely sensed and modelled soil moisture products using global ground-based in situ observations. *Remote Sensing of Environment*, 118, pp.215–226. Available at: http://dx.doi.org/10.1016/j.rse.2011.11.017.

Almazroui M., 2010. Calibration of TRMM rainfall climatology over Saudi Arabia, *Atmos.Res*, 99 (3-4) pp.400-414, doi; 10.1016/Jatmosres,2010.11.006.

Bangira T., 2013. Mapping of Flash Flood Potential Areas in the Western Cape (South Africa) Using Remote Sensing and in Situ Data. MSc Thesis. University of Twente, The Netherland.

Barnes K.N., Johnson D.J., Anderson M.D. and Taylor P.B., 2001. Important Bird Areas in Africa and associated islands – South Africa.

Baraldi A.N. and Enders C.K., 2010. An introduction to modern missing data analyses. *Journal of School Psycholology* 48(1) 5-37.

Bickerton I.B., 1984. Estuaries of the Cape. Part II. Synopses of available information on individual systems. Report no. 25: Heuningnes (CSW 19). Pp. 1–64 in Heydorn, A. E. F. and Grindley, J. R., eds. CSIR Report 424. CSIR, Pretoria.

Cai Y., Jin C., Wang A., Guan D., Wu J, Yuan F. and Xu L., 2015. Spatio-Temporal Analysis of the Accuracy of Tropical Multisatellite Precipitation Analysis 3B42 Precipitation Data in Mid-High Latitudes of China. PLoS ONE 10(4): e0120026. doi:10.1371/journal.pone.0120026

Campbell J.B., Wynne R.H., 2011. Introduction to .Remote Sensing, 5th ed, Guilford Press, 667p.

Campbell J.B., 2002. Introduction to Remote Sensing, 3rd ed, CRC Press, 621p.

Ceccato P.N. and Dinku T., 2010. Introduction to remote sensing for monitoring rainfall, temperature, vegetation and water bodies. International Research Institute for Climate and Society. Technical Report 10-04

Cheema M.J.M. and Bastiaanseen W.G.M., 2012, Local calibration of remotely-sensed rainfall from the TRMM satellite for different periods and spatial scales in the Indus Basin, *International Journal of Remote sensing*, 33(8) doi: 10.1080/01431161.2011.617397

Childs C., 2004. Interpolation surfaces in ArcGIS spatial analyst. ESRI education services. ArcUser. pp.32-35.

Ciach G.C., 2003. Local Random Errors in Tipping-Bucket Rain Gauge Measurements. IIHR–Hydroscience and Engineering, University of Iowa, Iowa City, Iowa. *Journal of Atmospheric and Oceanic Technology*, 20. pp.752-759

Coetzee E., 2008. SAEON research and monitoring sites. Available from: http://www.saeon-fynbos.org/#!home/c1cie

De Coning E., 2012. Satellite based precipitation estimation techniques for operational use over southern Africa. South African Weather Service. Pretoria, South Africa.

Dent J.E., 2012. Climate and Meteorological information requirements for water management: A review of issues. WMO-1094.

Dhib S., Mannearts C.M., Bargaoui Z., Retsios V., Mathuis B.H.P., 2017. Evalution ogf the MSG satellite Multi-Sensor Precipitation Estimate for extreme rainfall monitoring over northern Tunisia. *Weather and climate extremes*, 16. pp.14-22

Ebert E.E., 1997. Methods for verifying satellite precipitation estimates. pp.1–12.

Esien O., Frezzotti M., Genthon C., Isaksson E., Magard O., van den Broeke M.R., Dixon D.A., Holmlund P., Kameda T., Karlof L., Kaspari S., Lipenkov V.Y., Oerter H., Takahashi S. and Vaughan D.G., 2008. Ground-based measurements of spatial and temporal variability of snow accumulation in East Antactia, *Rev. Geophys*, 46, RG2001

Funk C., Peterson P., Landsfeld M., Pedreros D., Verdin J., Shukla S., Husak G., Rowland J., Harrison L., Hoell A. and Michaelsen J., 2015. The climate hazards infrared precipitation

with stations—a new environmental record for monitoring extremes. *Scientific Data*, 2, p.150066. Available at: http://www.pubmedcentral.nih.gov/articlerender.fcgi?artid=4672685&tool=pmcentrez&rendertype=abstract.

Gray W., 2003. The characterisation of orographic rainfall. *Meteorol. Appl*. 7, pp.105–119

Gerbera F., Furrera R., Schaepman-Strubb G., de Jongc R. and Schaepmanc M.E., 2016. Predicting missing values in spatio-temporal satellite data. University Zurich, Winterthurerstrasse 190, CH-8057 Zurich, Switzerland.

Gao, Y.C. and Liu, M.F., 2013. Evaluation of high-resolution satellite precipitation products using rain gauge observations over the Tibetan Plateau, *Hydrology and Earth system sciences*. 17(2), pp.837–849.

Gomez M. R. S., 2007. Spatial and temporal rainfall gauge data analysis and validation with TRMM microwave radiometer surface rainfall retrievals, I.T.C, International Institute for Geo-information science and earth observation, Nederlands.

Hardy S., Dugdale G., Milford J.R., and Sutcliffe J.V., 1989. The use of satellite derived rainfall estimates as inputs to flow prediction in the River Senegal Department of Meteorology, University of Reading, Reading, U.K.

Heinemann T., Latanzio A. and Roveda, F., 2002. The EUMETSAT multi-sensor precipitation estimate (MPE), *Second International Precipitation Working group (IPWG) Meeting* 2002, pp. 23-27.

Hughes D., 2006. Comparison of satellite rainfall data with observations from gauging station networks. *Journal of Hydrology*, **327**(3), pp. 399-410.

Helsel D.R. and Hirsch R.M., 2002. Statistical methods in Water Resources. Techniques of Water-Resources Investigations of the United States Geological Survey. Book 4, Hydrologic Analysis and Interpretation.

ICIMOD, 2013. International Center for Integrated Mountain Development (ICIMOD). China Environment and Health Resources Hub available at: http://www.icimod.org/?q=abt&page=abt

Jackson G.F., Huffman G., Stocker E., Petersen W., 2017., Successes of the Global Precipitation Measurement (GPM) Mission., NASA. Available at: https://ntrs.nasa.gov/archive/nasa/casi.ntrs.nasa.gov/20160008958.pdf

Jobard I., 2001. Status of Satellite Retrieval of Rainfall at Different Scales Using Multi-Source Data. In *MEGHA-TROPIQUES 2nd Scientific Workshop*. p. 10.

Jovanovic N., Dzikiti S., Maitre D., Roberts W., Ramoelo A. and Majozi N., 2013. Monitoring of water availability using Geo-spatial data and earth observation-Technical report. CSIR. Natural resource and the environment

Joyce R.J., Janowiack J.E., Arkin P.A., Xie., 2004. CMORPH: A Method that Produces Global Precipitation Estimates from Passive Microwave and Infrared Data at High Spatial and Temporal Resolution. *Journal of Hydrometeorology*, 5(3), pp.487–503.

Jung Y., Kim H., Baik J., Choi M., 2013. Rain gauge Network Evaluation Using Spatiotemperal Correlation Structure for Semi-mountainous. *Terr.Atmos.Ocean* 25(2) pp.267-278

Karimi P. and Bastiaanssen W.G.M., 2015. Spatial evapotranspiration, rainfall and land use data in water accounting-Part1: Review of accuracy of the remote sensing data. *Hydrology and Earth System Science* 19:507-532, 2015 doi: 10.5194/hess-+19-507-205

Kidd C., 2001. Satellite Rainfall Climatology: A Review. *International Journal of Climatology.*, 21(2001), pp.1041-1066

Kidd C., Kniveton D.R., Todd M.C. and Bellerby T. J., 2003. Satellite rainfall estimation using combined passive microwave and infrared algorithms. *J. Hydrometeor.*, 4, pp.1088–1104, doi:10.1175/1525-7541(2003)004,1088:SREUCP.2.0.CO;2.

Kruger A.G., Goliger A.M., Retief J.V. and Sekele S., 2010. Strong wind climatic zones in South Africa. *Wind and Structures*, An International Journal, 13(1), pp.37–55.

Kumar, D.N. and Reshmidevi, T., 2013. Remote Sensing Applications in Water Resources. *Journal of the Indian Institute of Science*, 93(2), pp.163–187.

Lakshmi V., 2004. The role of satellite remote sensing in the prediction of ungauged basins. *Hydrological Processes*, 18(5), pp.1029–1034.

Lensky M.I. and Levizzani V., 2008. Precipitation: Advances in Measurement. Estimation of precipitation from space-based platforms. pp.195-217. Springer. Berlin Heidelberg

Levizzani V., Amorati R. and Meneguzzo F., 2002. A review of satellite- based Rainfall estimation Methods, Multiple-sensor precipitation Measurements, Integration, Calibration and Flood Measurements, Integration, Calibration and Flood Forecasting (MUSIC), Deliverable 6.1 EVK-CT-2006-00058

Li Z.L., Tang R., Wan Z., Bi Y., Zhou C., Tang B., Yan G., and Zhang X., 2009. A review of current methodologies for regional Evapotranspiration estimation from remotely sensed data. *Sensors*, 9(5), pp.3801–3853

Liu Y.S., Islam M., and Gao J., 2003. Quantification of shallow water quality parameters by means of remote sensing. *Progress in Physical Geography*, 27(1), pp.24–43.

Lu G.Y. and Wong A.W., 2008. An adaptive inverse-distance weighting spatial interpolation technique. *Computers & Geosciences*, 34(9), pp.1044–1055.

Ly S., Charles C. and Degré A., 2013. Different methods for spatial interpolation of rainfall data for operational hydrology and hydrological modelling at watershed scale . A review, 17(2), pp.392–406.

Maidment R.I., Grimes D., Allan D.P., Tarnavsky E., Stringer M., Hewison T., Roebeling R, and E.B., 2014. Atmospheres And Time series (TARCAT) data set. *Journal of Geophysical Research:* Atmospheres, 119, pp.10619–10644.

Makapela L., Newby T., Gibson L.A., Majozi N., Mathieu R., Ramoelo A., Mengistu M.G., Jewitt G.P.W., Bulcock H.H., Chetty K.T., Clark D., 2015. Review of the use of Earth Observations Remote Sensing in Water Resource Management in South Africa. Water Research Commission, Pretoria, Report KV329/15

Maree G. and Govender S., 2013. State of Environment Outlook, Report for the Western Cape Province, Western Cape Department of Environmental Affairs & Development Planning, EADP2/2013.

Molini A., Lanza L.G. and Barbera P., 2005. The impact of tipping-bucket rain gauge measurement errors on design rainfall for urban-scale applications. Department of

Environmental Engineering. University of Genova, Genoa, Italy. *Hydrol. Process.* 19, pp.1073–1088 (2005)

Moses G., 2008. The establishment of the long-term rainfall trends in the annual rainfall patterns in the Jonkershoek valley, Western Cape, South Africa. UWC, Earth science.

Mu Q., Heinsch F.A., Zhao M., and Running S.W., 2007. Development of a global evapotranspiration algorithm based on MODIS and global meteorology data. *Remote Sensing of Environmen,* 111, pp.519-525

Najmaddin P.M., Whelan M.J., and Balzter H., 2017. Application of Satellite-Based Precipitation Estimates to Rainfall-Runoff Modelling in a Data-Scarce Semi-Arid Catchment, *Climate* ,5,32.

Ochieng W.O., 2009. Comparative study of performance of satellite derived rainfall estimates. University of Dar es Salaam. [Unpublished thesis]

Pahl-Wostl C., 2007. Transitions towards adaptive management of water facing climate and global change. *Water Resource Management* (2007) 21 pp.49–62. DOI 10.1007/s11269-006-9040-4

Pandey V. and Pandey P.K., 2010. Spatial and Temporal Variability of Soil Moisture. *International Journal of Geosciences*, 2010, 1, pp.87–98.

Peng J., Niese J., Loew A., Zhang S., and Wang J., 2015. Evaluation of Satellite and Reanalysis Soil Moisture Products over Southwest China Using Ground-Based Measurements. *Remote Sens.* 7(11*)*, pp.15729-15747.

Petty G.W. and Krajewski W.F., 1997. Satellite estimation of precipitation over land. *Hydrological Science,* 41(4) August 1996

Pimentel D., Berger B., Filiberto D., Newton M., Wolfe B., Karabinakis E., Clark S., Elaine Poon E., Abbett E., and Nandagopal S., 2004. Water Resources: *Agricultural and Environmental Issues*. 54(10), pp.909–918.

PSDF, 2005. The Western Cape Province today. Environmental planning, landscape architecture, urban design.

Qui Y., Fu B., Wand J., Chen L., 2001. Spatial variability of soil moisture content and its relation to environmental indices in a semi-arid gully catchment of the Loess Plateau, China. *Journal of Arid Environments*, 49(4), pp.723–750.

Qunwei L., 1996. The application of remote sensing in rainfall monitoring. Helsinki University of Technology, Finland.

Reddy M.K., Srinivas J., and Kumar B.N., 2008. Comparison of Mean Per Unit, Ration ABD Regression Estimators in Simple Random Sampling Using Simulation. Proceedings of the VI International Symposium on Optimization and Statistics, 29-31 Dec 2008, Aligarh, India.

Ritchie, J.C., Zimba, P. V & Everitt, J.H., 2003. Remote Sensing Techniques to Assess Water Quality. *Photogrammetric Engineering Remote Sensing*, 69(6), pp.695–704. Available at: http://www.asprs.org/a/publications/pers/2003journal/june/2003_jun_695-704.pdf.

Robert A. and Houze J., 2012. Orographic effects on precipitating clouds, *Rev. Geophys.*, 50, RG1001, doi:10.1029/2011RG000365.

Rodda J.C. and Dixon H., 2012. Rainfall measurement revisited. Centre for Ecology&Hydrology, Maclean Building, Gifford. Wallingford, Oxon. *Weather-May 2012.* 67(5)

Rogers P.P., Lamas R., and Martínez-Cortina L., 2006. *Water crisis: myth or reality*? London: Fundación Marcelino Botín, Taylor & Francis, 2. 331p

Ruhoff A.L., Paz A.R., Aragao L.E.O.C., Mu Q., Malhi Y., Collischonn W., Rocha H.R., and Running S.W., 2013. Assessment of the MODIS global evapotranspiration algorithm using eddy covariance measurements and hydrological modelling in the Rio Grande basin, *Hydrological Sciences Journal*, 58(8) DOI: 10.1080/02626667.2013.837578

Sadler R, 2010. Weather and Atmospheric phenomena, Southern Africa. Available at: http://www.southerncape.co.za/geography/weather/welcome.php

Sawunyama T. and Hughes D.A., 2010. Using satellite-based rainfall data to support the implementation of environmental water requirements in South Africa. *Water SA* (Online), 36(4) Available at: http://www.scielo.org.za/scielo.php?script=sci_arttext&pid=S1816-79502010000400001&nrm=iso.

Sivapalan M., Takeuchi K., Franks S.W., Gupta V.K., Karambiri H., Lakshmi V., Liang X., Mcdonnell J.J., Mendiondo E.M., O'connell P.E., Oki T., Pomeroy J.W., Schertzer D., Uhlenbrook S., and Zehe E., 2003. IAHS Decade on Predictions in Ungauged Basins (PUB), 2003–2012: Shaping an exciting future for the hydrological sciences, *Hydrological Sciences Journal*, 48(6), pp.857-880, DOI: 10.1623/hysj.48.6.857.51421

Schmugge T.J., William P., Kustas W.P., Ritchie J.C. and Jackson T.J., 2002. Remote sensing in hydrology. *Advances in Water Resources*, 25(8-12), pp.1367–1385.

Schulze S.E., 1997. South African Atlas of Agrohydrology and climatology. Report to the Water Research Commission, Report No. TT82/96. Pretoria, South Africa.

Sokolik I.N., 2013. Remote sensing of precipitation and clouds. School of Earth and Atmospheric Science. Georgia Institute of Technology. Available at: http://irina.eas.gatech.edu/EAS6145_Spring2013/Lecture12.pdf

Soley-Bori M., 2013. Dealing with missing data: Key assumptions and methods for applied analysis. Technical Report No. 4. Boston University. United State.

Tarnavsky E., Grimes D., Maidment R., Black E., Allan R.P., Stringer A., Chadwick R. and Kayitakire F., 2014. Extension of the TAMSAT satellite-based rainfall monitoring over Africa and from 1983 to present. *Journal of Applied Meteorology and Climatology*, 53(12), pp.2805–2822.

Teo C.T., 2006. Application of satellite-based rainfall estimates to Crop yield forecasting in Africa. Department of Meteorology. The University of Reading. England.

Toté, C., Patricio, D., Boogaard, H., van der Wijngaart, R., Tarnavsky, E. and Funk, C., 2015. Evaluation of satellite rainfall estimates for drought and flood monitoring in Mozambique. *Remote Sensing*, 7(2). pp.1758-1776. ISSN 2072-4292 doi: 10.3390/rs70201758 Available at http://centaur.reading.ac.uk/39190/

Tuo Y., Duan Z., Disse M. and Chiogna G., 2016. Evaluation of precipitation input for SWAT modeling in Alpine catchment : A case study in the Adige river basin (Italy). *Science of the Total Environment*, 573, pp.66–82. Available at: http://dx.doi.org/10.1016/j.scitotenv.2016.08.034.

Van Wyk D.B., 1987. Some effects of afforestation on streamflow in the Western Cape Province, South Africa. *Water SA* 13(1)

Wang G., Garcia D., Liu Y., de Jeu R. and Dolman A.J., 2011. A three-dimensional gap filling method for large geophysical datasets: Application to global satellite soil moisture observations. *Environmental Modelling & Software* 30 (2012) pp.139-142.

Wicht C.L., Meyburgh J.C., Boustead C.P., 1969. Rainfall at the Jonkershoek Forest Research Station. Volume 44, Serie A, no. 1. Annale University of Stellenbosch. South Africa

Wolters E.L.A., van den Hurk B.J.J.M., and Roebeling R.A., 2011, Evaluation of rainfall retrievals from SEVIRI reflectances over West Africa using TRMM-PR and CMORPH. *Hydrology and Earth System*, 15 pp.437-451,2011, doi: 10;5194/hess-15-437-2011

World Climate Programme, 1985. Review on requirements for area-averaged precipitation data, surface-based and space-based estimation techniques, Space and Time Sampling, Accuracy and Error; Data Exchange. WMO-No. 115. United State of America.

World Meteorological Organization, 2008. Guide to Meteorological Instruments and Methods of Observation, WMO-No. 8, 7th ed. Switzerland. Available at: https://www.wmo.int/pages/prog/gcos/documents/gruanmanuals/CIMO/CIMO_Guide-7th_Edition-2008.pdf

World Meteorological Organisation, 2008. Measurement of Precipitation. 8th ed. Chapter 6, Available at: https://www.wmo.int/pages/prog/www/IMOP/publications/CIMO-Guide/Ed2008Up2010/Part-I/WMO8_Ed2008_PartI_Ch6_Up2010_en.pdf

Yamana T.K., and Eltahir A.B., 2011. On the Use of Satellite-based Estimates of Rainfall Temporal Distribution to Simulate the Potential for Malaria Transmission in Rural Africa. *Water Resources Research* 47(2).

Yebra M., Van Dijk A., Leuning R., Huete A., Guerschman J.P., 2013. Evaluation of optical remote sensing to estimate actual evapotranspiration and canopy conductance. *Remote Sensing of Environment*, 129, pp.250–261. Available at: http://dx.doi.org/10.1016/j.rse.2012.11.004

Zhang C., Li W., and Travis D.J., 2009. Restoration of clouded pixels in multispectral remotely sensed imagery with cokriging. *International Journal of Remote Sensing*, 30(9), pp.2173–2195. http://doi.org/10.1080/01431160802549294

Data reference

NOAA GSoD :
http://gis.ncdc.noaa.gov/map/viewer/#app=clim&cfg=cdo&theme=daily&layers=0001&node=gis

CHIRPS:

ftp://ftp.chg.ucsb.edu/pub/org/chg/products/CHIRPS-2.0/

TAMSAT:

http://tamsat.org.uk/view/estimates/index.cgi/rainfall/

Daily MPE estimates from ITC:

ftp://ftp.itc.nl/pub/mpe

Appendix

Appendix 4.1: All the rain gauge stations that were used for this study.

Name	Latitude (°)	Longitude (°)	Elevation (m.a.s.l)		Name	Latitude (°)	Longitude (°)	Elevation (m.a.s.l)
Cape Agulhas	-34.833	20.016	14		Plettenburg	-34.09	23.327	141
Cape Point	-34.35	18.5	238		Porteville	-30.016	18.983	123
CTN INT	-33.964	18.601	46		Vanwykvlei	-30.35	21.816	962
Excelsior	-32.95	19.433	945		Robben island	-33.8	18.366	3
Geelbek	-33.2	18.116	7		Beaurtfort West	-32.35	22.55	900
George	-34.005	22.378	197		Willowmore	-32.35	23.5	842
Laingsburg	-33.2	20.866	656		19B	-33.976	18.948	300
Malmesbury	-33.466	18.716	102		11B	-33.959	18.939	408
Mossel bay	-34.183	22.15	59		15B	-33.966	18.940	319
Paarl	-33.716	18.966	104		14B	-33.982	18.976	500
Riverdale	-34.085	21.25	116		L500	-33.984	18.969	500
Robertson	-33.8	19.9	204		L600	-33.982	18.971	585
Stilbaai	-34.383	21.385	103		L700	-33.978	18.975	686
Struibaai	-34.8	20.066	4		L800	-33.978	18.983	805
Tigerhoek	-34.15	19.9	151		8B	-33.988	18.970	371
Cape columbine	-32.835	17.85	67		5B	-33.954	18.947	688
Knysna	-34.05	23.083	54		Dwarsberg	-33.999	19.013	1200
Lambertbay	-32.035	18.33	94		20B	-33.988	18.951	397
Nieuwouldtvilee	-31.35	19.083	731		12B	-33.973	18.949	340
Langabaan	-32.968	18.16	33		9B	-33.979	18.951	300
Vredendal	-31.64	18.544	52		13B	-33.976	18.957	446
Worcester	-33.9	18.5	16		Vissersdrift	-34.688	19.996	135
De aar(AU)	-30.666	24.016	1287		Spanjaardskloof	-34.540	19.739	135
Fraserburg	-31.916	21.516	1268		Napier	-34.468	19.909	10
Patensie	-33.766	24.816	85					

Appendix 4.2: Description of the MPE missing data, including the exact dates, data handling and communication with data providers.

Initially from ITC downloaded daily data, there were 66 days missing, 28 days were filled using raw data from the EUMETSAT. Therefore, 38 (10.4%) missing days remained between September and Mid-October as shown in the figure below. However when requested an explanation for the remainder of the days, the EUMETSAT IOP helpdesk responded "MPE product relies on the availability of Meteosat image data and an externally provided data (SSMIS). The SSMIS was not available for the time; therefore no MPE product for that time frame". The figure below also shows that there was rain estimated by the MPE during the August month which rises alarm/concern (Figure A1). To verify this, raw data from the EUMETSAT was again used, there were no evident problems. (The problem might have been internally if there any e.g the logarithm itself)

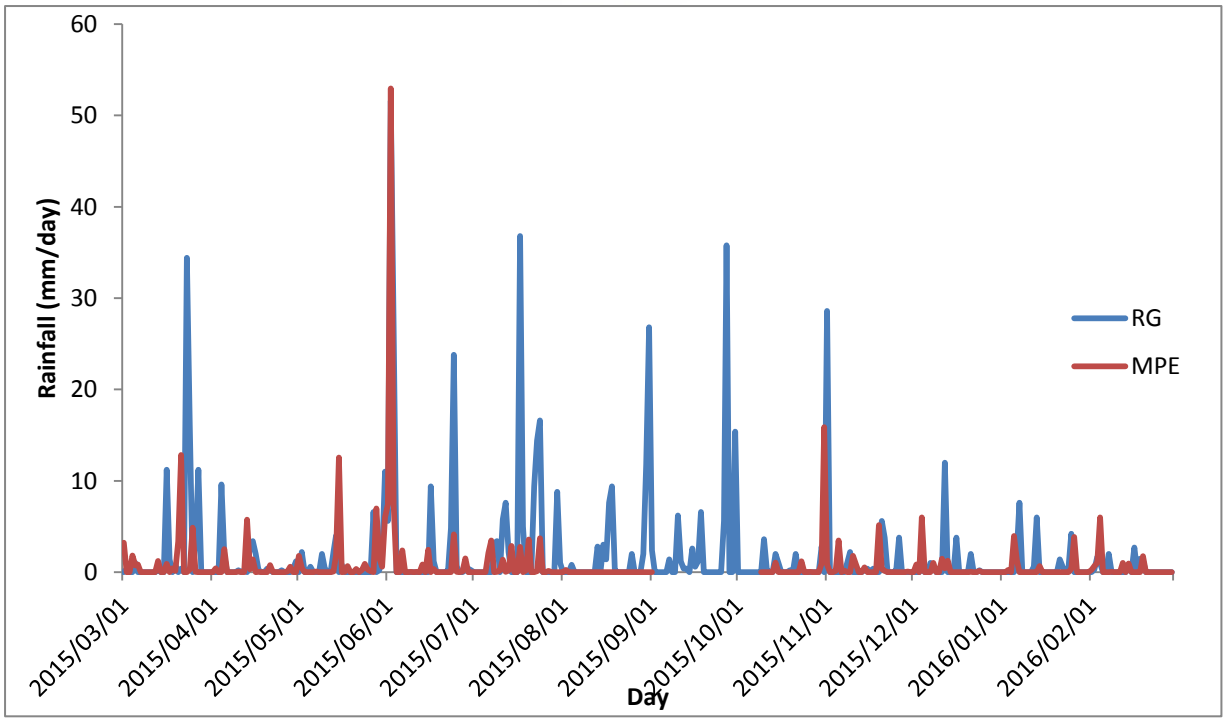

The rain gauge (RG) data and MPE estimates, the red gap shows the period of the missing data from 2015/09/01 to 2015/10/09.

Handling the remotely-sensed missing data

An investigation was done into how to handle missing remotely-sensed data. Many studies (Gerbel *et al.*, 2016; Wang *et al.*,2011; Zhang *et al.*, 2009) have been done in the spatial part of missing that due to cloud cover for instance, Figure A2 provides an MPE example, but

insufficient information in terms of when there image is not available at all, like in this case with MPE. When part of the image is corrupt, it can be completed through interpolation. Remotely-sensed data can also not be filled by nearest neighbour system like the rain gauge data as each product has its principle data and algorithm, therefore it cannot be filled using another product. Also infilling will be like creating an estimate on top of the estimate. Therefore the best way was to use the commonly used likewise/listwise deletion methods (Soley-Bori, 2013; Baraldi and Enders, 2010), which means that the missing data (days/months) were simply excluded from the analyses to have a fair comparison; statistics such as correlation have this as default. However, the results have to interpreted with caution.

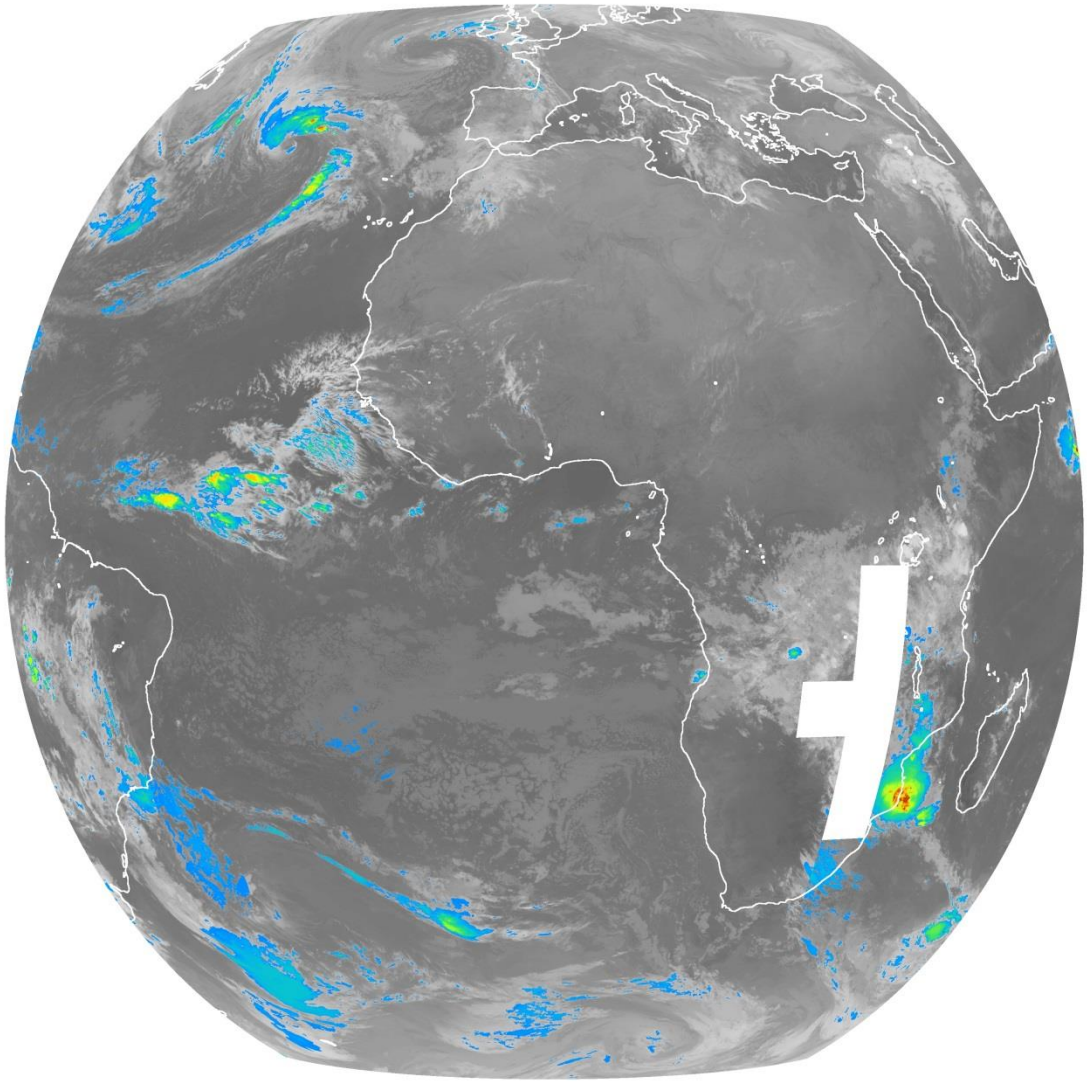

An example of the MPE with patch of missing data on 20151208.

Appendix 4.3: Additional materials of the results chapters

Correlation of the daily rainfall between rain gauge stations in the Jonkershoek catchment used for infilling of data and for the selection of the most representative rain station of the catchment. SAEON fynbos node(2016)

	19B	11B	5B	15B	8B	14B	L500	L600	L700	L 800	DWS	20B	12B	9B	13B
19B	1														
11B	0.98	1.00													
5B	0.96	0.98	1.00												
15B	0.99	0.98	0.95	1.00											
8B	0.91	0.91	0.89	0.92	1.00										
14B	0.95	0.96	0.95	0.93	0.89	1.00									
L500	0.86	0.87	0.85	0.87	0.91	0.85	1.00								
L600	0.83	0.86	0.86	0.85	0.89	0.88	0.97	1.00							
L700	0.81	0.83	0.82	0.82	0.88	0.83	0.96	0.99	1.00						
L800	0.78	0.82	0.84	0.79	0.86	0.85	0.93	0.96	0.97	1.00					
DWS	0.59	0.64	0.67	0.58	0.63	0.74	0.76	0.85	0.80	0.88	1.00				
20B	0.96	0.95	0.95	0.94	0.87	0.92	0.82	0.79	0.77	0.77	0.57	1.00			
12B	0.99	0.99	0.96	1.00	0.93	0.95	0.88	0.86	0.83	0.81	0.61	0.94	1.00		
9B	0.60	0.61	0.62	0.55	0.45	0.70	0.45	0.48	0.32	0.51	0.51	0.68	0.58	1.00	
13B	0.99	0.98	0.94	0.98	0.89	0.96	0.82	0.80	0.79	0.74	0.40	0.94	0.99	0.50	1

Appendix 4.4: Some of the reasons for missing data at Jonkershoek

Station number	Station name	Fire date	Fire damage repair action	Rainfall data gap	Davis re-installation	Radiation shield re-installation
7B	Weikamp	10 March 2015	Davis gauge damaged. Install Nipher funnel on 10 April 2015 (2pm)	10 March to 10 April 2015	28 April 2015	28 April 2015
8B	Langrivier	10 March 2015	Davis burnt to nothing, logger destroyed, replaced with Nipher funnel	26 February to 16 April 2015	31 March 2015	10 April 2015
9B	Tierkloof	10 March 2015	Davis burnt to nothing, logger destroyed, replaced with Nipher funnel	26 February to 16 April 2015	10 April 2015	10 April 2015
12B	Skag	11 March 2015	Davis gauge damaged. Install Nipher funnel on 31 March 2015	11 - 31 March 2015	10 April 2015	21 April 2015
14B	Langrivier	09 March 2015	Davis gauge damaged. Nipher funnel installed on 16 March 2015	9 - 16 March 2015	31 March 2015	21 April 2015
15B	Lambrechtbos	11 March 2015	Davis gauge damaged. Install Nipher funnel on 31 March 2015.	11 - 31 March 2015	10 April 2015	21 April 2015
19B	Biesievlei	11 March 2015	Installed new Davis funnel on 16th, tipping mechanism was fine. Rad shield destroyed	11 - 16 March 2015	16 March 2015	21 April 2015
20B	Lookout	11 March 2015	Davis burnt to nothing. No Nipher installed.	26 February to 31 March 2015	31 March 2015	21 April 2015

L500	Langrivier 500	09 March 2015	Sustained severe fire damage between 6-7pm on 9 March 2015. As a result of this, there is a data gap for all sensors from this time until 3pm on 16 March 2015 when we could visit the site to repair parts of it	09 March to 17 March 2015		
L600	Langivier 600	09 March 2015	Sustained severe fire damage between 6-7pm on 9 March 2015. As a result of this, there is a data gap for all sensors from this time until 17 March 2015 when replacement sensors could be installed	09 March to 17 March 2015		
L700	Langrivier	09 March 2015	Sustained severe fire damage between 6-7pm on 9 March 2015. As a result of this, there is a data gap for all sensors from this time until 17 March 2015 when replacement sensors could be installed.			

Appendix 6.1: The number and percentage of rainy day correctly detected by TAMSAT at various intensities at Spanjaardskloof in the Heuningnes catchment.

Intensity	no. of observed events	no. of correctly estimated events by TAMSAT	% of corrected estimated
1-5	61	4	6.56
>5-10	16	3	18.75
>10-20	9	1	11.11
>20-30	4	1	25
>30	4	2	50

Appendix 6.2: The number and percentage of rainy day correctly detected by CHIRPS at various intensities at Spanjaardskloof in the Heuningnes catchment.

Intensity	no. of observed events	no. of correctly estimated events by CHIRPS	% of corrected estimated
1-5	61	8	13.11
>5-10	16	3	18.75
>10-20	9	3	33.33
>20-30	4	0	0
>30	4	3	75

Appendix 6.3: The number and percentage of rainy day correctly detected by MPE at various intensities at Spanjaardskloof in the Heuningnes catchment.

Intensity	no. of observed events	no. of correctly estimated events by MPE	% of corrected estimated
1-5	55	12	21.82
>5-10	14	2	14.28
>10-20	8	3	37.5
>20-30	4	3	75
>30	3	2	66.66

Appendix 6.4: The number and percentage of rainy day correctly detected by TAMSAT at various intensities at Jonkershoek catchment.

Intensity	no. of observed events	no. of correctly estimated events by TAMSAT	% of corrected estimated
1-5	36	3	8.33
>5-10	22	4	18.18
>10-20	11	1	9.09
>20-30	10	1	10
>30	5	1	20

Appendix 6.5: The number and percentage of rainy day correctly detected by CHIRPS at various intensities at in the Jonkershoek catchment.

Intensity	no. of observed events	no. of correctly estimated events by CHIRPS	% of corrected estimated
1-5	36	8	22.22
>5-10	22	5	22.72
>10-20	11	3	27.27
>20-30	10	4	40
>30	5	1	20

Appendix 6.6: The number and percentage of rainy day correctly detected by CHIRPS at various intensities at in the Jonkershoek catchment.

Intensity	no. of observed events	no. of correctly estimated events by MPE	% of corrected estimated
1-5	33	6	18.18
>5-10	19	7	36.84
>10-20	9	4	44.44
>20-30	7	2	28.57
>30	5	3	60